IFM-GEOMAR REPORT

# IFM-GEOMAR

Leibniz-Institut für Meereswissenschaften
an der Universität Kiel

# FS SONNE
# Fahrtbericht / Cruise Report
# SO206

Caldera, Costa Rica – Caldera, Costa Rica
30.05. – 19.06.2010

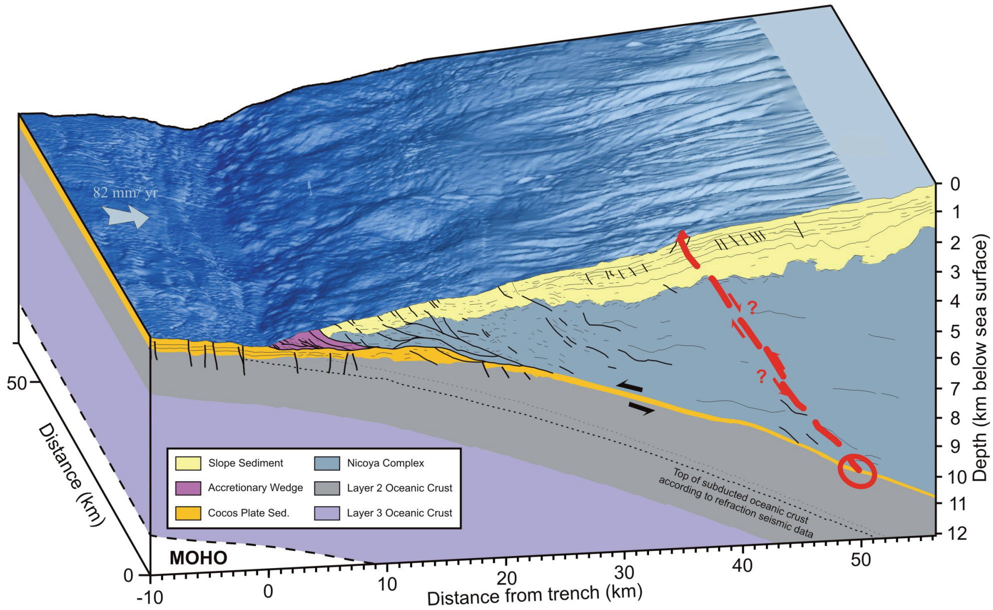



Berichte aus dem Leibniz-Institut
für Meereswissenschaften an der
Christian-Albrechts-Universität zu Kiel

**Nr. 41**
Dezember 2010

IFM-GEOMAR

Leibniz-Institut für Meereswissenschaften
an der Universität Kiel

# FS SONNE
# Fahrtbericht / Cruise Report
# SO206

Caldera, Costa Rica – Caldera, Costa Rica
30.05. – 19.06.2010

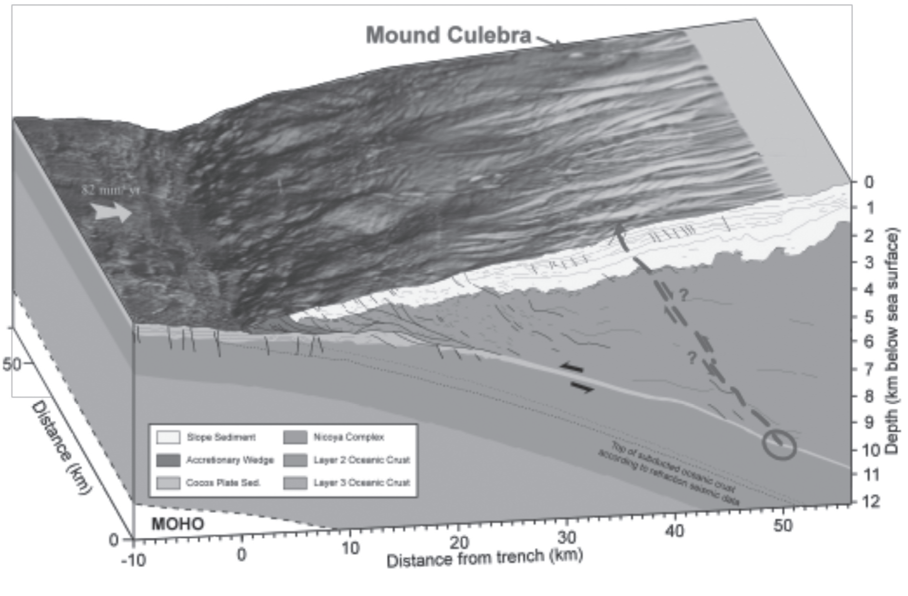


Berichte aus dem Leibniz-Institut
für Meereswissenschaften an der
Christian-Albrechts-Universität zu Kiel

**Nr. 41**
Dezember 2010

ISSN Nr.: 1614-6298

IFM-GEOMAR
Leibniz-Institut für Meereswissenschaften
an der Universität Kiel

Das Leibniz-Institut für Meereswissenschaften
ist ein Institut der Wissenschaftsgemeinschaft
Gottfried Wilhelm Leibniz (WGL)

The Leibniz-Institute of Marine Sciences is a
member of the Leibniz Association
(Wissenschaftsgemeinschaft Gottfried
Wilhelm Leibniz).

**Herausgeber / Editor:**
Christian Hensen

**IFM-GEOMAR Report**
ISSN Nr.: 1614-6298

**Leibniz-Institut für Meereswissenschaften / Leibniz Institute of Marine Sciences**
IFM-GEOMAR
Dienstgebäude Westufer / West Shore Building
Düsternbrooker Weg 20
D-24105 Kiel
Germany

**Leibniz-Institut für Meereswissenschaften / Leibniz Institute of Marine Sciences**
IFM-GEOMAR
Dienstgebäude Ostufer / East Shore Building
Wischhofstr. 1-3
D-24148 Kiel
Germany

Tel.: ++49 431 600-0
Fax: ++49 431 600-2805
www.ifm-geomar.de

Table of Contents

# 1 Summary

RV Sonne cruise 206 started on the 31st of May in Caldera (Costa Rica) and ended there on the 18th of June 2010. An international group of 23 scientists and 2 guests from Costa Rica set out to perform geophysical, biogeochemical, and sedimentological investigations at and around a number of submarine cold seeps that are ubiquitous along this convergent continental margin. The cruise was predominantly conducted as a pre-site survey for IODP (proposal 633Full-2; Costa Rica Mounds) in order to fill existing gaps in the seismic record at two of the proposed drill locations. A 2D seismic survey was conducted running over the large-scale seamount subduction slide “Jaco Scarp” yielding a highly improved image of the structural pattern within the upper 1000 m of the sedimentary sequence. In addition, high-resolution 3D seismic data, roughly covering the uppermost 300 m, could be obtained in the Mound 11/12 area, which will allow for a detailed analysis of the internal structure of these mud volcano-like features and help to understand the complex relation to the upward directed material flow. Moreover, a total number of 36 sediment cores (TV-guided multicorer, gravity corer) were successfully retrieved from active cold seeps and submarine slides and a large number of sub-samples were taken for subsequent geochemical and microbiological analyses. Overall, all major tasks of this cruise could successfully be fulfilled and the results will help to further our understanding of mechanisms controlling fluid flow in the deep subsurface of active continental margins.

## Zusammenfassung

Die Reise 206 des FS Sonne vom 31. Mai bis zum 18. Juni 2010 (Caldera - Caldera) hatte zum Ziel, geophysikalische, biogeochemische und sedimentologische Untersuchungen an “Cold Seeps” am aktiven Kontinentalrand vor Costa zu untersuchen. Basierend auf umfangreichen Vorkenntnissen von früheren Expeditionen in dieses Gebiet sollte die Fahrt vor allem dazu dienen, detaillierte seismische Untersuchungen im Rahmen eines „pre-site survey“ (IODP proposal 633Full-2; Costa Rica Mounds) durchzuführen. Zwei Gebiete standen dabei im Vordergrund: Zum einen wurden mehrere Profilschnitte über die geplanten Bohrlokationen und „Cold Seeps“ im Bereich der „Jaco Scarp“ Rutschung aufgenommen. Hier konnte ein deutlich verbessertes, strukturelles Bild der Sedimente bis zu einer Tiefe von ca. 1000 m oberhalb des subduzierten „Seamounts“ gewonnen werden. Darüber hinaus war es möglich, hochauflösende 3D-Seismikdaten der oberflächennahen Sedimente an zwei schlammvulkan-ähnlichen Strukturen („Mound 11/12“) zu gewinnen. Diese Daten lassen eine detaillierte Analyse des strukturellen Aufbaus insbesondere in Hinblick auf potentielle Aufstiegswege von Fluiden und Sedimenten zu. IN Ergänzung des seismischen Programms wurden insgesamt 36 erfolgreiche Kernnahmen mit Schwerelot und TV-gesteuertem Multicorer an verschiedenen „Cold seeps“ und submarinen Rutschungen durchgeführt sowie zahlreiche geochemische und mikrobiologische Proben für Folgeuntersuchungen entnommen. Insgesamt konnten alle Ziele des Vorhabens erreicht werden. Die erzielten Ergebnisse werden insgesamt dazu beitragen, ein besseres Verständnis hinsichtlich der Mobilisierung und Freisetzung von Fluiden an aktiven Kontinentalrändern zu erhalten.

# 2 Participants

## Scientists

**Table 2-1** Participants - Scientists

| | | | |
|---|---|---|---|
| 1 | Dr. Christian Hensen | IFM-GEOMAR | Chief Scientist |
| 2 | Dr. Joerg Bialas | IFM-GEOMAR | P-Cable / DTMCS |
| 3 | Prof. Dr. Sebastian Krastel | IFM-GEOMAR | P-Cable / Processing |
| 4 | Dr. Dirk Klaeschen | IFM-GEOMAR | Data Processing |
| 5 | Dr. Cord Papenberg | IFM-GEOMAR | Navigation Multibeam WCI |
| 6 | Wiebke Brunn | IFM-GEOMAR | OBS / DTMCS Watch |
| 7 | Dr. Ingo Klaucke | IFM-GEOMAR | DTSS / Multibeam WCI |
| 8 | Dr. Ivonne Aden-Arroyo | SFB 574 | OBS / DTSS Watch |
| 9 | Katja Lindhorst | IFM-GEOMAR | DTMCS |
| 10 | Patrick Schroeder | IFM-GEOMAR | DTSS Technician |
| 11 | Klaus Steffen | IFM-GEOMAR | Airgun / OBS Technician |
| 12 | Torge Matthiessen | IFM-GEOMAR | P-Cable Technician |
| 13 | Dr. Elena Piñero Melgar | IFM-GEOMAR | Geochemistry |
| 14 | Maik Lange | IFM-GEOMAR | MUC / GC Coring |
| 15 | Anke Bleyer | IFM-GEOMAR | Geochemistry |
| 16 | Dr. Marianne Nuzzo | LNEG | Geochemistry |
| 17 | Renate Ebbinghaus | IFM-GEOMAR | Geochemistry |
| 18 | Dr. Andy Dale | IFM-GEOMAR | Geochemistry |
| 19 | Nicolaas Glock | IFM-GEOMAR | Geochemistry |
| 20 | Philipp Steeb | SFB 574 | Microbiology |
| 21 | Stefan Krause | IFM-GEOMAR | Microbiology |
| 22 | Andrea Anasetti | IFM-GEOMAR | Sedimentology |
| 23 | Dr. Daniel Winkelmann | IFM-GEOMAR | Sedimentology |
| 24 | Emelina Corrales-Cordero | UNA, Heredia | Observer, Costa Rica |
| 25 | Dr. Maria Martinez Cruz | UNA, Heredia | Observer, Costa Rica |

IFM-GEOMAR
Leibniz-Institut of Marine Sciences
IFM-GEOMAR
Wischhofstr. 1-3
24148 Kiel
Germany

Collaborative Research Centre 574
Christian-Albrechts-University, Kiel
Wischhofstr. 1-3
24148 Kiel
Germany

LNEG
Laboratório Nacional de Energia e Geologia, I.P.
Estrada da Portela, Bairro do Zambujal – Alfragide
Apartado 7586 - 2720-866 Amadora
Portugal

UNA
Universidad Nacional
OVSICORI-UNA
P.O. Box 86-3000, Heredia
Costa Rica

**Figure 2-1:** Scientific party of SO 206

## Crew

**Table 2-2:** Participants - Crew

| | | |
|---|---|---|
| 1 | Oliver Meyer | Captain / Master |
| 2 | Nils-Arne, Aden | Chief Officer |
| 3 | Carsten Cordes | 2. Officer |
| 4 | Heinz-Ulrich Büchele | 2. Officer |
| 5 | Anke Walther | Surgeon / Ship's Doctor |
| 6 | Joerg Leppin | Electronic Engineer |
| 7 | Matthias Grossmann | System Manager |
| 8 | Wolfgang Borchert | System Manager |
| 9 | Werner Guzman-Navarrete | Chief Engineer |
| 10 | Klaus Dieter Klinder | 2. Engineer |
| 11 | Dieter Hermesmeyer | 2. Engineer |
| 12 | Uwe Rieper | Electrician |
| 13 | Andreas Moritz | Deck Fitter |
| 14 | Holger Zeitz | Motorman |
| 15 | Tim Henning | Motorman |
| 16 | Frank Tiemann | Chief Cook |
| 17 | Antony Ganagaraj | 2$^{nd}$ Cook |
| 18 | Andreas Pohl | Chief Steward |
| 19 | Harald Schmandke | 2$^{nd}$ Steward |
| 20 | Hans-Peter Mucke | Boatswain |
| 21 | Dirk Dehne | A.B. |
| 22 | Ingo Fricke | A.B. |
| 23 | Torsten Bierstedt | A.B. |
| 24 | Mario Beyer | A.B. |
| 25 | Hans Mehlhase | A.B. |
| 26 | Valerie F. Globke | A.B. |
| 27 | Denis Altendorf | S.M. / Apprentice |
| 28 | Steven Ide | S.M. / Apprentice |
| 29 | Oliver Eidam | S.M. / Apprentice |
| 30 | Michael Peplow | S.M. / Apprentice |

# 3 Research Program

## 3.1 Scientific background

While mud volcanoes and mud diapirs have extensively been described in accretionary settings forming seaward of the outer deformation front of accretionary prisms, they have rarely been reported in the context of erosive convergent margins like the Central America trench. Positive seafloor anomalies related to mud advection are known in the area since more than a decade (Kahn et al., 1996). Extensive multibeam bathymetry off the Costa Rica and Nicaragua margin has revealed the widespread occurrence of mound-like structures along the middle to upper slope of the margin (Sahling et al., 2008; Ranero et al., 2008). In general, the collective term "mound" is used, because it is difficult to clearly categorize these structures as mud volcanoes, mud diapirs or any other type of mud extrusion feature. Together with other types of dewatering features (slides and faults) more than 100 of these mounds have clearly been identified to date (Figure 3-3). Geologically, the mounds are underlain by little deformed slope sediment, which rests in turn on the basement of the continental framework. Normal faulting has been imaged seismically across the mid-slope (Ranero and von Huene, 2000) indicating that the mounds are typically associated with faults.

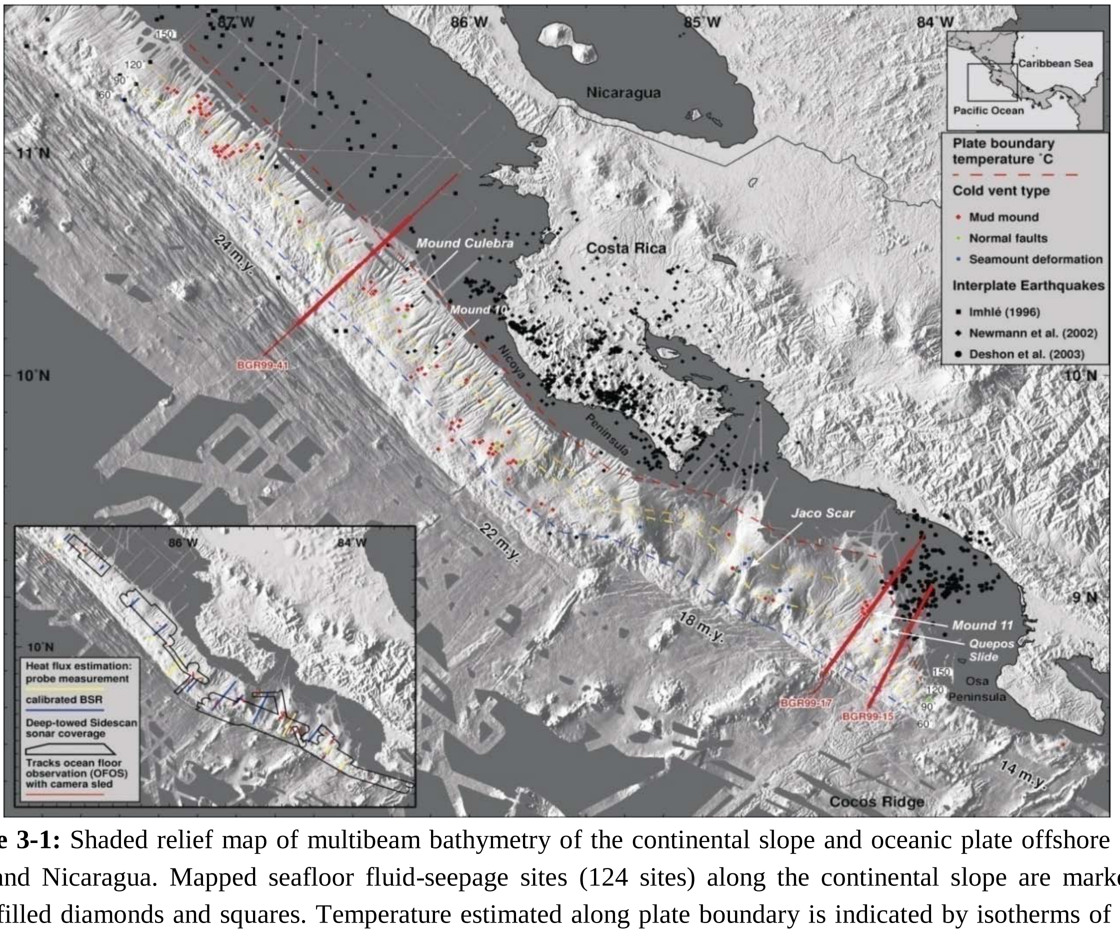


**Figure 3-1:** Shaded relief map of multibeam bathymetry of the continental slope and oceanic plate offshore Costa Rica and Nicaragua. Mapped seafloor fluid-seepage sites (124 sites) along the continental slope are marked by color-filled diamonds and squares. Temperature estimated along plate boundary is indicated by isotherms of 60°C, 90°C, 120°C and 150°C. Age of the oceanic plate at the trench axis is indicated in million years (m.y.). Black-filled symbols are well-located interplate earthquakes. Red lines are tracks of BGR99 seismic reflection profiles. Inset with relief map shows coverage of deep-towed side scan sonar and tracks of ocean floor observations. The inset also shows profiles with heat flux measurements from cruise Meteor 54 and bottom simulating reflectors used to estimate plate boundary temperatures (from Ranero et al., 2008).

Subduction of large seamounts and ridges (up to 2-3 km high and 15-20 km wide) is ubiquitous mainly offshore central Costa Rica (Figure 3-3) and correlates with enhanced forearc deformation, subduction erosion and along-trench changes in seismicity patterns. As they underthrust the continental margin and move down the subduction zone they leave behind a bathymetric furrow that marks the path of subducting seamounts (Figure 3-2) and also intensely deforms upper plate structure as observed in seismic records (Ranero and von Huene, 2000; von Huene et al., 2004). The fractures related to seamount subduction may break the upper plate providing persistent conduits across the entire upper plate. Fluids moving along the plate boundary will tend to rise along the flanks of the subducted seamount and infiltrate the fractured upper plate basement and eventually reach the overlying sediment. Fluids may flow along particular strata with enhanced porosity and vent at the plateau of the updoming sediments or at failure-related scarps behind the subducting seamount. Chemosynthetic fauna has been observed at the seafloor along most of the scarp and on top of the uplift area and there is direct evidence for major seepage creating significant plumes of methane in the water column (Mau et al., 2004; Figure 3-2).

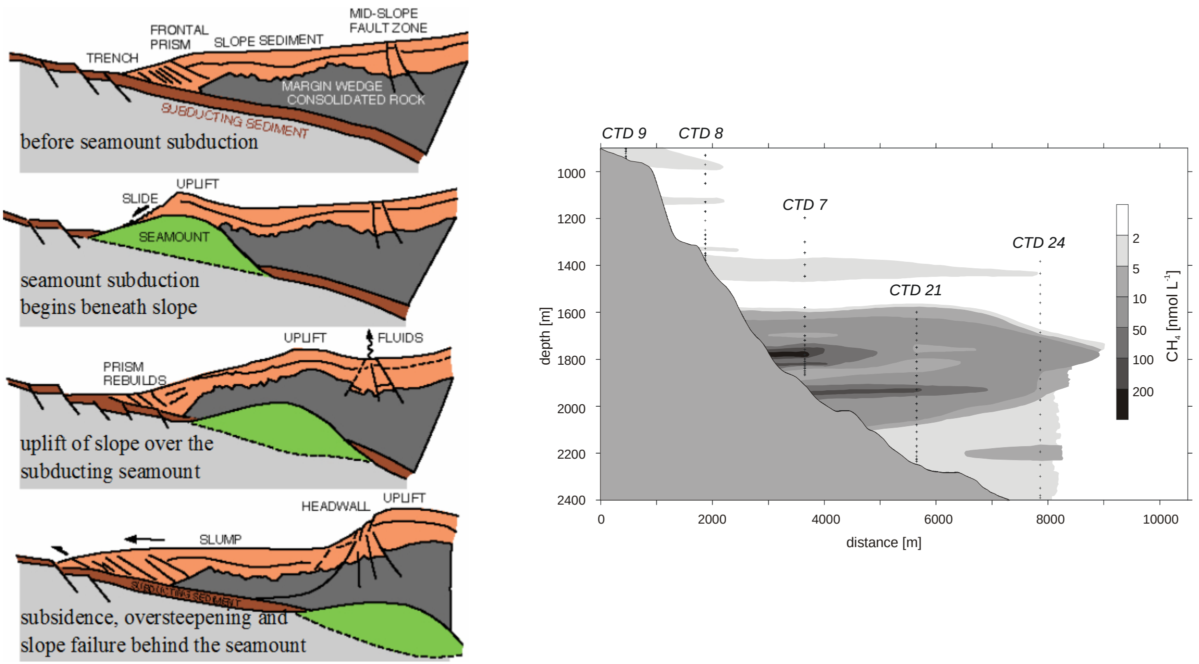


**Figure 3-2:** Development of seamount subdcution (after von Huene et al., 2004; left) and methane plume at the slide plane of Jaco Scarp (after Mau et al., 2004).

Geochemical data sampled on cruises with RV METEOR and RV SONNE in 2002, 2003, and 2005 clearly shows that fluids expelling at a number of mounds and seamount scarps at the Central American convergent margin are originating from deep sources. In general, fluids are significantly depleted with respect to seawater chloride and other major elements, suggesting that the general source of freshwater is clay-mineral dehydration (Hensen et al. 2004). Since the temperature range required for this process is not reached within the sediment cover of the upper plate, it has been hypothesized that the fluids are derived from subducting sediments and migrate upward along deep-seated faults (Hensen et al. 2004; Ranero et al. 2008; Figure 3-2). Thus, the Costa Rican mud diapirs may be less related to compressive forces in the upper plate than to the rise of deep-seated fluids from the subducted slab.

Based on results from expeditions with RV SONNE (SO163, SO173) and RV METEOR (M54, M66) a general model of fluid turnover in the forearc has been developed (Figure 3-3) and a number of hypothesis have been formulated that shall be tested by deep drilling into some of the key sites (IODP-proposal 633): (1) Numerous mounds found on the Costa Rica and Nicaragua margin are manifestations of dewatering pathways that essentially control and balance the overall fluid budget at this erosive convergent margin. (2) The internal dynamics of dewatering are driven by smectite dehydration in subducting sediments on the oceanic plate. (3) Seamount subduction at the Central America continental margin provides an unquantified mechanism for devolatilisation of slope sediments by creating deep reaching faults and fractures and causing large collapse structures on the slope. (4) Episodic release of deep, freshened fluids controls mud mobilization and hence the formation of the mounds and their internal structure. This will have major implications for the development of flow conduits and the internal mixing of fluids, which in turn may have major implications for total fluid and element budgets and the evolution cycle of the mounds. IODP-drilling has been proposed for 3 key sites (Jaco Scarp, Mound 11/12, Mound Culebra) which represent typical end-members of the observed dewatering structures at the continental margin off Costa Rica.

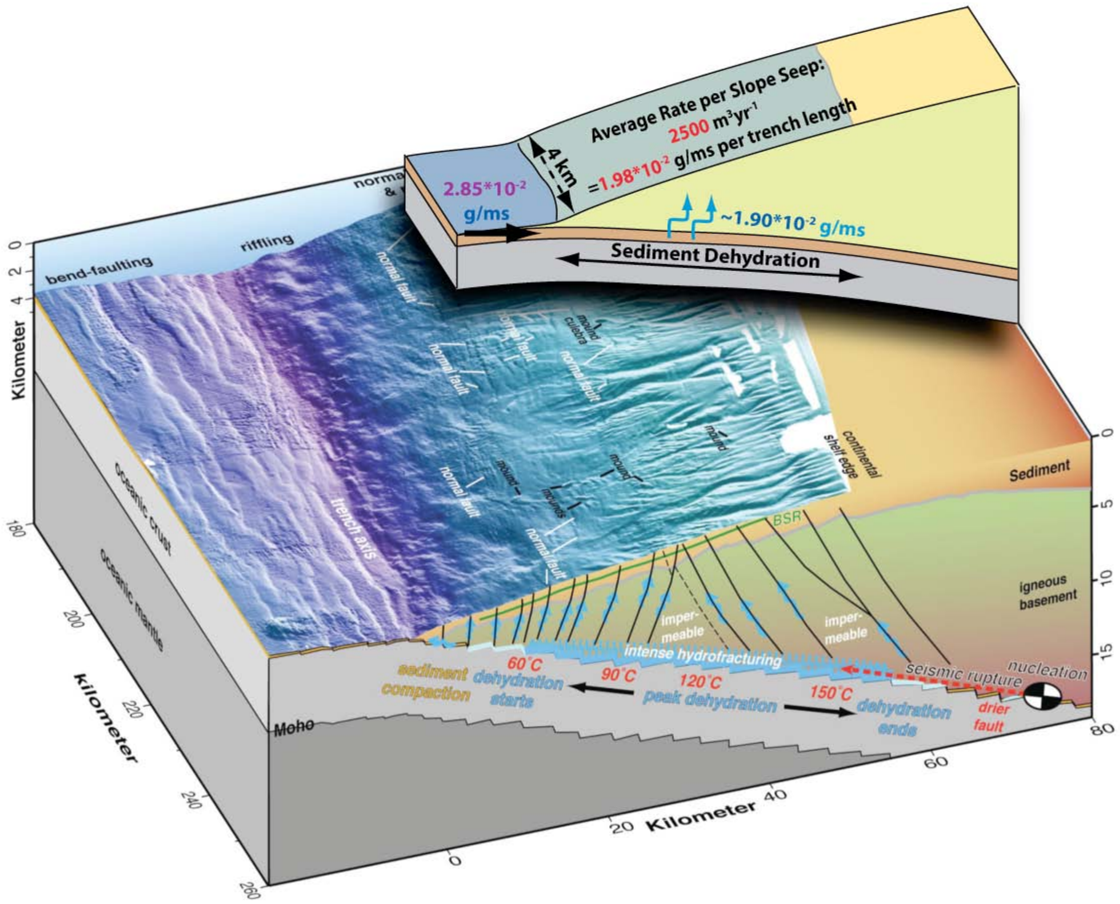


**Figure 3-3:** Conceptual 3-D illustration of structure and processes acting at the erosional Central American plate boundary indicating temperature-controlled dehydration of subducted material and fluid ascent along forearc fractures (from Ranero et al., 2008). Superimposed is the budget for the recycling of mineral-bound water for the forearc of the Central American subduction zone.

## 3.2 Objectives of the cruise

The proposed cruise aimed at collecting essential seismic and geochemical data at and around cold seepage sites located on the active continental margin off Costa Rica in order to improve our knowledge on the subsurface structure of these features and by this get a better understanding of the dewatering system at an active and erosive continental margin. The major target sites were two mud volcano – like structures (Mound 11/12) and a large-scale slide caused by subducting seamounts (Jaco Scarp) which both are key targets of IODP proposal 633 that aims to enhance the general understanding on complex forearc dewatering processes of an erosive subduction system. In order to approve drilling by IODP essential high-resolution seismic data were required. For this purpose a conventional MCS-streamer and 3-D SwathSeis system was applied. In addition to seismic investigations, geochemical and microbiological investigations were conducted at various cold seeps. Existing porewater data from these sites support the hypothesis that upward migration of fluids along deep-seated fault systems is an important mechanism of forearc dewatering. However, previously obtained geochemical information is not unambiguous, and hence additional samples were retrieved for analyses of noble and hydrocarbon gases, microbial populations and turnover rates, sediment biomarkers, and pore fluid composition.

# 4 Narrative of the cruise

(*Christian Hensen*)

FS Sonne left the port of Caldera (Costa Rica) in the early evening of the $31^{st}$ of May 2010 with an international group of 25 scientists onboard. The start of the cruise was delayed, because 7 members of the scientific crew arrived with considerable delay of more than 2 days caused by complications concerning the entry to the territory of Costa Rica from Caracas (Venezuela). In addition, important spare parts for the use of video-guided instruments were delivered one day late. In the early morning of June, 1 we started mounting the trawl doors for running the 3D seismic system (3D MCS) on the outside back of the vessel while still staying in quiet waters of the Gulf of Nicoya. In the early afternoon of the same day these preparatory works were completed and a few hours later FS Sonne arrived at the first working area of Jaco Scarp, where seamount subduction caused a large-scale submarine slide. For this area two IODP drill-holes were proposed and high quality seismic data were urgently required. After running a CTD for calibration of the SIMRAD system and a releaser test, 6 OBS were deployed along two cross-sections over Jaco Scarp. In the following ~30 hours the first section of the standard seismic profile (2D MCS) were shot with a shot frequency of 60 seconds in order to obtain optimal records by the OBS. In the evening of June, 3 the seismic program was interrupted for collecting sediment cores with gravity corer (GC) and TV-guided multicorer (TV-MUC) at a known cold seepage site (Pockmark) about 10 nautical miles southeast of the headwall of Jaco Scarp. Thereafter, the 2D MCS was repeated in opposite direction with a higher shot frequency of 15 seconds. Finally, the 6 OBS along the seismic transect were picked up in the morning of June, 5.
Afterwards, the scientific program had to be interrupted and FS Sonne sailed back to Caldera, because one of the crew members needed urgent dental care on land. After a very quick and successful medical treatment, FS Sonne could already leave Caldera in the late afternoon of the same day and the scientific program was continued. The first station was a TV-MUC on top of

Jaco Scarp followed by a Multibeam (MB) and Parasound (PS) survey in the BGR-slide region northeast of Jaco Scar. In the morning of June, 6 we returned to the Pockmark site and continued sediment sampling with TV-MUC and GC. Afterwards, GC sampling was continued at four selected sites at and the around the BGR-slide. Overnight, a video survey with the TV-multicorer was performed at a newly discovered cold seep site northwest of Pockmark. Since the video survey revealed clear indications for active expulsion of methane enriched fluids, TV-MUC and GC sampling was continued over the next day at this site. Thereafter, we transferred again to the BGR-Slide working area. Here we repeated coring at 2 of the GC locations from the day before using a longer core barrel and finalized the MB/PS survey in this region over night.

In the morning of June, 8 we started coring with TV-MUC and GC in the easternmost working area at Quepos Slide. From past cruises it was known that below the headwall (ca. 400 m water depth) of this less than 1 km wide feature, the expulsion of methane rich fluids created an abundant chemoautotrophic life with a vast area of the seafloor covered by bacterial mats. Sampling with the TV-MUC was difficult in the beginning, because of the very soft ground below the bacterial mat patches. In total, 6 TV-MUCs and 1 GC were taken at this location. For the rest of the day and the following night we again returned to the BGR-slide to deploy 6 OBS and start a seismic survey. For the next day, we again returned to the easternmost working area and started coring with GC and TV-MUC at Mound 11, another proposed IODP drilling-location. In the following night the OBS-survey was completed.

At this time it was not possible to run streamer seismics (2D-MCS and 3D-MCS) due to a complete system failure, which could not be repaired onboard. Hence, once again the scientific program had to be interrupted for enabling technical support in Caldera in order to fix the seismic equipment. In the morning of June, 10 a technician of the company Geometrics came onboard. After exchanging spare parts and a successful repair of the system, FS Sonne left Caldera in the late afternoon and headed towards the BGR-Slide area to pick up the 6 OBS. The next morning was dedicated to sample more cores with TV-MUC in the Mound 11/12 area and to prepare the 3D-MCS for deployment. In the afternoon of June, 11 the 3D-MCS was deployed southeast of Mound 11 to record high-resolution subsurface information for the area beneath Mounds 11 and 12. On June, 13 the 3D-MCS survey had to be interrupted because of technical problems with the streamer array. While these problems were fixed, two more GCs were taken at Mound 11 and in the vicinity of Mound 12 followed by a MB/PS at the shelf break further north. On Monday the 14$^{th}$ of June the 3D-MCS was deployed again at Mound 11/12 and recording of data continued until the morning of June 16. After deploying a GC reference station in the vicinity of Mound 12, we left this working area. In the afternoon of the same day a final 2D-MCS was started at BGR-Slide in order to connect to previously recorded seismic data in this area. In the early morning of June, 17 the seismic program was completed. The rest of the day was used for a MB/PS survey in the area east of the BGR-slide area to complete the high-resolution bathymetric data set off Costa Rica. The scientific program of SO 206 ended at 20:00 on June 17, 2010. After waiting about 16 hours outside the harbour, RV Sonne finally moored at pier of Caldera at 00:15 in the morning of June 19, 2010.

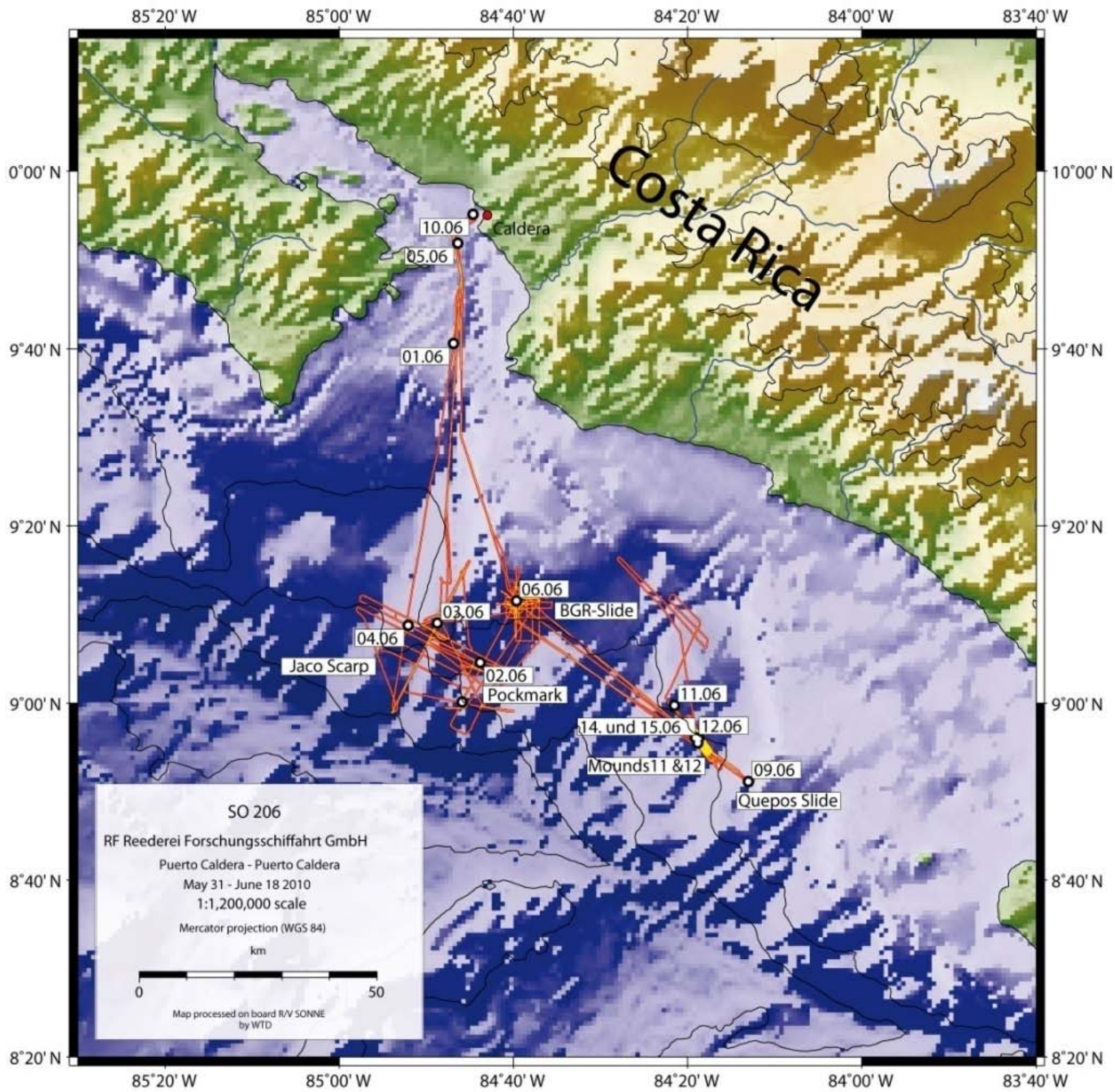


**Figure 4-1** Cruise plot of SO 206

# 5 Preliminary Results

## 5.1 EM 120 bathymetric and backscatter mapping

*(Sebastian Krastel, Ingo Klaucke, Ivonne Aden-Arroyo, Katja Lindhorst)*

Bathymetric mapping has been carried out with the Kongsberg multibeam echo sounder system EM120 hull-mounted onboard the RV Sonne (Figure 5-1). This system operates using sonar frequencies ranging from 11.25 to 12.75 kHz and that are split into up to nine (in deep water) different sectors with 191 beams per ping. Beam spacing can be either equidistant or equiangle with a maximum total swath of 150°. The ping rate only depends on the round trip travel time of sound in water. In addition to travel times, the Simrad EM120 also records the amplitude of the backscattered signal that is used to produce seafloor backscatter maps.

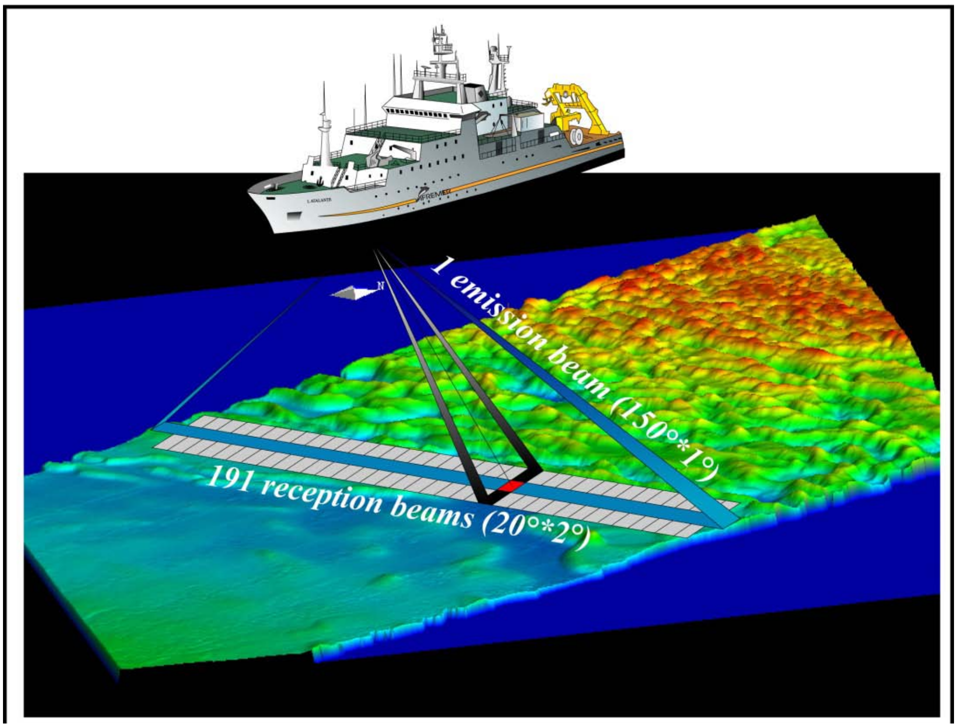


**Figure 5-1:** SIMRAD EM120 multibeam system (here shown on RV L'Atalante).

Most of the study area had already been mapped during various cruises in the past. Consequently, acquiring new bathymetry was not a major objective of this cruise. As seismic acquisition was generally carried out at low survey speed and with closely spaced survey lines, bathymetric grids were thought to be improved by choosing a reduced swath opening angle of 80°. While this produced good results in deeper water (roughly below 1000 metres water depth in this case), the overlapping footprints of the system in shallow water resulted in numerous side echoes and erroneous depth recordings (Figure 5-2). An additional dedicated bathymetric survey on the upper slope was consequently carried out with 120° total swath width.

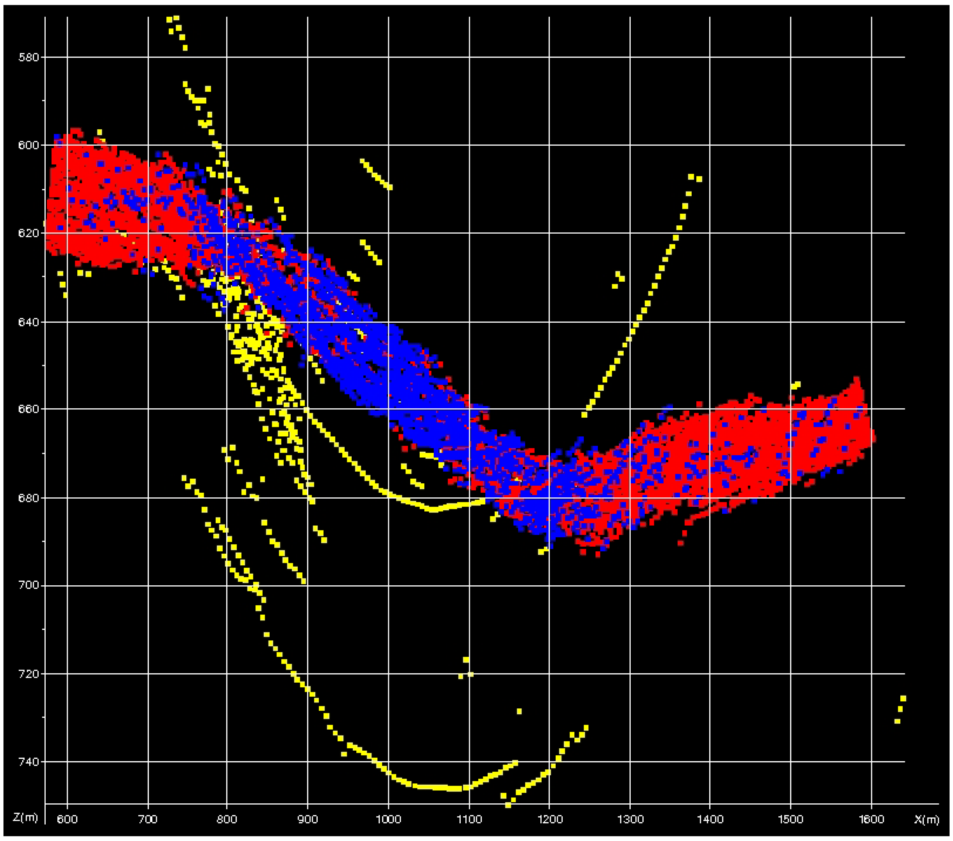


**Figure 5-2:** Bathymetric swaths showing erroneous curved soundings that are probably due to side echoes at narrow beam width in "shallow" water.

The raw bathymetric have been processed and edited onbord RV Sonne using the software package Caraibes for both bathymetry and backscatter mapping. The data are of generally good quality except for the above mentioned erroneous data due to side echoes and some miscalibration or inappropriate sound velocity profile (Figure 5-3). A sound velocity profile (Figure 5-4) has only been taken once at the beginning of the cruise and water column conditions might have changed during the duration of the cruise. The bathymetric data have been gridded with a grid cell size of 50 metres (Figure 5-5, Figure 5-6) except for the area of the BGR slide (Figure 5-7) and the area of mounds 11 and 12 (Figure 5-8), where a grid cell size of 25 and 10 metres, respectively, could be achieved. Backscatter data have been processed using the edited soundings and gridded at 25 metres, interpolated and finally filtered for speckle removal (Figure 5-9). The backscatter data underline coarse-grained deposits along sediment pathways and authigenic carbonate precipitates at cold seep sites that both produce high backscatter intensity.

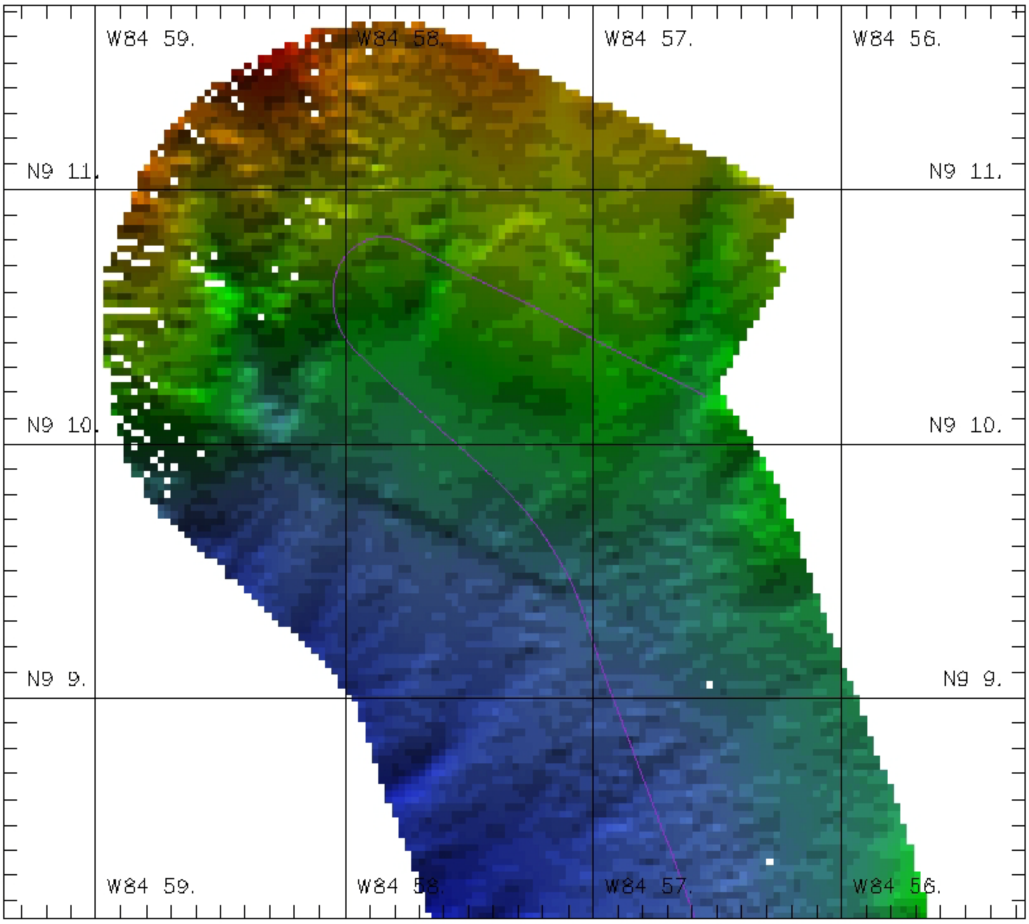


**Figure 5-3:** Mismatch between adjacent tracks.

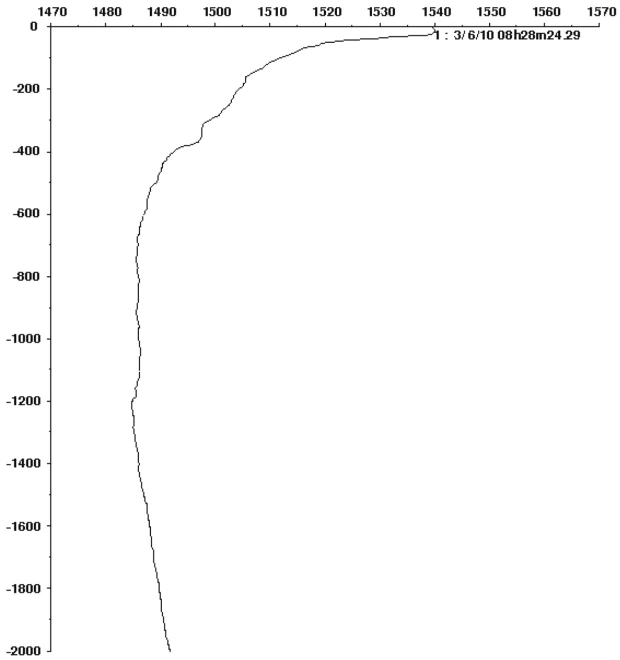


**Figure 5-4:** Sound velocity profile taken during SO206.

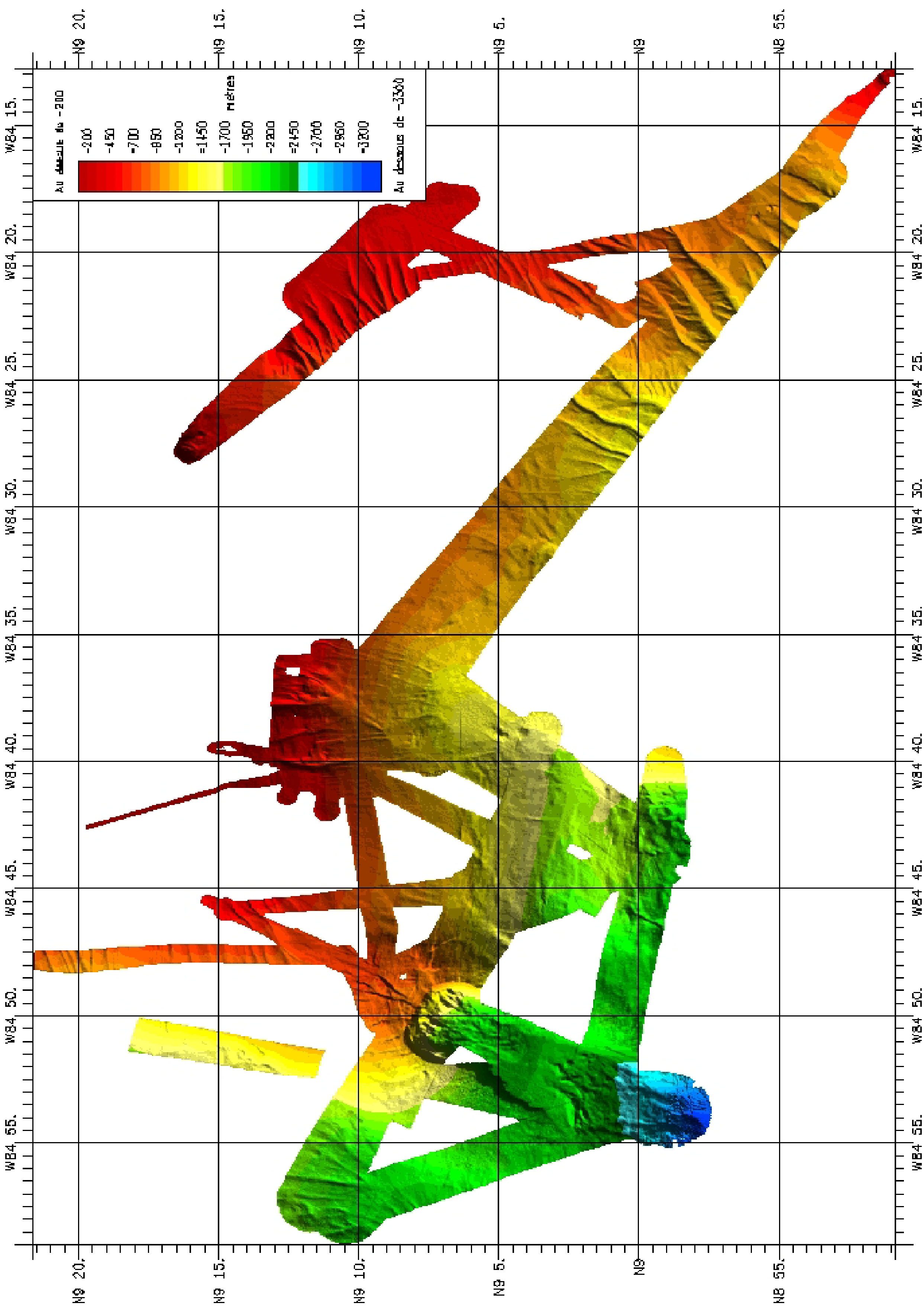


**Figure 5-5:** Shaded-relief map of the study area during SO 206. Grid cell size is 50 metres.

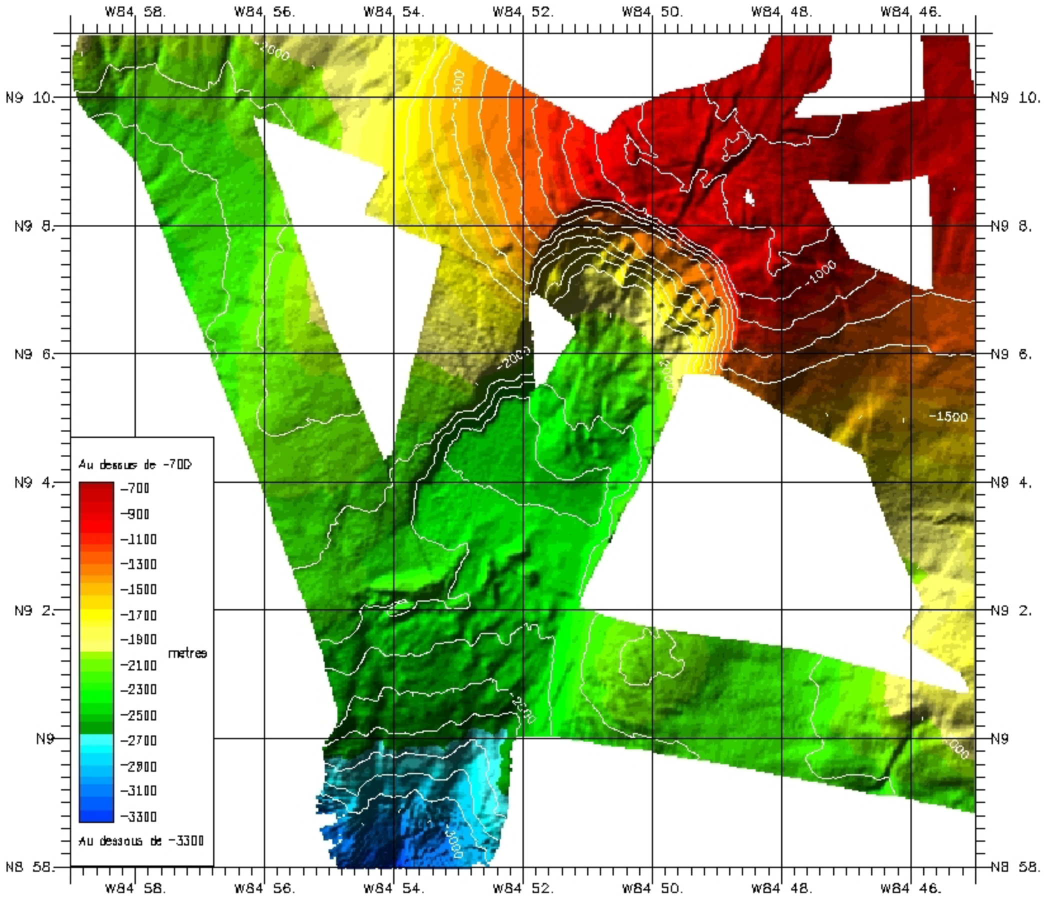


**Figure 5-6:** Shaded-relief map of the Jaco Scar area. Grid cell size is 50 metres.

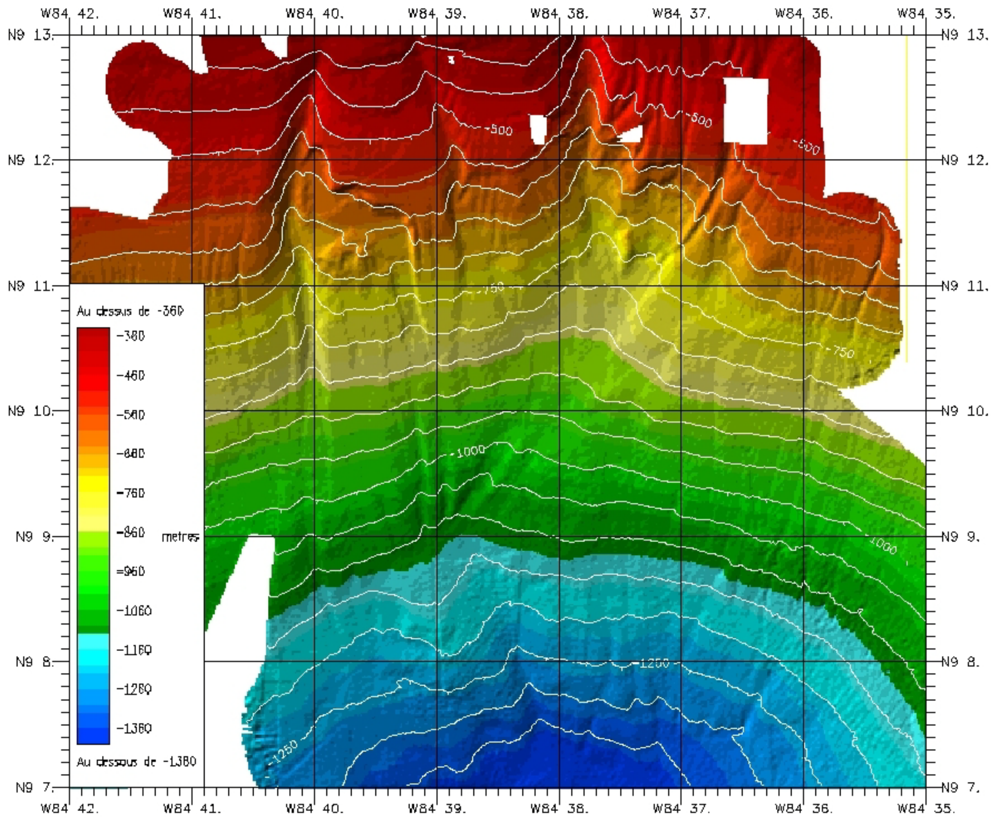


**Figure 5-7:** Shaded-relief bathymetric map of the area of the BGR slide. Grid cell size is 25 metres.

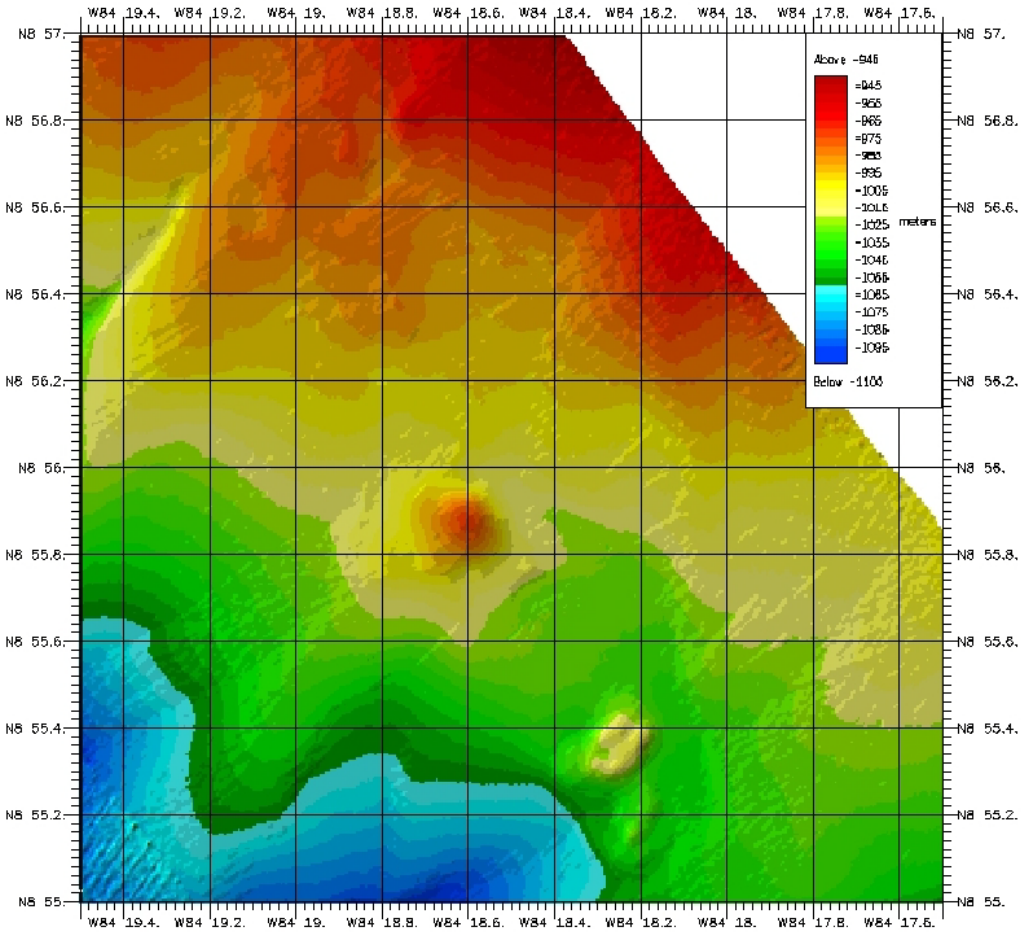


**Figure 5-8:** Shaded-relief bathymetric map of mounds 11 and 12. Grid cell size is 10 metres.

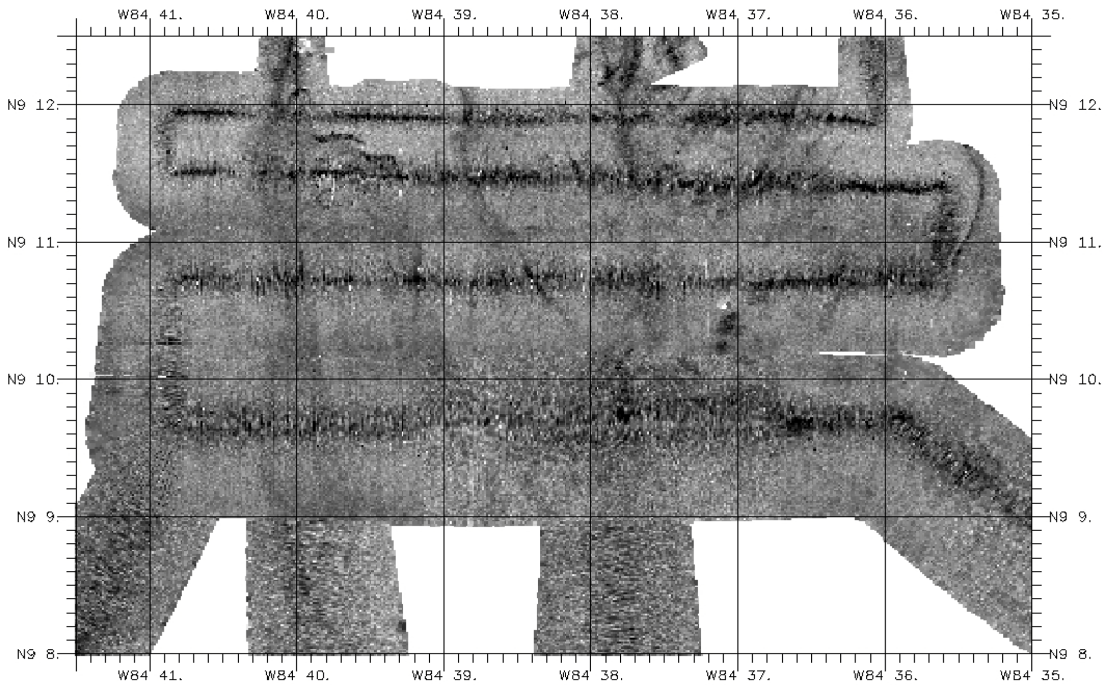


**Figure 5-9:** Multibeam backscatter map of the BGR slide area. High backscatter is dark underlining sediment pathways and possible fluid-escape structures at W84 37.0.

## 5.2 Sub-bottom profiling – Parasound

*(Sebastian Krastel, Ivonne Aden-Arroyo, Katja Lindhorst, Daniel Winkelmann)*

In parallel to the bathymetric mapping, the hull mounted parametric subbottom profiler Parasound P70 (Atlas Hydrographic GmbH, Bremen) was operated on a 24 hour schedule to provide high resolution information of the uppermost 50-100 m of sediment. Parasound P70 works as a narrow beam sediment echo-sounder, providing primary frequencies of 18 (PHF) and adjustable 18.5 – 28 kHz, thus generating parametric secondary frequencies in the range of 0.5 – 10 kHz (SLF) and 36.5 – 48 kHz (SHF), respectively. The secondary frequencies develop through nonlinear acoustic interaction of the primary waves at high signal amplitudes. This takes place only in the emission cone of the high frequency primary signals, which is limited to an aperture angle of only 4° for the Parasound P70. This is achieved by using a transducer array of 128 transducers on a rectangular plate of approximately 1 m² in size. Therefore the footprint size is only 7% of the water depth and vertical and lateral resolution is significantly improved compared to conventional 3.5 kHz echosounder systems. The fully digital system provides important features like recording of the 18 kHz primary signal and both secondary frequencies, continuous recording of the whole water column, beam steering, different types of source signals (continuous wave, chirp, barker coded) and signal shaping. However, many of the new features are still in an experimental state. Digitization takes place at 96 kHz to provide sufficient sampling rates for the high secondary frequency. A down-mixing algorithm in the frequency domain is used to reduce the amount of data and allow data distribution over ethernet. For the standard operation a parametric frequency of 4 kHz and a sinusoidal source wavelet of 2 periods was chosen to provide a good relation between signal penetration and vertical resolution. The 18 kHz signal was recorded permanently.

At the beginning of the cruise the system was operated in a Quasi-Equidistant-Transmission mode with EM120 depth as system depth. However, this mode caused major data gaps because wrong depth values resulted in a wrong pinging sequence. To overcome this problem, we operated the Parasound P70 with system depth obtained from the Parastore Post processing software both in Quasi-Equidistant-Transmission and single pulse mode. These settings caused regular ftp-errors between the different components of the Parasound system and a reboot of the entire system was necessary after such an error. Rebooting the entire system took at least 10 minutes causing major data gaps. Therefore we changed the pinging mode to a single pulse mode with manual system depth that had to be adapted constantly by the watch keepers about 200 m below PHF arrival. This mode worked very reliable.

All raw data were stored in the ASD data format (Atlas Hydrographic), which contains the data of the full water column of each signal as well as the full set of system parameters. Additionally a 300 m long reception window centered on the seafloor was recorded in compressed PS3 data and SEGY format with Phase and Carrier what allows processing with a standard seismic processing software (e.g. VISTA Seismic Processing). All profiles were first plotted with SeNT for Windows 7 to split the SEGY files into profiles. Processing included adding of delay, applying a wide band pass filter to improve the signal-to-noise ratio, stacking of 2 adjacent traces and writing a navigation file. All lines were then loaded to a Kingdom Suite Project. From these plots, a first impression of variations in sea floor morphology, sediment coverage and sedimentation patterns along the ship’s track could be obtained.

## 5.3 Seismics

*(Jörg Bialas, Sebastian Krastel, Dirk Klaeschen, Cord Papenberg, Ingo Klaucke, Ivonne Aden-Arroyo, Wiebke Brunn, Katja Lindhorst, Torge Matthiesen, Klaus-Peter Steffen, Patrick Schroeder)*

### 5.3.1 Seismic instrumentation

#### 5.3.1.1 Airguns

During cruise SO-206 three different airguns were available. One cluster with two 520 cinch G-guns, a GI-gun with 210 cinch and a GI-gun with 355 cinch. All guns were operated at 210 bar provided by the second stage compressor of R/V SONNE.

To improve the gun position information a GPS system was towed 2 m in front of the guns. Towing for the G-gun Cluster was 40 m behind the stern, while the GI-guns were towed at 20m offset (Figure 5-10).

Trigger signals were generated by an Ashtec AC12 GPS receiver, and an attached switch box. A wheel selector on the switch box was set to the desired shot interval. A SD card inside the switch box is used to store the NMEA string for each trigger signal. The trigger was distributed to the gun controller, the Geometrics streamer recording software, the Eiva navigation system and for secondary storage captured by a HyperTerminal.

Shot intervals were chosen to 60 sec for wide angle OBS records, 10 sec. For 2-D seismic operation with the G-guns, and 5 sec with the GI-guns.

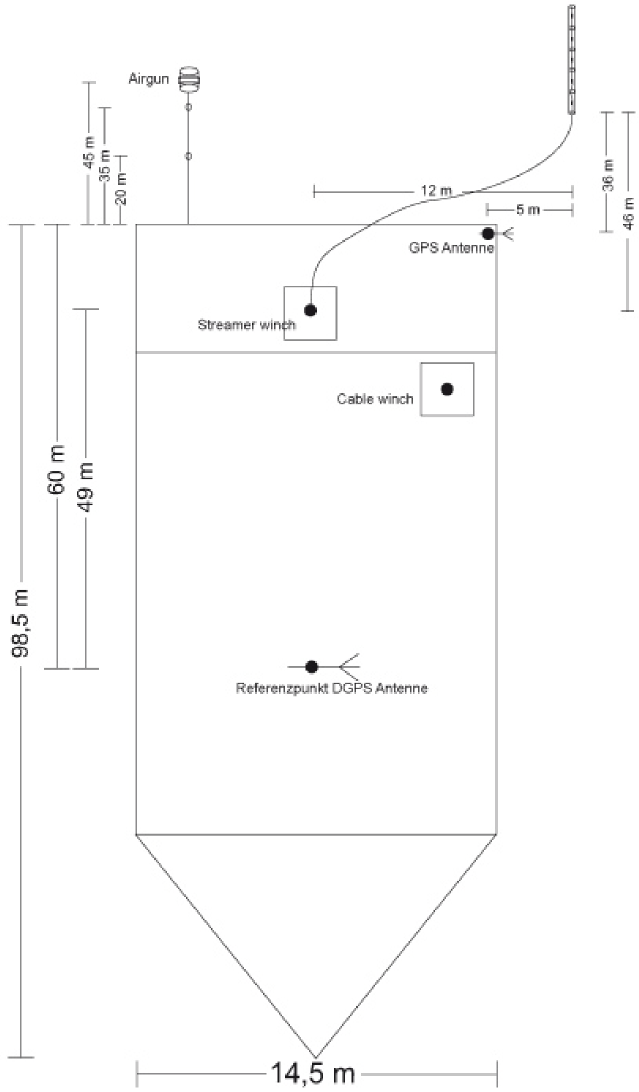


**Figure 5-10:** Drawing of the aft of R/V SONNE with the locations of the seismic systems Offsets are given in meters.

### 5.3.1.2 Navigation

Several Ashtec AC12 GPS receivers were set up to provide position information of the various systems. Onboard a GPS antenna was mounted on the port side airgun rail next to the stern of the ship (Figure 5-10). Additional GPS receivers were mounted on the airgun float, and the two trawl doors for the 3-D P-Cable system. NMEA strings from the remote GPS were transmitted via radio link onboard R/V SONNE. RS232 links submitted the position information to the Eiva system. Additional backup for the online data processing was done through HyperTerminal capturing (Figure 5-11).

Although the GPS receivers were setup with same parameters two of them showed unstable position delivery. For unknown reasons the system could track only two satellites over shorter or wider time spans, sometimes the tracking was lost for several hours. At the same time a third receiver on the second trawl door and the shipboard receiver behaved well.

With the P-Cable system the streamer sections are not distributed along a straight line. Due to drag forces in the water the cross cable can best be described forming a shape somewhere between a triangular and a half circle. Navigation processing sets out to calculate the exact shape by using the GPS positions of the trawl doors and the first arrival time of the direct wave from the airgun signal. During the course of profiling the trawl doors were effected by water currents and sea state. Therefore offsets between starboard and port side door and the airgun in the centre are varying depending on the heading of the sail line (Figure 5-12). Based on GPS positions of the trawl doors and the first arrival of the airgun shots at the streamer hydrophones the position of each streamer segment is calculated. Triangulation is applied and provides coordinates for the streamer groups within a range of less than 5 m. The assumption of catenary shaped outline for the cross cable provides best results (Figure 5-13). Based on the resulting shot table interpolation, stacking and migration of the entire data cube can be done. For the raw processing onboard R/V SONNE a migration grid of 6.25 m * 6.25 m could be achieved.

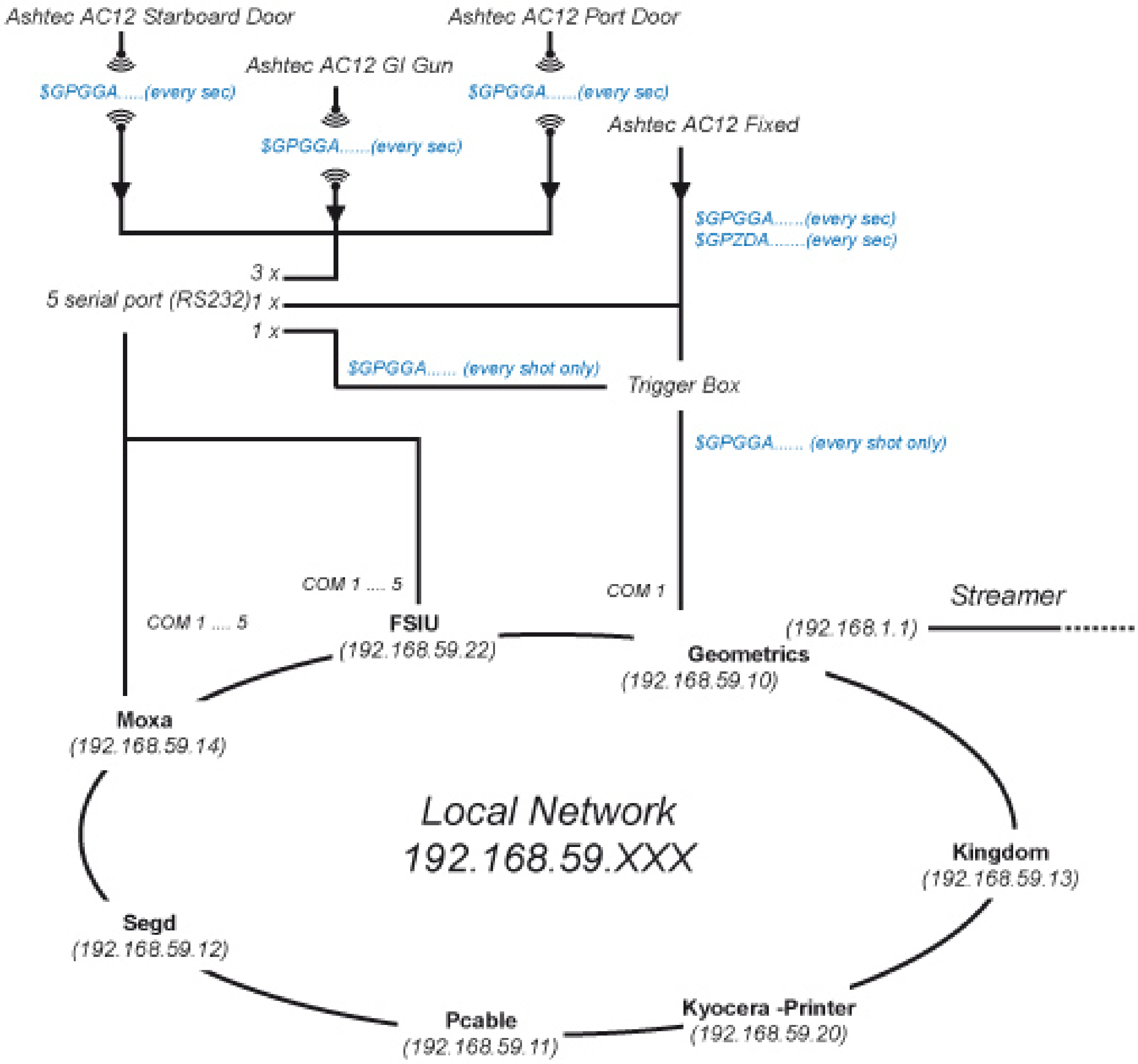


**Figure 5-11:** Data flow diagram of the seismic navigation system onboard R/V SONNE during SO-206.

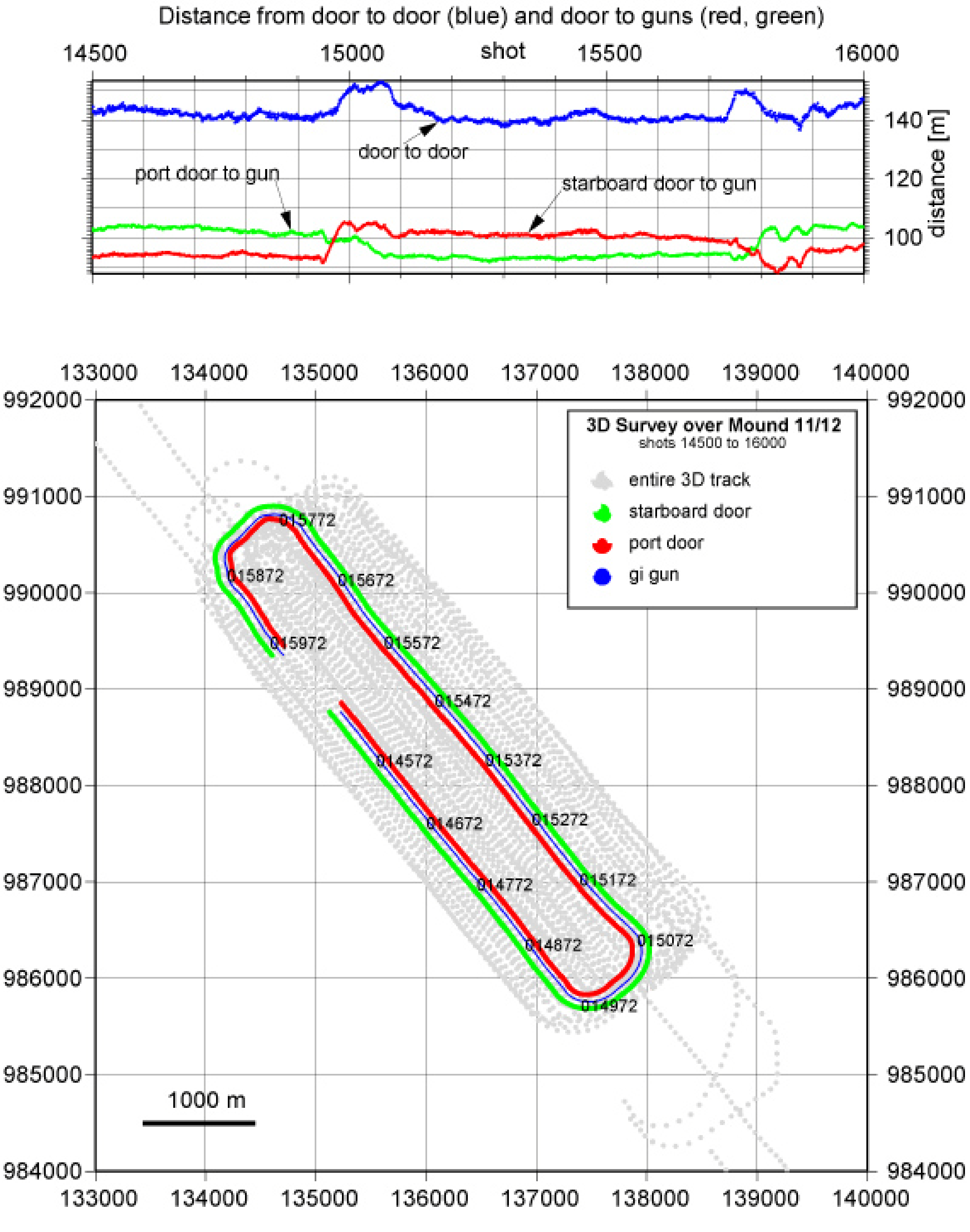


**Figure 5-12:** Track plot of trawl doors and gun during the 3-D seismic profiling Water currents and sea state influence the sail line of the trawl doors and cause varying offsets between airgun and doors during the course of profiling.

### 5.3.1.1 MCS Streamer 2-D and 3-D mode

For the multichannel seismic data acquisition a Geometrics GeoEel streamer system was available. The streamer sections were build by two hydrophones per group, each group separated by 1.5 m. Eight groups are included in one 12.5 m long streamer section, which is controlled by an eight channel A/D converter bottle. As the same system is used for the 3-D P-Cable acquisition system the A/D bottles need to be manually reconfigured for 3-D application. 19 streamer sections and A/D converter were available. Three of the sections were returned from a previous application with traces of damages, that could not be tested in the institute before shipping. Inspection onboard showed that only 16 sections were available for recording. During the cruise damages occurred in one tow cable and salt water penetration happened into one section. Both events did cause a sever short cut in the SPSU onboard controller and its spare unit. Intensive telephone and email correspondence with the manufacturer did not help to fix the failure with available spare parts. As the operation area is within a few hours off port of Caldera it was decided to fly in a technician with additional spare parts. During one day of inspection and repair both SPSU streamer controller could be activated again and the seismic work could be continued. The sensibility of the controllers to seaward short cuts is reported to be known by the manufacturer and additional security circuits are under development but were not available for the two IFM-GEOMAR systems.

During 2-D profiling three GeoSpace Navigator birds were attached to the 200 m long streamer providing a towing depth of 3-4 m.

For the 3-D P-Cable application the streamers were reconfigured for parallel connection along a cross cable (Figure 5-13). Two trawl doors were deployed spanning the 180 m long cross cable rectangular to the ships course. With trials of two different lengths of the trawl wires and after repair of the cross cable the width between the two trawl doors varied between 120 m and 145 m (Figure 5-13).

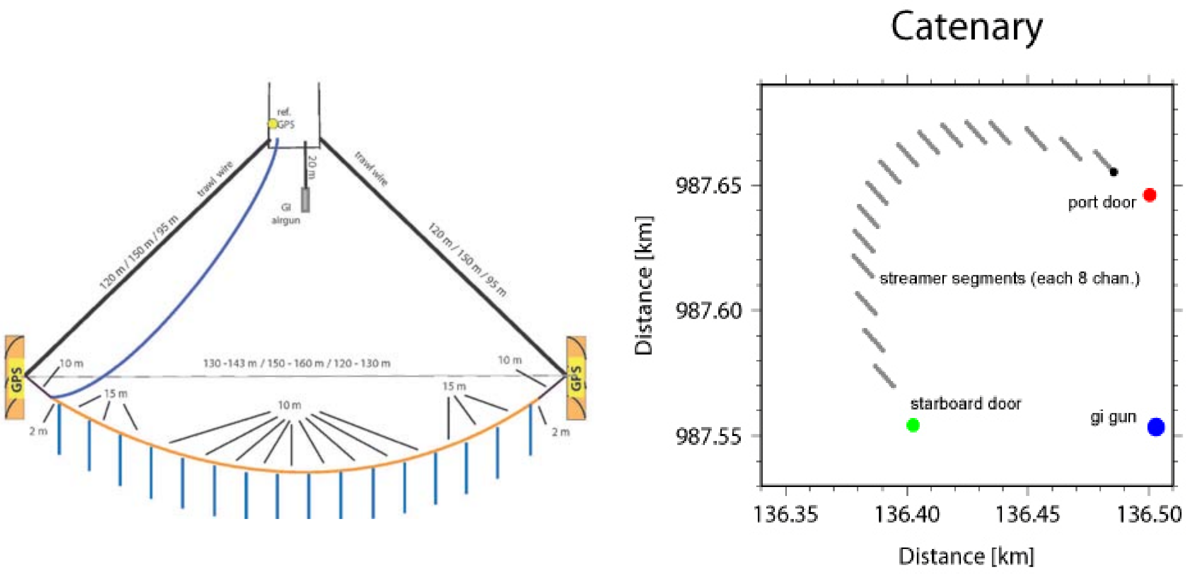


**Figure 5-13:** Triangulation of the P-Cable 3-D streamer setup in the water Depending on drag forces in the water and the pull of the trawl doors the stretch of the cross cable will deviate from a straight line. Expecting the shape of the cross cable to follow the behaviour of a catenary seems to be the best assumption.

### 5.3.2 Results

#### 5.3.2.1 Jaco Scarp and Pockmark area

Jaco Scarp is located southwest of Port of Caldera. A prominent head wall shows up at about 1000 m water depth with heights of more than 1000 m. A Parasound profile crossing the scar in a downslope direction is shown in (Figure 5-14). The penetration depth along the profile is limited due to the rough topography. However, the steep head scrap, some slide blocks along the upper part of the profile, and slide deposits indicated by transparent units in the deeper part can be observed.

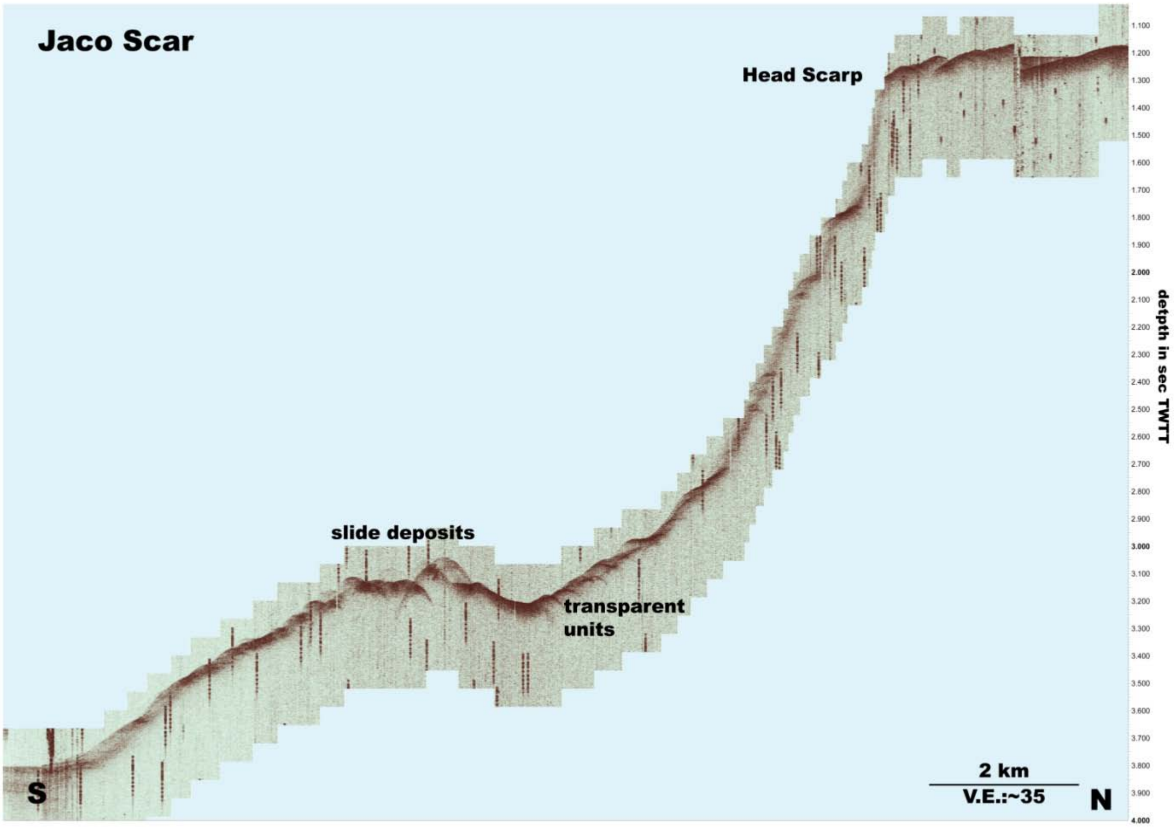


**Figure 5-14:** Parasound profile crossing Jaco Scarp in a downslope direction.

To further support the IODP drilling proposal at Jaco Scar several seismic profiles were scheduled crossing the drill locations in various directions. At the same time 6 OBS were deployed to provide wide angle offset records, which will be used for a velocity depth model. The seismic profiles were sailed two times, first with a shot interval of 60 sec. To avoid increased noise levels on the OBS records, and a second time to serve for a suitable MCS coverage by the 2-D streamer (Figure 5.15). As the goal of the survey was to cover the upper 1 km of sediment shots were provided by the G-gun cluster.

Onboard processing of the seismic lines already provided constant velocity Post-Stack Migration data. Clear images of the Jaco Scar structure can be traced to 500 ms TWT. Comparison with the profile SO81-13 (Figure 5-16) shows the increase in resolution with the new data set at shallow depth. All OBS were successful recovered and provided good data. Refracted events were recorded over the complete length of the profile and should provide the required velocity depth information of the upper 1 km of the seafloor (Figure 5-17).

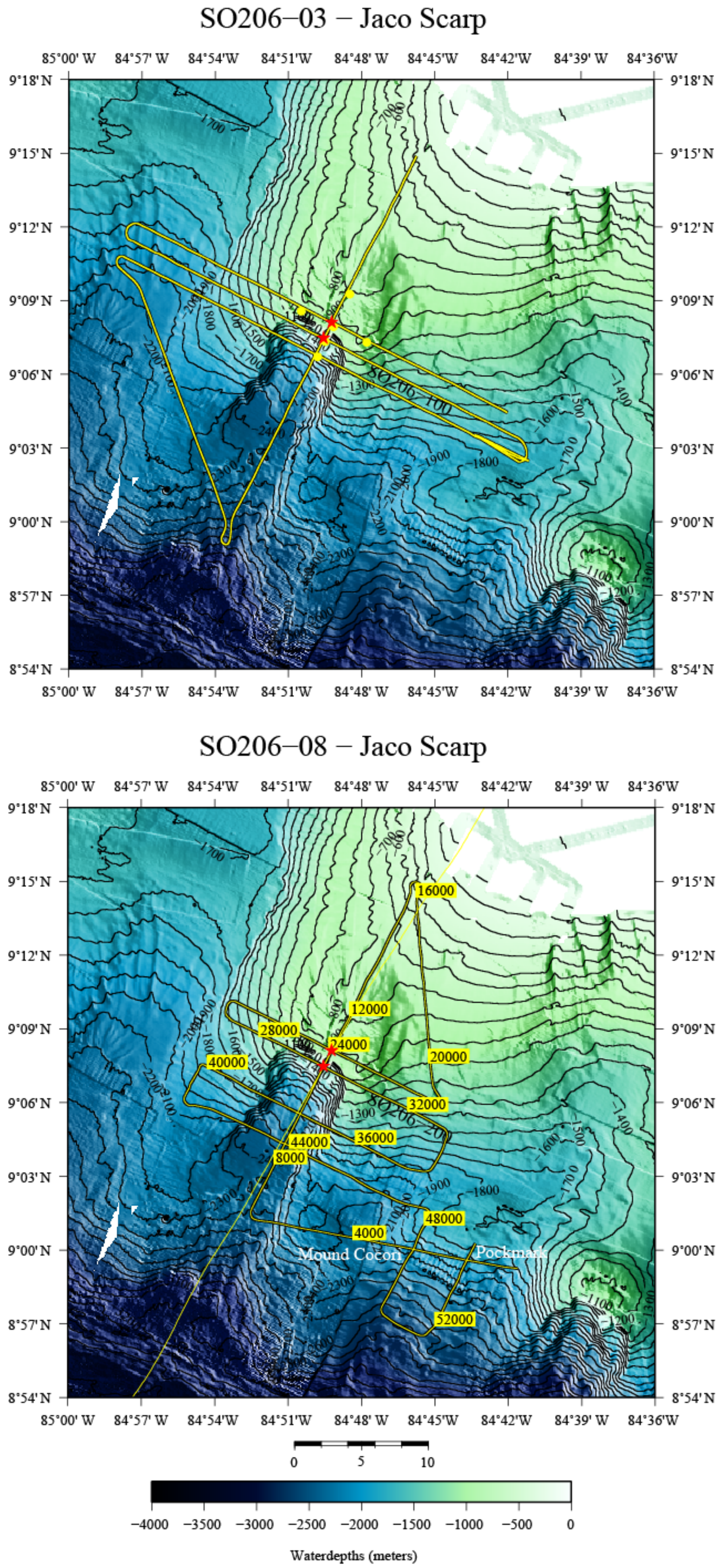


**Figure 5-15:** Upper panel: OBS locations and seismic profile over jaco scarp (60 secs shot interval). Lower panel: MCS profile over Jaco Scarp an adjacent seep locations.

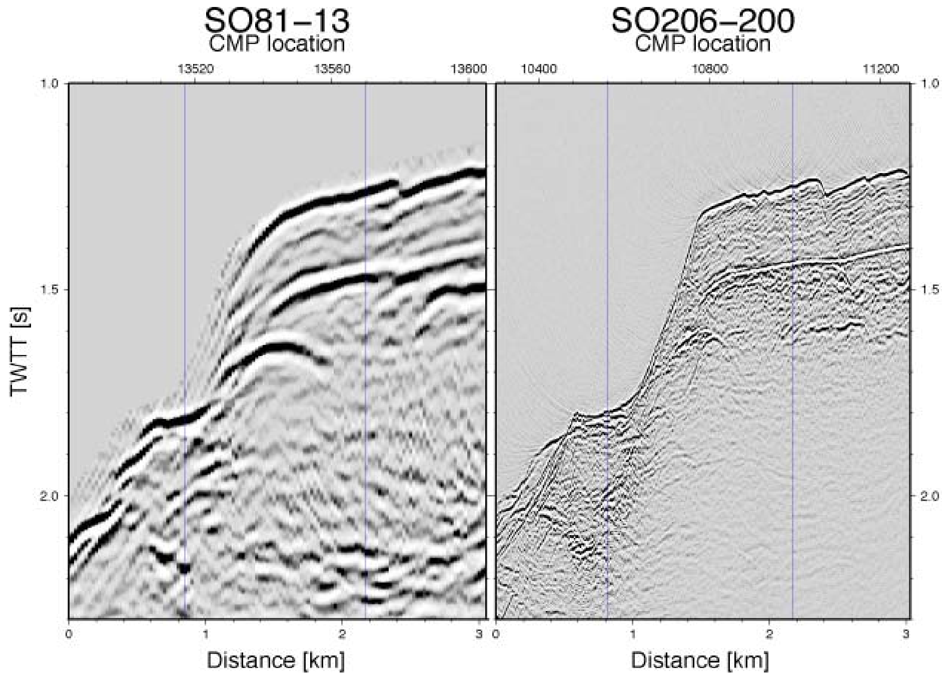


**Figure 5-16:** Comparison of seismic data sampled across Jaco Scar – left: deep penetrating MCS data collected during SO-81 – right: new high resolution data acquired during SO-206.

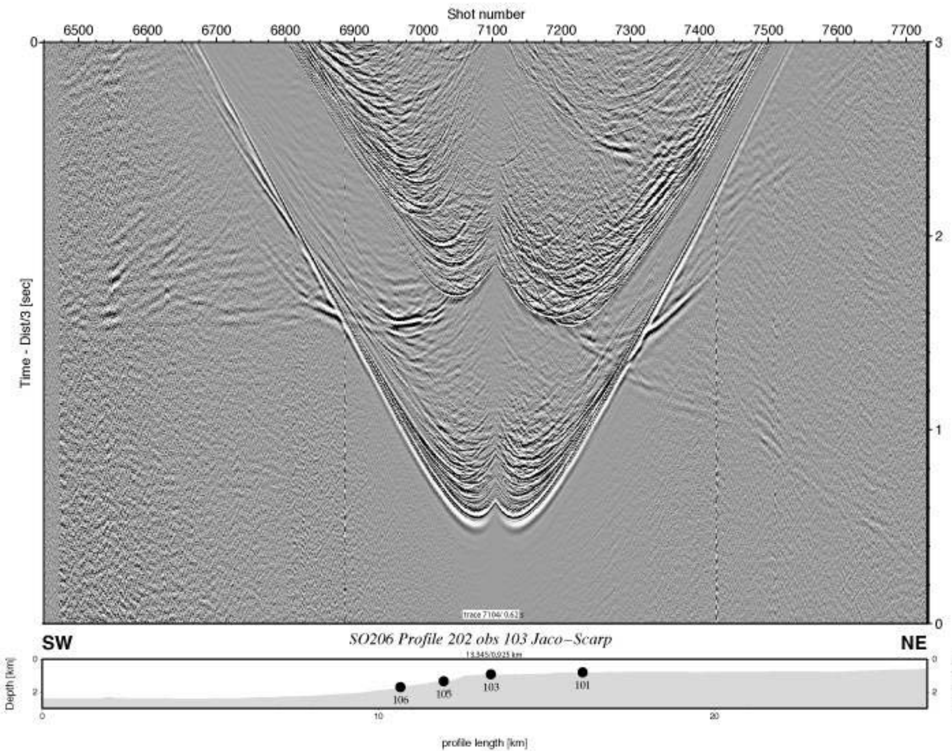


**Figure 5-17:** Seismic section of OBS 103 along seismic line 200-13 Section is reduced at 3 km/s. Refracted events are clearly visible across the entire profile length.

In the course of the MCS profiling additional profiles were shot across the Pockmark structure and a second, yet unclear image, identified in the Sidescan map. Both structures are underlain by an interrupted BSR reflection. Underneath the Pockmark the BSR is slightly uplifted and discontinuous where the feeder channel for the upward migration of fluids is expected (Figure 5-18).Underneath the second structure the BSR is clearly interrupted and bended upward. It is missing underneath the structure (Figure 5-19). The upward bending of the BSR reflection is much more pronounced and interpreted as indication for more intensive upward migration of warm fluid flow from below modifying the pressure and heat relation, avoiding the formation of gas hydrates. In the online Parasound image lateral limited flow structures were observed. Together with the positive seafloor anomaly this might be interpreted as a mud volcano. Clasts found in a gravity core from this site (see section 5.4.2.1) further support this interpretation.

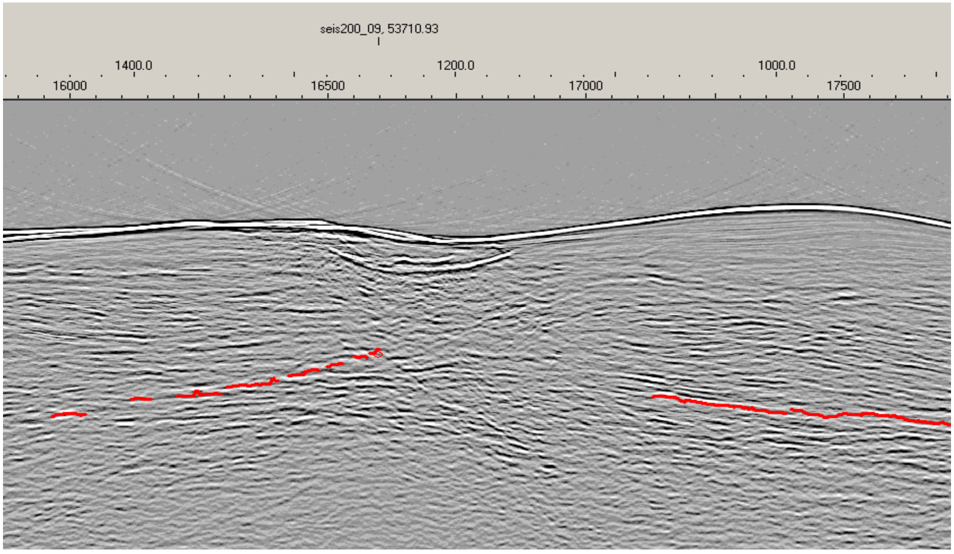


**Figure 5-18:** 2-D MCS section across the Pockmark structure. The BSR is interrupted underneath the structure and might continue in various length elements.

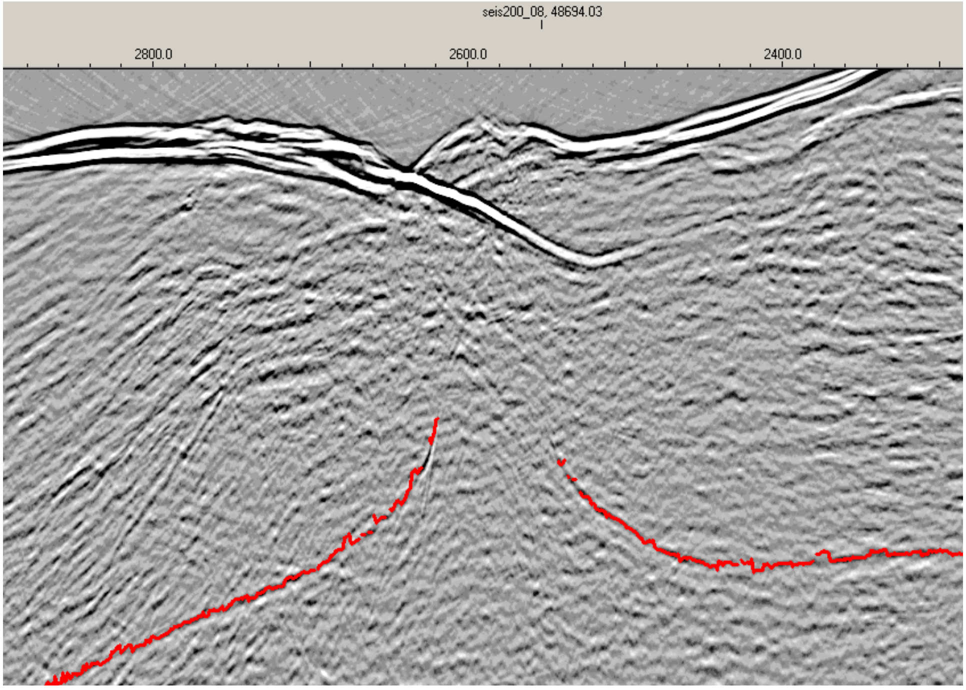


**Figure 5-19:** 2-D MCS section across the mud volcano west of Pockmark. The BSR is interrupted underneath the structure. Upward bending of the BSR underneath the mud volcano indicates upward migration of warm fluids and hence a reduced hydrate stability field.

#### 5.3.2.2 Mound 11/12

A Parasound profile crossing mounds 11 & 12 is shown in Figure 5-20. The mounds interrupt well stratified sediments. No sub-bottom penetration is reached beneath the mounds indicating the occurrence of free gas.

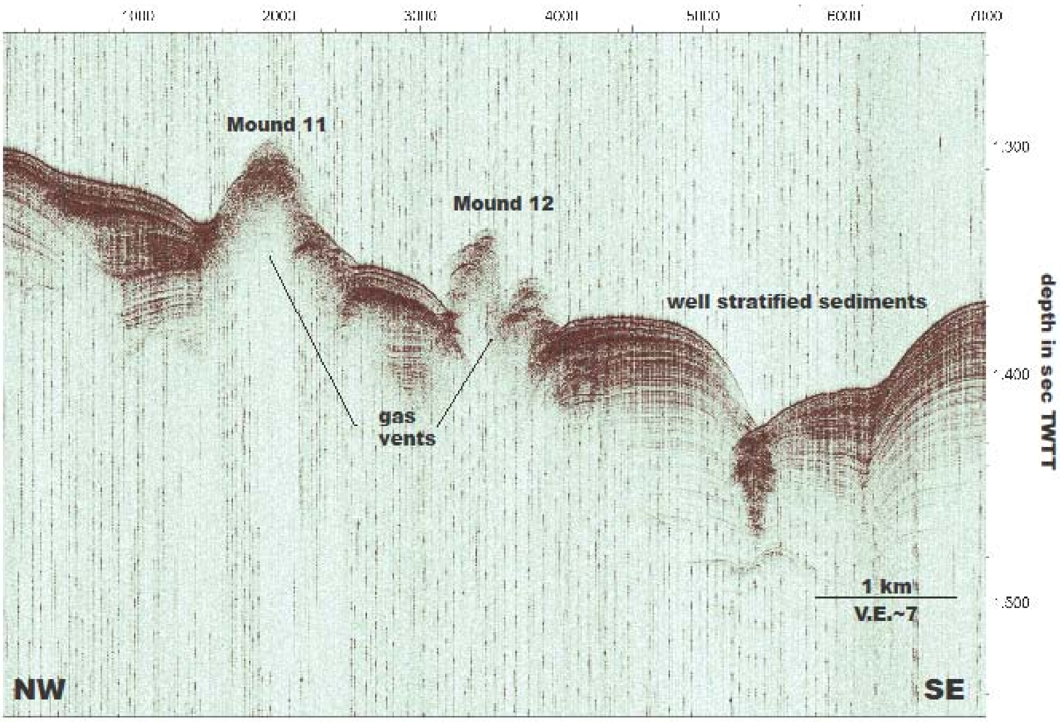


**Figure 5-20: Parasound profile crossing mounds 11 & 12.**

The area of mounds 11 & 12 was chosen for the 3-D seismic survey (Figure 5-21). Although the BSR as indicator for a high level of free gas accumulation is widely spread all along the Costa Rican margin during more than 10 years of continuous research no active gas expulsion has been observed here. With their exposed bathymetric structure the mounds are a prominent indicator for upward migration of ocean sediment material. High resolution study of their subsurface structure should indicate if single or multiple feeder channels can be imaged and how they are distributed. Vertical cuts along and across the 3-D data cube reveal the internal structure of mound 11 & 12 (Figure 5-22). Clearly visible is the interruption of the reflecting layers underneath the structures. Cuts through their centres reveal upward bending reflection events, which indicate upward material flow (Figure 5-22). The internal structure of the mounds should be compared with seeps or mud volcanoes, found in other margins of the world, which act as migration pathway for fluids. Cold seeps were mostly found along active acreational margins like the Hikurangi Margin in New Zealand and are associated with various types of pathways guiding fluids through the hydrate stability field. Mud volcanoes on the other hand are examples of vertical material transport from greater depth to the seafloor. Examples form the Mediterranean coast of Egypt or the Crimean Peninsula in the Black Sea have been found to be active not only during periods of mud movement. Gas expulsion and transport from greater depth has been reported in both areas, independent of a hydrate stability layer.

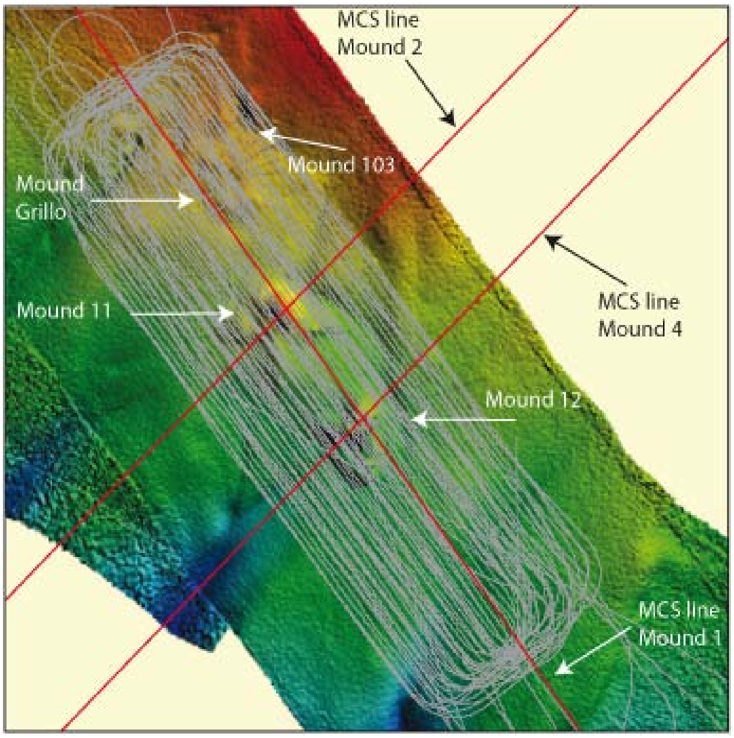


**Figure 5-21:** 3-D MCS profile track crossing Mounds 11 and 12. Grey: ships course during the SO-206 3-D data acquisition. Red: MCS track lines of R/V LANGSETH.

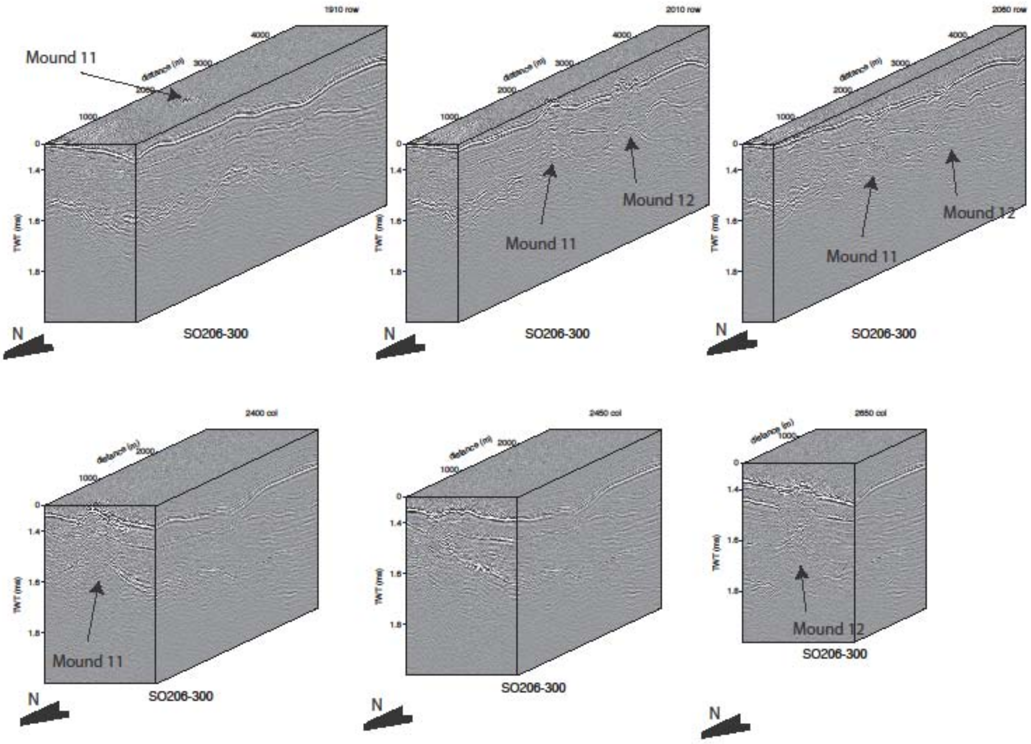


**Figure 5-22:** 3-D view of the subsurface structure at Mounds 11 and 12 recorded with the P-cable system.

#### 5.3.2.3 BGR-Slide

The BGR-Slide and additional smaller slides are located in an area north of the Jaco scar. Previous investigations showed that these slide events are relatively young. Headwalls are typically found in about 600m water depth. This depth roughly corresponds with the upper limit of the gas hydrate stability zone. Hence it was suggested that the failures are closely related to the occurrence as or the formation and/or dissociation of gas hydrates in this area. A BSR is clearly imaged in greater water depth close to these slides. Hence gas hydrates are widespread at this part of the margin. The main motivation of the additional investigations during SO206 was to further study a possible genetic link between gas hydrate occurrence and slope (in)stability.
A dense net of Parasound profiles were collected across this structure. A typical example is shown on (Figure 5-23). The area above the headwall is characterized by well stratified sediments. These sediments onlap an older surface. Varying accumulation rates might suggest that contour currents played an important role for the deposition and re-deposition of sediments in this area. The headwall cuts the well stratified sediments. Headwall height is ~40m. The area immediately beneath the headwall seems to represent the glide plane of this slide not covered by significant slide deposits or a post slide sediment drape. Further downslope, chaotic to transparent slide deposits indicate the main depositional are of this slide. The data image deposits of more than one slide events. Several cores were taken along this profile (see section 5.4.2.4).

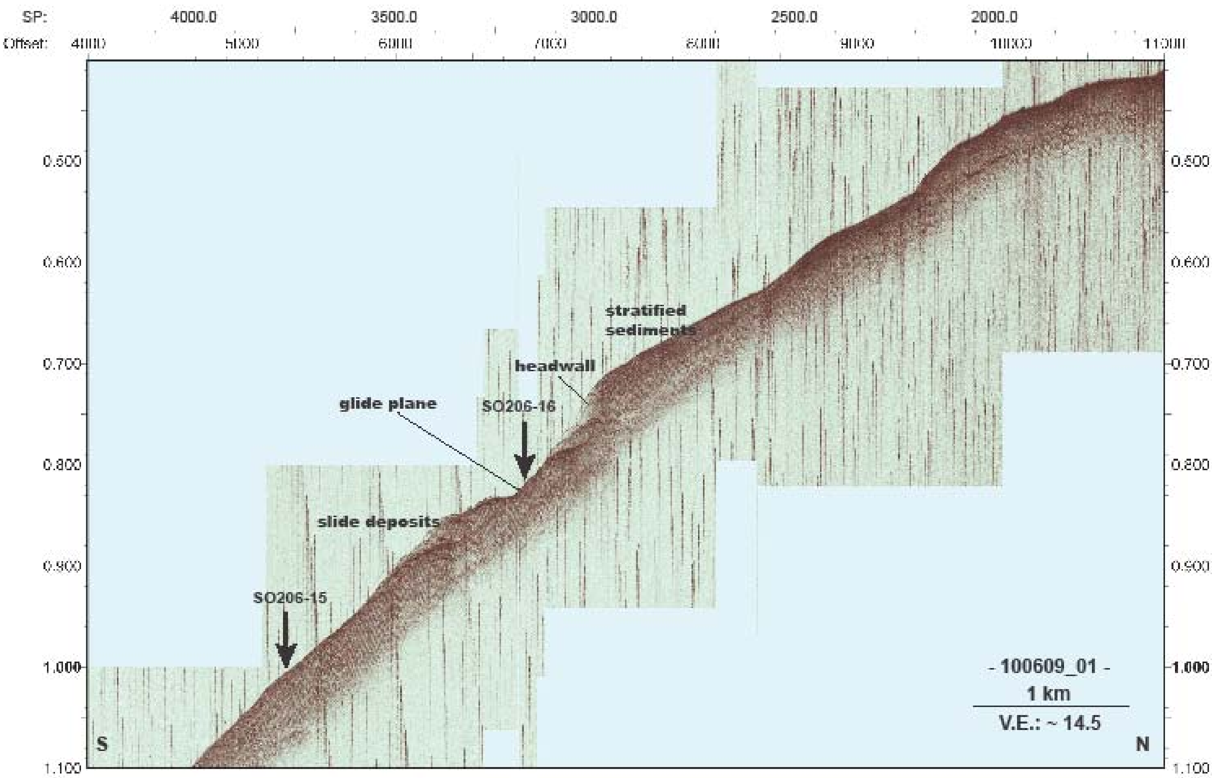


**Figure 5-23:** Parasound Profile crossing the headwall scar of the BGR slide.

The BGR slide area was target of two seismic surveys. During the first survey (P300) 6 OBS were deployed along two perpendicular lines with distances between the instruments of 1000-1600m. Airgun shooting with a 1.7l Gig-Gun was along the two main OBS-lines and numerous additional lines across all OBS-stations (Figure 5-24).

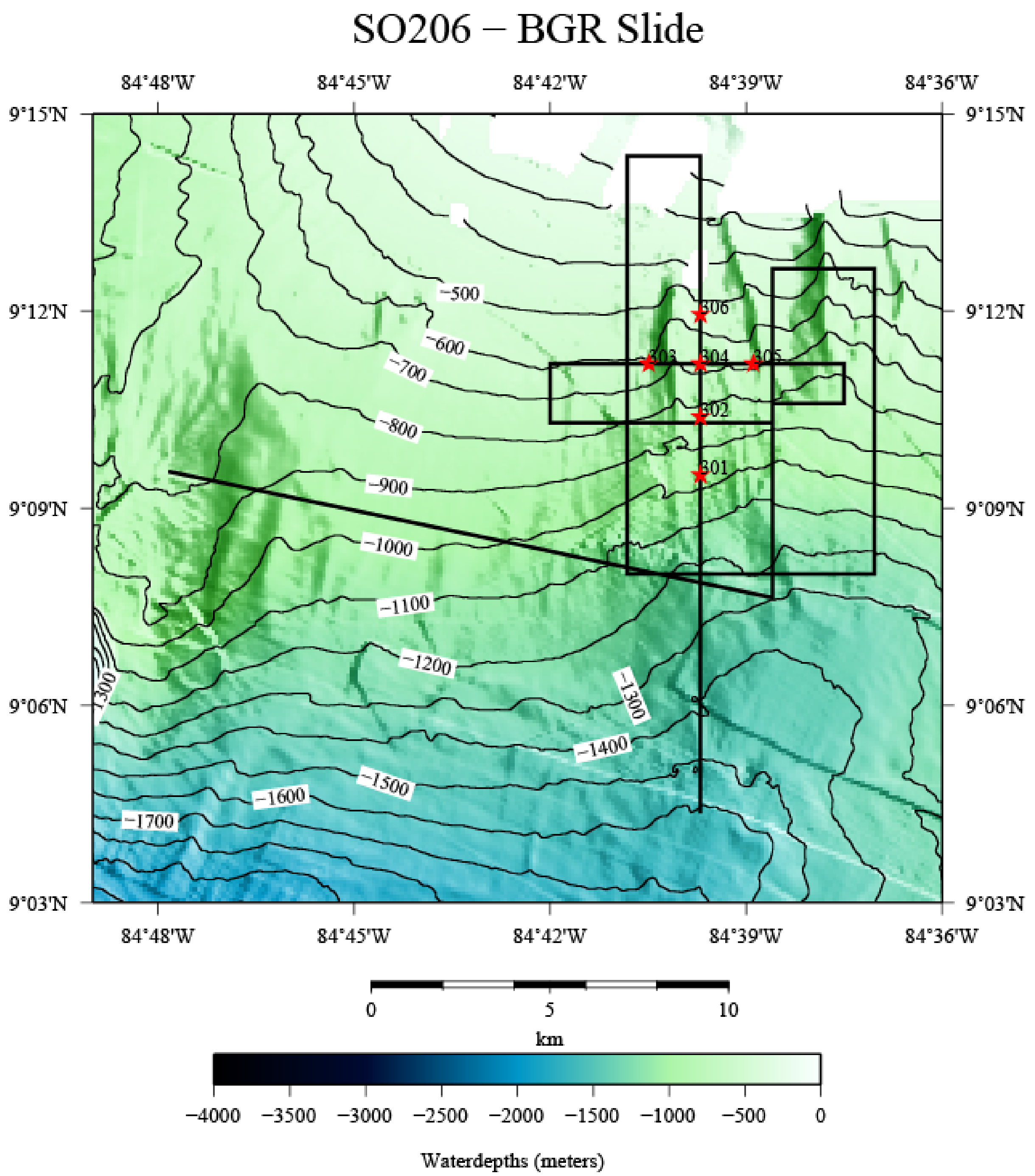


**Figure 5-24:** OBS locations and MCS-profile over BGR slide.

Due to the damage of the SPSU, no streamer was available at that time. The main motivation of this survey was a mirror imaging in order to produce a structural image of the subsurface. An example of the migrated mirror images along a slope parallel line is shown in (Figure 5-25).

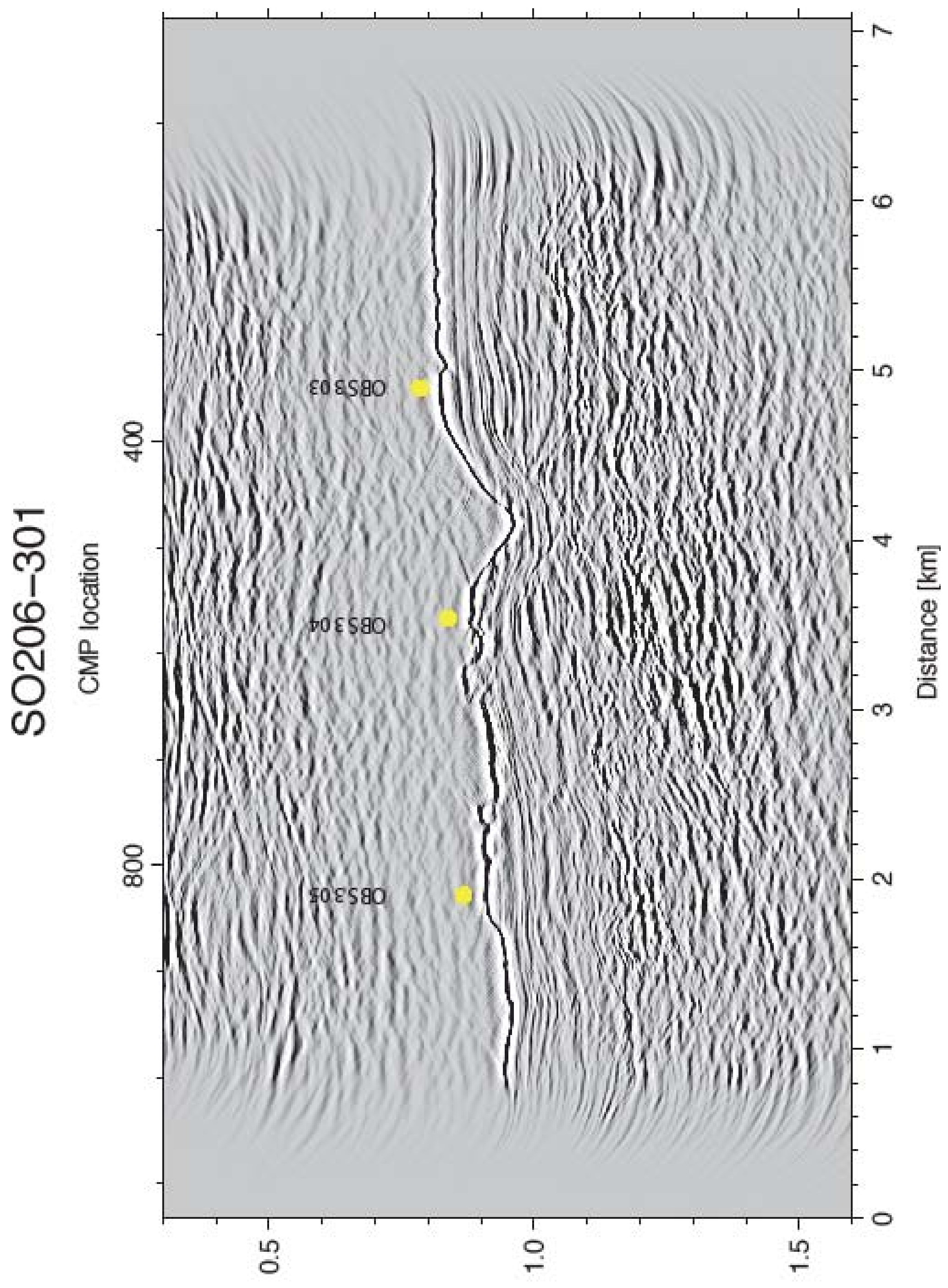


**Figure 5-25:** Migrated mirror image along a slope parallel line.

Close to the end of the cruise, additional reflection seismic data with the GeoEel streamer and a 1.7l GI-Gun were collected along several lines (Survey P500) (Figure 5-24). A 100m-long 64 channel streamer was used during this survey. In total we collected 100km of profiles during a 16h long survey. In addition several seismic lines were collected across numerous slide events. The new line shows a complex pattern of faulting, erosion, as well as deposition and redeposition of sediments (Figures 5-26, 5-27). The final line to the west connects the new data with deep seismic data (Line BGR99-059) collected by the BGR in 1999 and a new line of Cruise SO206 across the Jaco scar. A BSR is clearly visible on these lines. A careful analysis of the new net of seismic data will be used to investigate the role of gas hydrates for slope failures in this area.

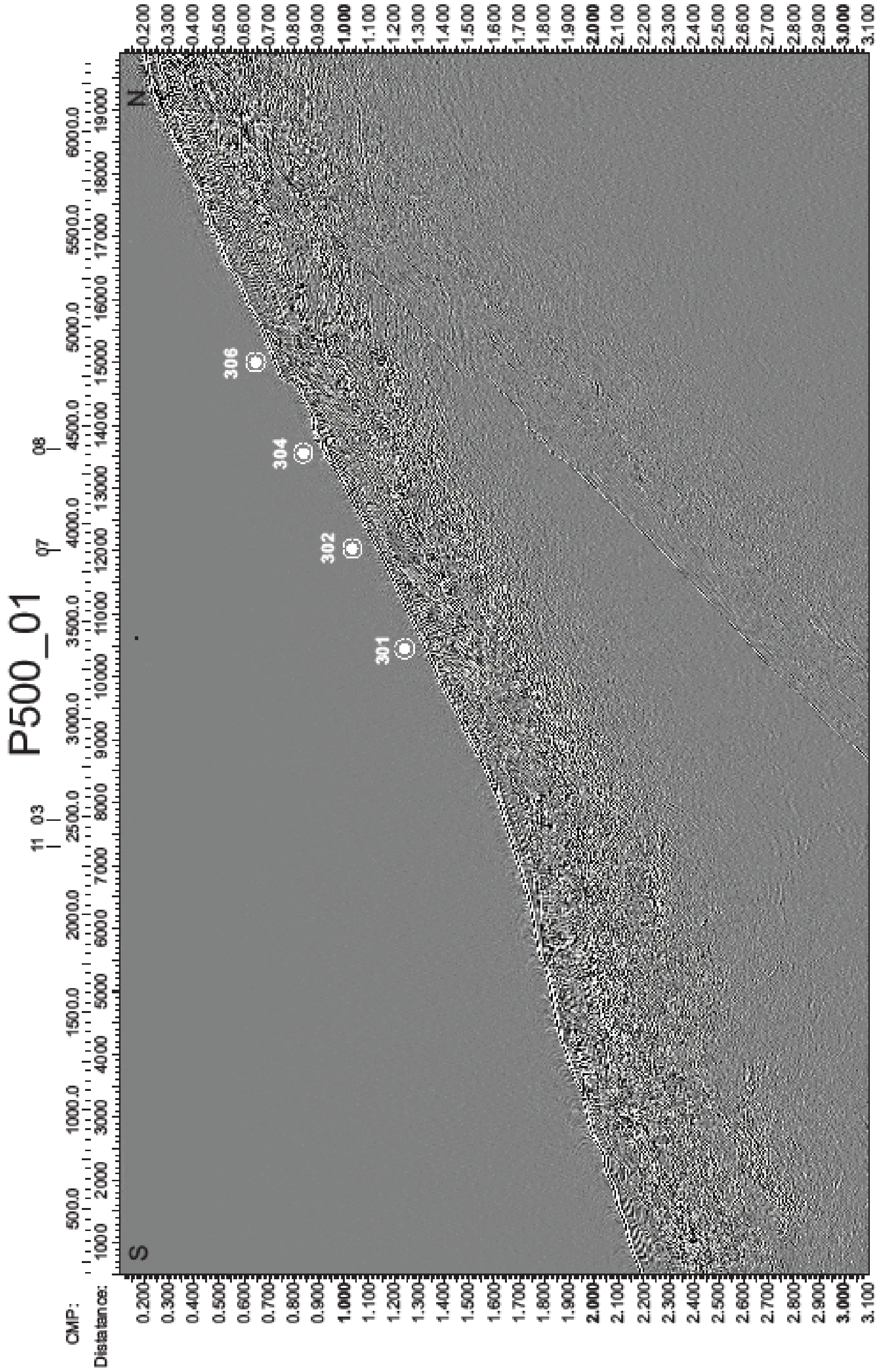


**Figure 5-26:** Reflection seismic profile P500_01 crossing the headwall area of the BGR slide. The OBS-locations of deployment P300 are shown as well.

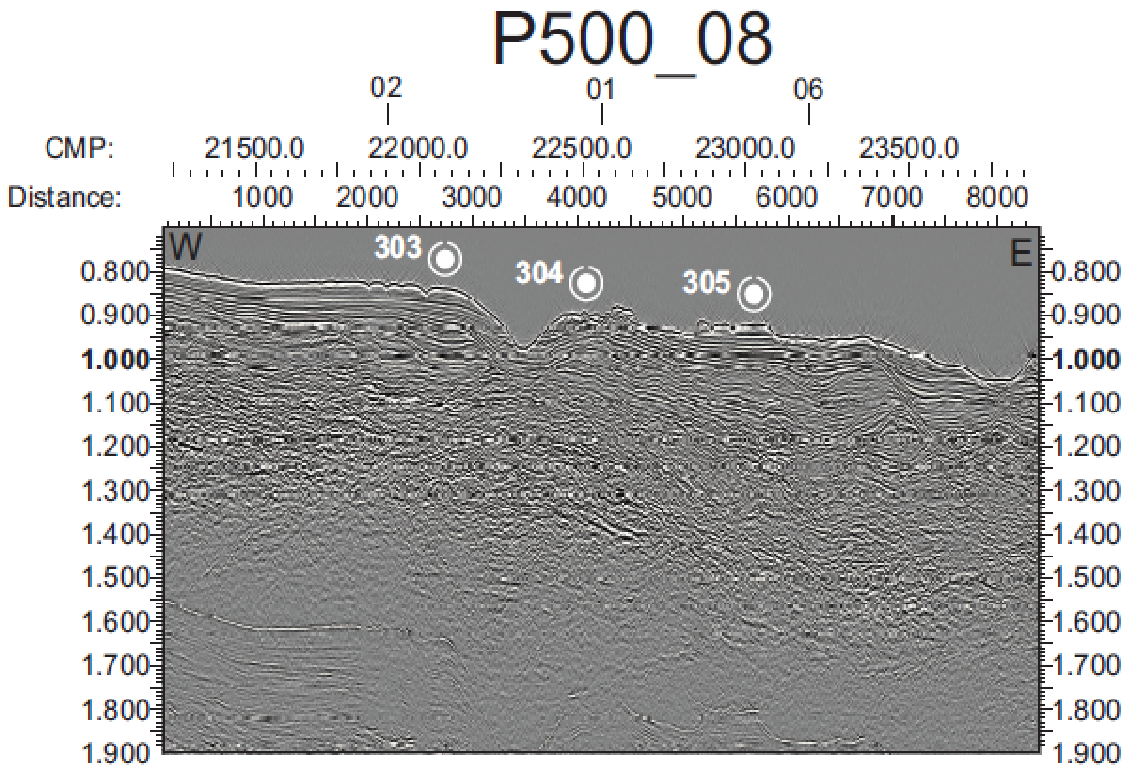


**Figure 5-27:** Reflection seismic profile P500_08 running along slope across the BGR slide. The OBS-locations of deployment P300 are shown as well.

## 5.4 Sedimentology

(*Daniel Winkelmann, Andrea Anasetti, Maik Lange, Christian Hensen)*

### 5.4.1 Geological Sampling

The sediment sampling program during SO206 focused on two topics: i) the recovery of surface sediments and long gravity cores from cold seeps for detailed geochemical analysis and ii) the recovery of long gravity cores from submarine slope failures at the upper continental slope. Both topics aim in concert with the seismic and hydro-acoustic investigations on understanding of the fluid flow and its impact on the slope stability of the active continental margin offshore Costa Rica.

Sediment sampling of cold seeps (i) was accomplished by application of the TV-equipped multicorer (TV-MUC, Figure 5-). The synoptical investigation of the targeted seafloor via online TV allowed the controlled placement of the corer into desired spots on site. In addition, a 5m gravity corer was used for recovery of long cores. Both coring systems were equipped with an additional Posidonia acoustic positioning system to detect their precise position over the sea ground. A complete overview of all sampling stations is presented in Figure 5-29.

In total, 19 cores (62,37 m) were recovered (Table 5-1). 41,67 m were opened and investigated aboard. The cored sediment is dominated by terrigenous silt with small proportions of clay. Abundant carbonaceous shells of foraminifers, bivalves and gastropods were found in most core sections. Authigenic carbonate precipitation in form of nodules and/or more diffuse aggregates were found at sites of higher fluid flow. Gas hydrates containing methane were cored from these sites too (Pockmark and Mound 11/12).

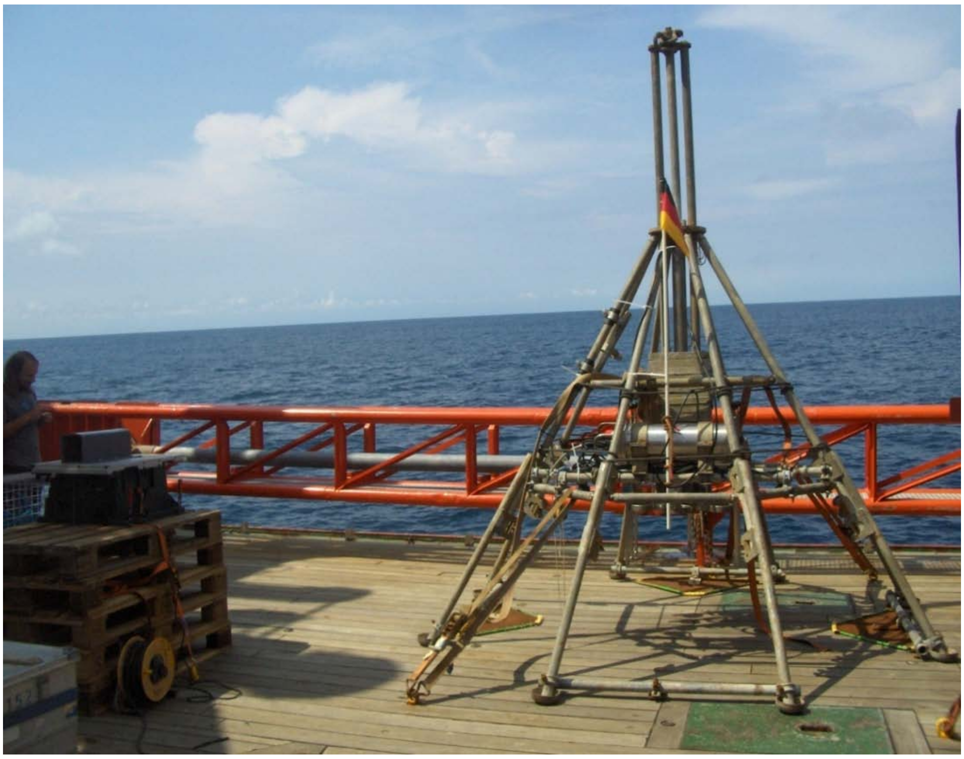

**Figure 5-28:** TV-MUC and GC used in sampling program.

**Table 5-1:** Position, depth and recovery of gravity cores.

| Core | Latitude | Longitude | Depth | Recovery |
|---|---|---|---|---|
| SO206-05 | 8° 59,58' N | 84° 43,69' W | 1909 m | 0 (gas hydrate) |
| SO206-06 | 8° 59,53' N | 84° 43,70' W | 1896 m | 100 cm |
| SO206-13 | 8° 59,58' N | 84° 43,72' W | 1905 m | 319 cm |
| SO206-14 | 8° 59,58' N | 84° 43,72' W | 1895 m | 230 cm |
| SO206-15 | 9° 10,69' N | 84° 39,72' W | 766 m | 498 cm |
| SO206-16 | 9° 11,54' N | 84° 39,72' W | 623 m | 262 cm |
| SO206-17 | 9° 11,93' N | 84° 39,40' W | 525 m | 519 cm |
| SO206-18 | 9° 11,65' N | 84° 37,08' W | 673 m | 500 cm |
| SO206-21 | 9° 00,20' N | 84° 45,90' W | 2017 m | 300 cm |
| SO206-22 | 9° 00,14' N | 84° 45,84' W | 2011 m | 386 cm |
| SO206-23 | 9° 11,95' N | 84° 39,42' W | 518 m | 759 cm |
| SO206-24 | 9° 11,64' N | 84° 37,05' W | 671 m | 450 cm |
| SO206-32 | 8° 51,13' N | 84° 13,06' W | 398 m | 281 cm |
| SO206-36 | 8° 55,34' N | 84° 18,21' W | 1006 m | 0 |
| SO206-37 | 8° 55,34' N | 84° 18,21' W | 1013 m | 81 cm |
| SO206-38 | 8° 55,33' N | 84° 18,22' W | 1020 m | 357 cm |
| SO206-50 | 8° 55,33' N | 84° 18,23' W | 1005 m | 300 cm |
| SO206-51 | 8° 56,41' N | 84° 19,00' W | 982 m | 395 cm |
| SO206-54 | 8° 56,39’ N | 84° 19,02’ W | 988 m | |

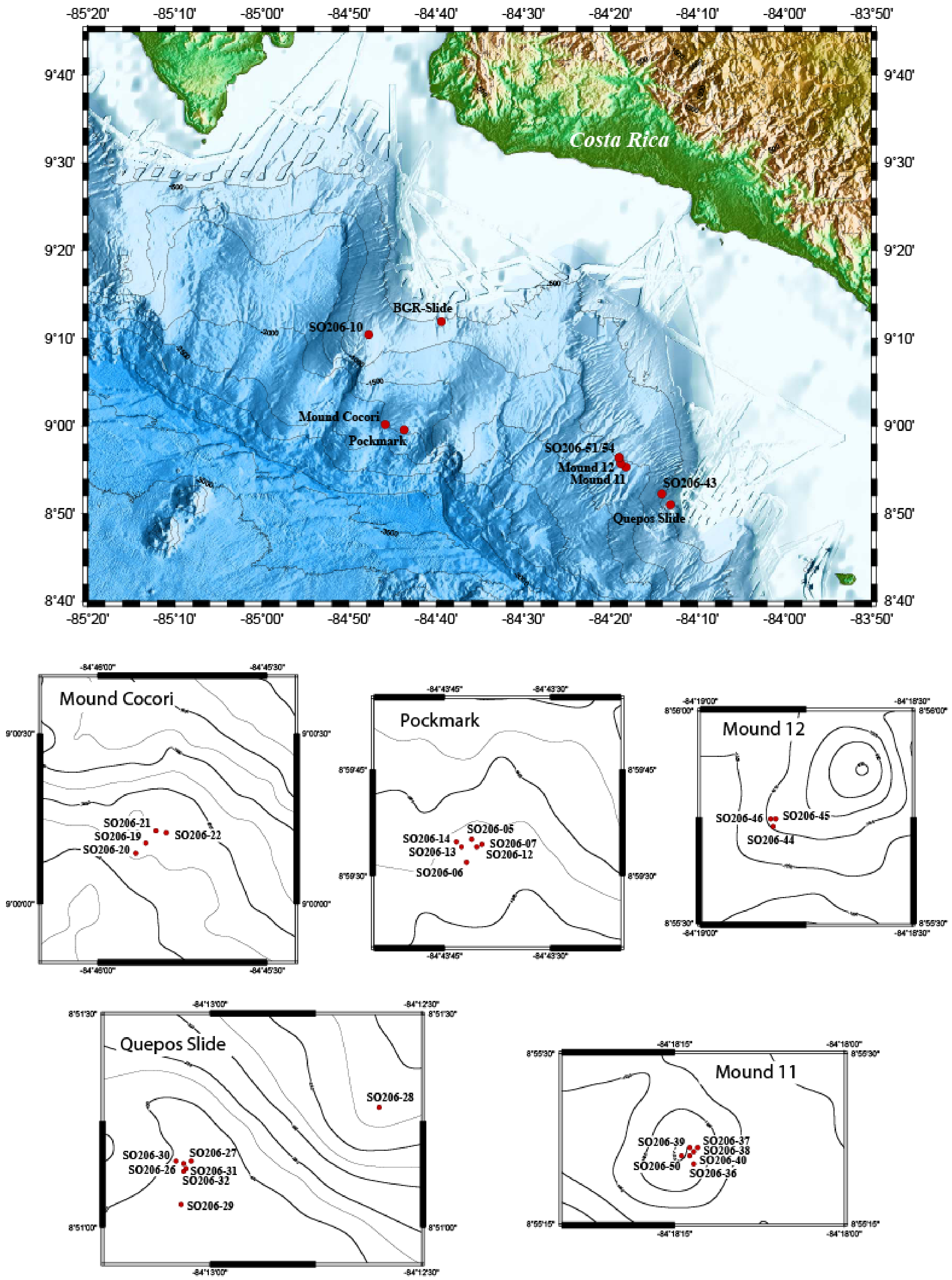


**Figure 5-29:** TV-MUC and GC sampling stations on cruise SO 206. For locations at BGR-Slide see Figure 5-31.

### 5.4.2 Results

#### 5.4.2.1 Jaco Scarp and Pockmark area

**Mound Cocori**

Core SO206-21 recovered 3 m of sediment. The upper unit consists of a dark olive grey mud with high water content and large fragments of clam shells (in situ). The underlying unit consist of a dark greenish grey mud with large amounts of mud clasts and authigenic carbonate nodules. An intensive smell of $H_2S$ was noticed. The boundary between both units is sharp and characterised by step in consolidation. The existences of highly consolidated mud clasts clearly identifies this structure as a mud volcano.

**Pockmark**

Core SO206-13 was placed on the Pockmark at 1905 m water depth near Jaco Scarp. It recovered a 319 cm long monotonous record of dark greenish grey mud with authigenic carbonate nodules. Tubeworm fragments and the associated burrow were found as sign of modern bioturbation at 106-111 cm.

#### 5.4.2.2 Mound 11/12

Gravity cores SO206-36, SO206-37, SO206-38 and SO206-50 were recovered at Mound 11. SO206-51 was taken to obtain a reference record near the mound 11/12 area. The 4 m long reference record consists of dark olive grey bioturbated mud. The mud (clayey silt) contains abundant foraminifers, small shells and shell fragments. Tephra layers (201-205 cm core depth) and a turbidite at the base of the core accentuate this background sedimentation.

At Mound 11 fluid seepage and associated phenomena overprint the mud. SO206-38 cored 3,57 m of sediment. A sharp boundary divides the uppermost 9 cm of slurry clayey silt from the underlying more consolidated mud. Macroscopic bioturbation characterises the upper core. Burrows originating from the sharp boundary reach down to 80 cm of core depth. At this depth a transition (80-100 cm) to dark greenish colour of the mud indicates a change in geochemical regime. Below, the mud is affected by formation of authigenic carbonate. SO206-50 shows a similar sequence down to 272 cm core depth. Below this depth a massive gas hydrate layer containing significant amounts of methane was cored. The hydrate layer was formed of nodular bodies forming a conglomerate of gas hydrate and relict sediment (Figure 5-30).


**Figure 5-30:** Conglomerate of nodular gas hydrate and relict sediment (core SO206-50, 272-300 cm).

### 5.4.2.3 Quepos Submarine Slide

Core SO206-32 was recovered from the Quepos Slide area. It cored a sequence of consolidated dark greenish grey mud that is overlain by a dark olive grey slurry mud. The boundary between both units is sharp indicating a hiatus. Its irregular shape and inclination (with respect to the core record) points to an erosive surface. The consolidated mud appears to be homogenous and contains authigenic carbonate nodules accompanied by a colour changes in the corresponding core intervals. A second sharp and probably erosive boundary is present at 239 cm and separates a consolidated dark olive grey mud from the overlaying units. The upper unit represents the youngest sedimentation at the site and can be interpreted as drape. The underlying sediment is difficult to interpret. It may represent a sliding surface (glide plane and intact sediments below) or and intact slided block from the debris facies of a slope failure.

### 5.4.2.4 BGR-Slide

The gravity coring program on submarine slides of the upper slope used 5 and 10m gravity corer. Six cores were taken from four key sites of the BGR and Geomar Slides (Figure 5-31). The focus was on a key Parasound profile across the BGR slide (Figure 5-23). Two cores were intended to recover a reference record above the headwalls. The other cores were placed on the glide plane and slide deposits for post-cruise dating of the failure event(s).

The total recovery varied according to the targeted sites between 7,59 and 2,62 metres. Cores were cut and cool-stored directly after recovery for post-cruise analysis. Samples for gas analysis (especially methane) were taken from each core section directly after cutting. Cores SO206-16 GC and SO206-23 GC were opened, described and sampled for porewater geochemistry aboard RV “Sonne”.

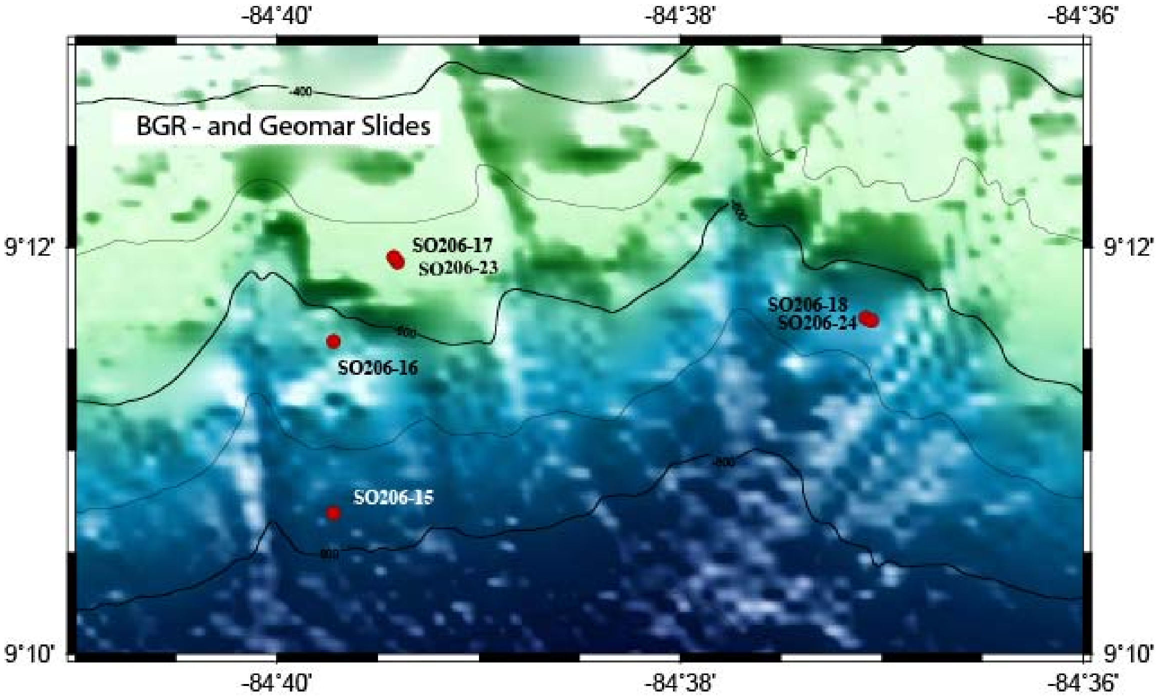


**Figure 5-31:** Overview map with coring stations at BGR and Geomar submarine slides of the upper continental slope offshore Costa Rica.

The 7,59 m long reference record of core SO206-23 consists of bioturbated olive grey mud (clayey silt). It contains abundant foraminifers, shells, shell and plant fragments. This background sedimentation is accentuated by turbidites and tephra layers (Figure 5-32).

Core SO206-16 GC was placed on the exposed glide plane of the BGR Slide at 623 m water depth. It cored 2,62 m of the uppermost sediment at site. The glide plane was recovered at 30 cm of core depth. It is overlain by soft olive grey clayey silt which represents the most recent sedimentation (Figure 5-33). Burrows into the underlaying older and consolidated mud reach down to 55 cm and are filled by the soft surface sediment. This points to a relatively young age of the BGR Slide.

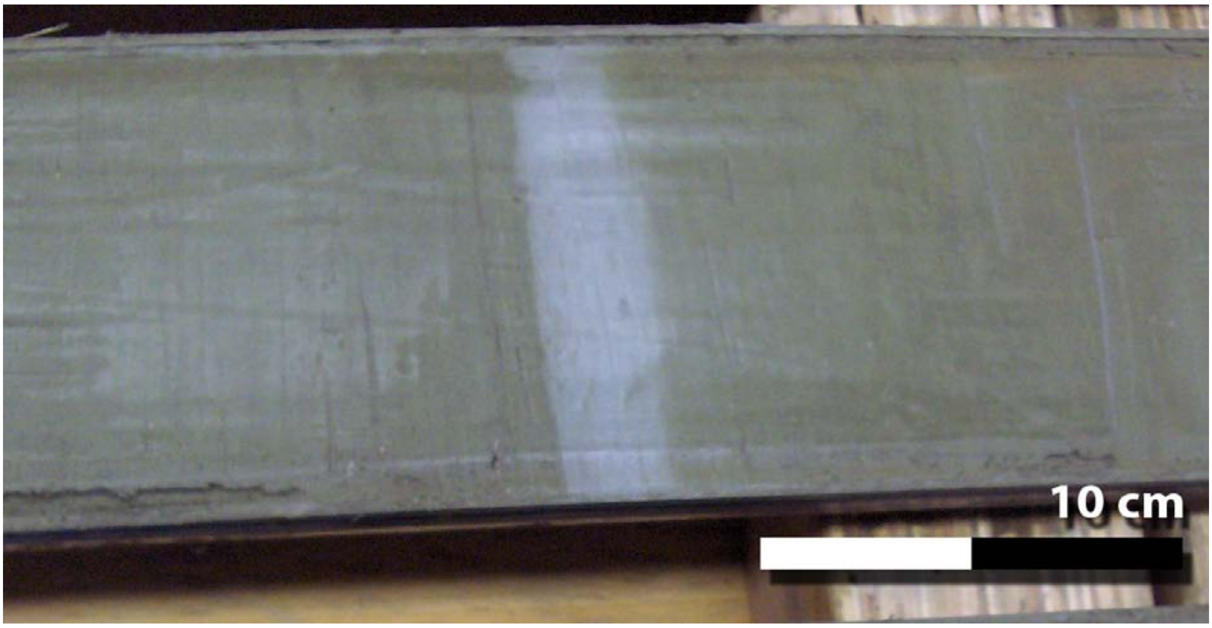


**Figure 5-32:** Tephra layer at 596-598,5 cm of the reference core SO206-23 above the BGR Slide.

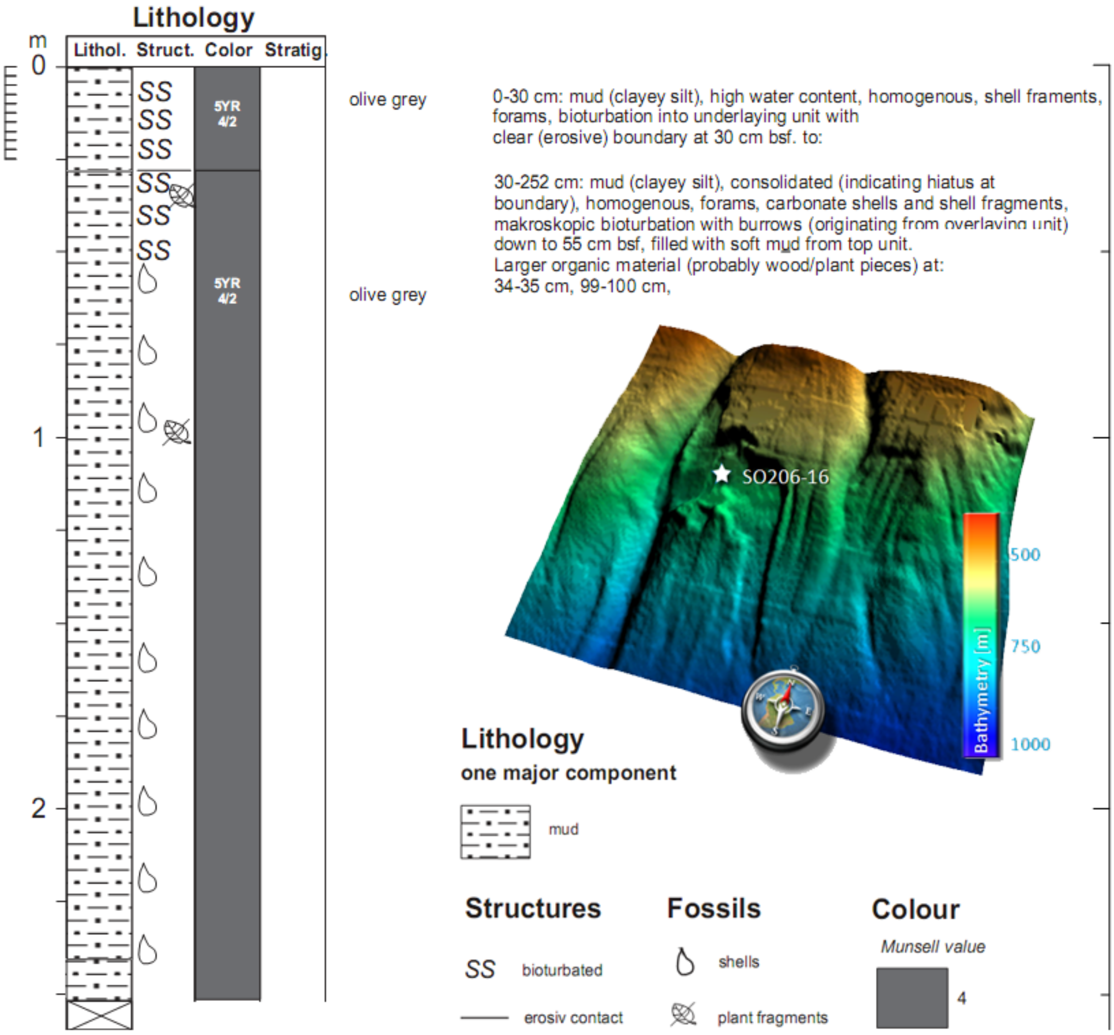


**Figure 5-33:** Core SO206-16 GC recovered the glide plane of the BGR Slide below a thin cover of young sediments at 30 cm bsf.

## Porewater geochemistry

*(Andy Dale, Marianne Nuzzo, Elena Piñero, Anke Bleyer, Renate Ebbinghaus, Emelina Corrales, Maria Martinez, Christian Hensen)*

The initial results presented in this report address the porewater geochemistry at selected sites along the Costa Rica subduction zone. The main objectives of performing a detailed porewater analysis are (i) to quantify the rates of abiotic and biotic geochemical processes in the upper sediments, (ii) to quantify the exchange fluxes between the sediments and the ocean, and (ii) to investigate the major geochemical processes occurring in the deep-seated upper plate sediments.

### 5.5.1 Methodology

#### 5.5.1.1 Sampling

In total, the porewater was analyzed at 22 sites at specific locations along the continental margin off Costa Rica. Samples were taken with a TV-guided multi-corer (MUC) and a gravity corer (GC) at the locations listed in Table 5-2. After sampling with the GC, the core liner was immediately sectioned on deck into lengths of≤ 1 m and samples for methane ($CH_4$) were taken using cut-off 10 ml polypropylene syringes from the ends of each core section. Each section was then sealed, labeled and split open lengthways inside the on-board cold room at 4 $^{o}$C. One (archive) half was described for sedimentological characteristics and the other (work) half was processed for geochemical analysis. Short sediment cores retrieved with the MUC were transferred into the cold room immediately after retrieval and the supernatant was filtered for subsequent analysis.

The sediments were mainly sampled for porewater by squeezing in a press under Argon gas (1-5 bar). This procedure was performed rapidly to minimize the effect of exposure to air on the porewater geochemistry. In selected cores, the porewater was sampled using 42hizome filters which were inserted through pre-drilled holes in the MUC liners or pushed into the work-half of the gravity core sediments. With this technique, the porewater is extracted anaerobically by suction using 10-20 ml plastic syringes and required 1-2 hours for the more consolidated sediments. The first 0.5 ml of porewater filtered from the sediment through the rhizones were discarded. Additional sediment sub-samples were taken in pre-weighed plastic vials for the determination of physical sediment properties such as porosity in addition to inorganic and organic particulate carbon and total particulate nitrogen.

**Table 5-2:** List of stations sampled where the geochemistry of solutes and dissolved gases in the porewater were analyzed simultaneously. Cores sub-sampled for He isotopes, acetate and biomarkers are also indicated. Note that dissolved gases were analyzed at a further 4 stations (15GC, 17GC, 18GC, 24GC) with no accompanying porewater analysis.

| Station SO206- | Date 2010 | Gear | $^3He/^4He$ | Biomarkers | Acetate | Lat. N | Long. W | Water depth (m) | Working area |
|---|---|---|---|---|---|---|---|---|---|
| 6 | 03.06 | GC | | X | X | 8°59.568’ | 84°43.720’ | 1920 | Pockmark |
| 10 | 03.06 | MUC | | | | 8°59.540’ | 84°43.720’ | 1933 | Pockmark |
| 12 | 06.06 | MUC | | X | X | 8°59.547’ | 84°43.657’ | 1938 | Pockmark |
| 13 | 06.06 | GC | | X | | 8°59.585’ | 84°43.714’ | 1896 | Pockmark |
| 14 | 06.06 | GC | X | | | 8°59.597’ | 84°43.727’ | 1892 | Pockmark |
| 16 | 06.06 | GC | | | | 9°11.530’ | 84°39.680’ | 623 | BGR Slide |
| 19 | 06.06 | MUC | | | | 9°00.236’ | 84°45.917’ | 2027 | Mound Cocori |
| 21 | 07.06 | GC | | X | X | 9°00.280’ | 84°45.921’ | 2023 | Mound Cocori |
| 22 | 07.06 | GC | X | X | | 9°00.175’ | 84°45.879’ | 2013 | Mound Cocori |
| 23 | 07.06 | GC | | | | 9°11.950’ | 84°39.420’ | 520 | BGR Slide |
| 26 | 08.06 | MUC | | X | X | 8°51.110’ | 84°13.080’ | 398 | Quepos Slide |
| 29 | 08.06 | MUC | | X | X | 8°51.110’ | 84°13.080’ | 399 | Quepos Slide |
| 31 | 08.06 | MUC | | X | X | 8°51.120’ | 84°13.050’ | 396 | Quepos Slide |
| 32 | 08.06 | GC | X | | X | 8°51.110’ | 84°13.080’ | 396 | Quepos Slide |
| 38 | 09.06 | GC | X | X | | 8°55.358’ | 84°18.225’ | 1013 | Mound 11 |
| 39 | 09.06 | MUC | | X | X | 8°55.330’ | 84°18.212’ | 1013 | Mound 11 |
| 40 | 09.06 | MUC | | | | 8°55.330’ | 84°18.220’ | 1002 | Mound 11 |
| 44 | 11.06 | MUC | | X | | 8°55.727’ | 84°18.787’ | 1005 | Mound 12 |
| 46 | 11.06 | MUC | | X | X | 8°55.721’ | 84°18.830’ | 998 | Mound 12 |
| 50 | 13.06 | GC | | X | X | 8°55.349’ | 84°18.241’ | 1003 | Mound 11 |
| 51 | 13.06 | GC | | X | X | 8°56.409’ | 84°18.997’ | 987 | ref site |
| 54 | 16.06 | GC | | | | 8°56.393’ | 84°19.018’ | 985 | ref site |

#### 5.5.1.2 Inorganic geochemical analysis

Water samples were analyzed on-board for dissolved silicate ($H_4SiO_4$), ammonium ($NH_4^+$), total dissolved sulfide ($TH_2S$) and total alkalinity (TA). $H_4SiO_4$, $NH_4^+$ and $TH_2S$ were determined using standard photometric procedures following Grasshoff et al. (1999). TA was measured by titrating porewater aliquots with 0.02 M HCl (Ivanenkov and Lyakhin, 1978) which was standardized using an IAPSO seawater solution.

In selected samples, a 2 ml porewater aliquot was passed through a Cd catalyst which reduces nitrate ($NO_3^-$) to nitrite ($NO_2^-$) and the latter was then analyzed on-board using photometry. Since $NO_2^-$ is a transient intermediate species in the benthic N cycle and is generally present at lower concentrations than $NO_3^-$, the $NO_2^-$ concentration determined is assumed to represent the concentration of $NO_3^-$.

Porewater and bottom water aliquots were also taken for shore-based chemical analysis. 2 ml of water were transferred to acid-cleaned plastic vials and acidified with supra-pure $HNO_3$ for ICP-OES analysis. 1.7 ml were added to plastic vials for ion-chromatography for the determination of the major seawater ions (K, Li, B, Mg, Ca, Sr, Mn, Br, I) and trace elements. In addition, 1.7 ml of porewater was added to glass vials containing 3 µL of $HgCl_2$ to poison microorganisms for later analysis of DOC and DIC and their isotopes ($\delta^{13}C$). 1.7 ml was separated and stored in glass vials for $\delta\ ^{18}O$ isotope analysis and, depending on the volume of porewater extracted from the sediments, 1.7 ml was taken for analysis of Sr and Cl isotopes. A detailed description of the analytical methods can be found on the website of IFM-GEOMAR (www.ifm-geomar.de).

### 5.5.1.3 Organic geochemical analysis

Porewater light volatile hydrocarbon gases were stripped from the sediments following the method of McAullife (1971). The sediment plugs sampled from the GC sections on deck were immediately injected into 30 ml glass vials filled with 10 ml of 10 % KCl to poison the bacteria. The vials were sealed and vigorously shaken to disaggregate the mud and to stop all bacterial activity. The samples were stored upside-down to minimize the potential gas exchange with the atmosphere and were allowed to equilibrate with the vial headspace for 24 to 48 h. The gas was extracted in a syringe by injecting an equivalent amount of 10% KCl solution into the vials. The headspace gas was later transferred into a 20 ml sterile serum vial filled (bubble-free) with 10 % KCl solution at pH 1 by displacement of an equivalent amount of solution. The vials were again stored upside-down to minimize the potential for gas exchange with air through the septum. The $CH_4$ concentration was determined onboard by Gas Chromatography-Flame Ionization Detection (GC-FID) using a Shimadzu GC14A instrument fitted with a Restek Rt® Alumina Bond/KCl capillary column (50m, 0.53mm ID). $N_2$ was used as a carrier gas. The headspace samples were stored for further analysis by GC-FID at the onshore IFM-GEOMAR laboratory to quantify $CH_4$ homologues as well as the stable carbon isotope composition of $CH_4$ by GC-combustion-isotope ratio Mass Spectrometry (GC-irMS).

Aliquots (2 to 4 ml) of porewater were filtered using acetate-free regenerated cellulose filters (0.2 µm; Wheaton®) and placed into pre-furnaced glass chromatography vials. The samples were immediately frozen at -20°C for the identification and quantification of organic acids by Liquid Chromatography-Mass Spectrometry at the onshore laboratory.

Sediments were also collected in pre-furnaced glass vials and immediately stored at -20 °C for the analysis of lipid biomarkers at the on-shore laboratory. Lipids will be extracted from the sediments using a modified Blye and Dyer method and separated into fractions of increasing chemical polarity by column chromatography prior to the identification and quantification of biomarker compounds by GC-MS and GC-FID, respectively. Compound-specific isotope analyses will also be performed on selected samples by GC-irMS. All methods are described by Elvert et al. (2003).

### 5.5.1.4 He-sampling methodology

For selected methane-rich 1 m GC sections (Table 5-2), sediment samples were taken by squeezing the sediment inside the core liner using a horizontal press in the on-board laboratory at ambient temperature. Prior to squeezing, air-tight fittings were inserted into pre-drilled and threaded fittings in the core liner (previously sealed with tape before coring) into which 3/8” or 1/2” diameter copper tubes were attached. The tubes were then flushed with sediment by squeezing the core section from both ends and then sealed with stainless steel clamps for shore-based analyses of He isotopes ($^{3}He/^{4}He$) and other noble gases. Preferentially, two sediment samples from the deepest section of the core were taken. Two reference cores were also sampled (51GC and 54GC, Table 5-2).

### 5.5.2 Results

A selection of porewater profiles from sediment cores retrieved from each working area and analyzed on board are shown in (Figure 5-34 – Figure 5-38) and described below.

#### 5.5.2.1 Pockmark and Mound Cocori

The Pockmark and Mound Cocori lie to the west of the study area targeted during the cruise (see Fig. 5-29 map). Extensive carbonate protrusions at the sediment surface were present at both sites and observations from the video equipment of the TV-MUC indicated that a thin veneer of sediment covered yet more subsurface carbonates. Consequently, only the upper 10 cm of sediment at both sites could be sampled using the TV-guided MUC (Figure 5-34, Figure 5-35). The recovered sediments showed no conspicuous bacterial mats on the sediment surface. The rapid increase in sulfide and alkalinity in the upper sediment layers from Mound Cocori (Figure Figure 5-35) is a clear indication for intense anaerobic oxidation of methane (AOM) coupled to sulfate reduction. It is highly likely that methane-rich fluids are advected to the surface sediments driven by deep clay dewatering in the crustal sediments. Chloride determinations in the on-shore laboratory will be useful in quantifying the fluid advection velocity at this site. Sulfide, alkalinity and methane data from the gravity cores at Mound Cocori indicate a deeper zone (200-300 cm) of AOM which likely reflects the varying intensity of fluid advection across the mound (Figure 5-35). Interestingly, sulfide is depleted above and below the AOM zone at station 21GC which either indicates a sink for sulfide due to reductive (sulfidic) dissolution of iron oxide minerals or lateral and horizontal fluid circulation within the sediment. The gravity core data from the Pockmark (Figure 5-34) reveal higher concentrations of sulfide, methane and alkalinity in the upper meter of sediments than at Mound Cocori. In particular, at the Pockmark (core 6GC) the high methane and sulfide concentrations in the upper 50 and 20 cm, respectively, are attributed to the presence of thawed gas hydrate inclusions in the sediment. The occurrence of small and dispersed gas hydrate crystals in the very shallow sediments at the pockmark was observed in core 5GC, that recovered only few cm of sediments and was therefore not sampled.

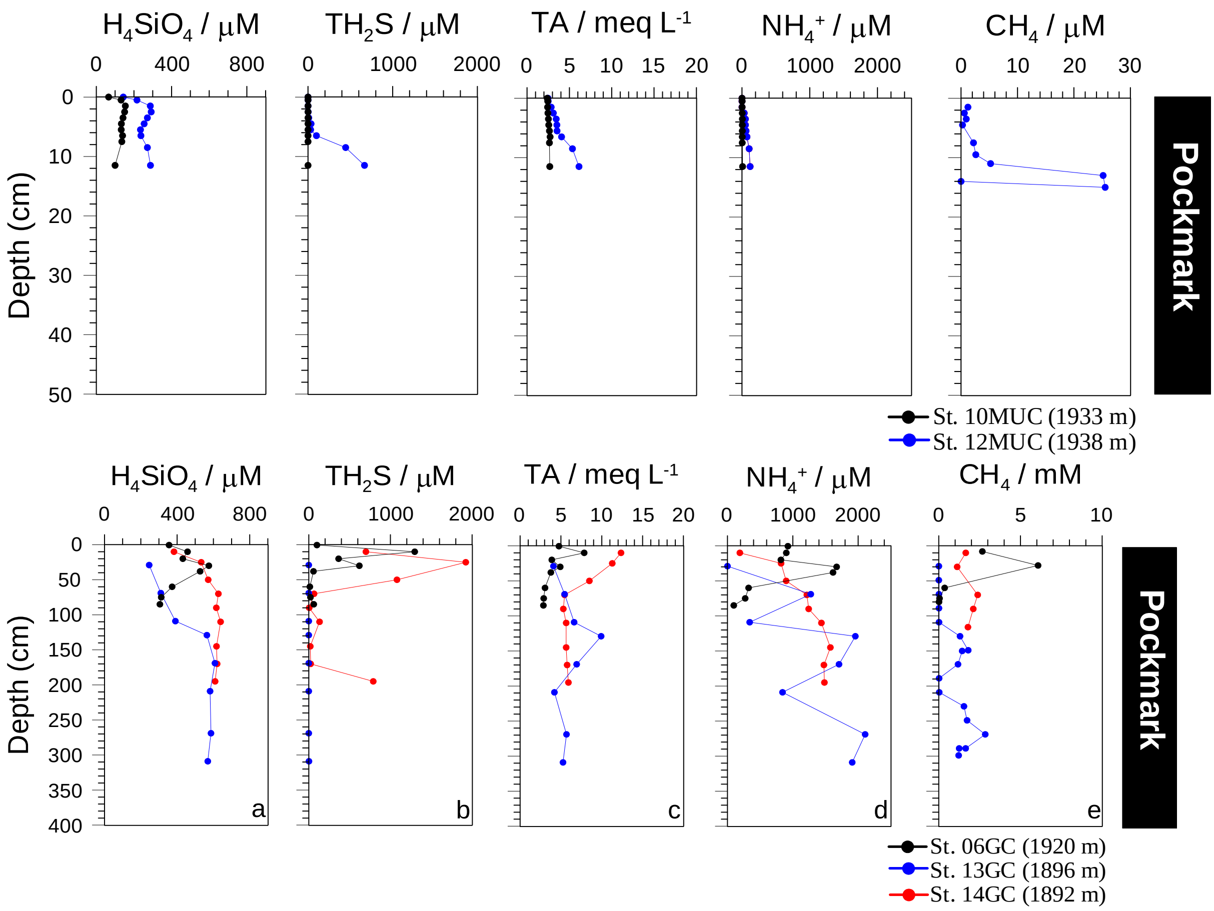


**Figure 5-34:** Porewater profiles from the Pockmark sampled using the MUC (top) and GC (bottom). Note different concentration scales for $CH_4$.

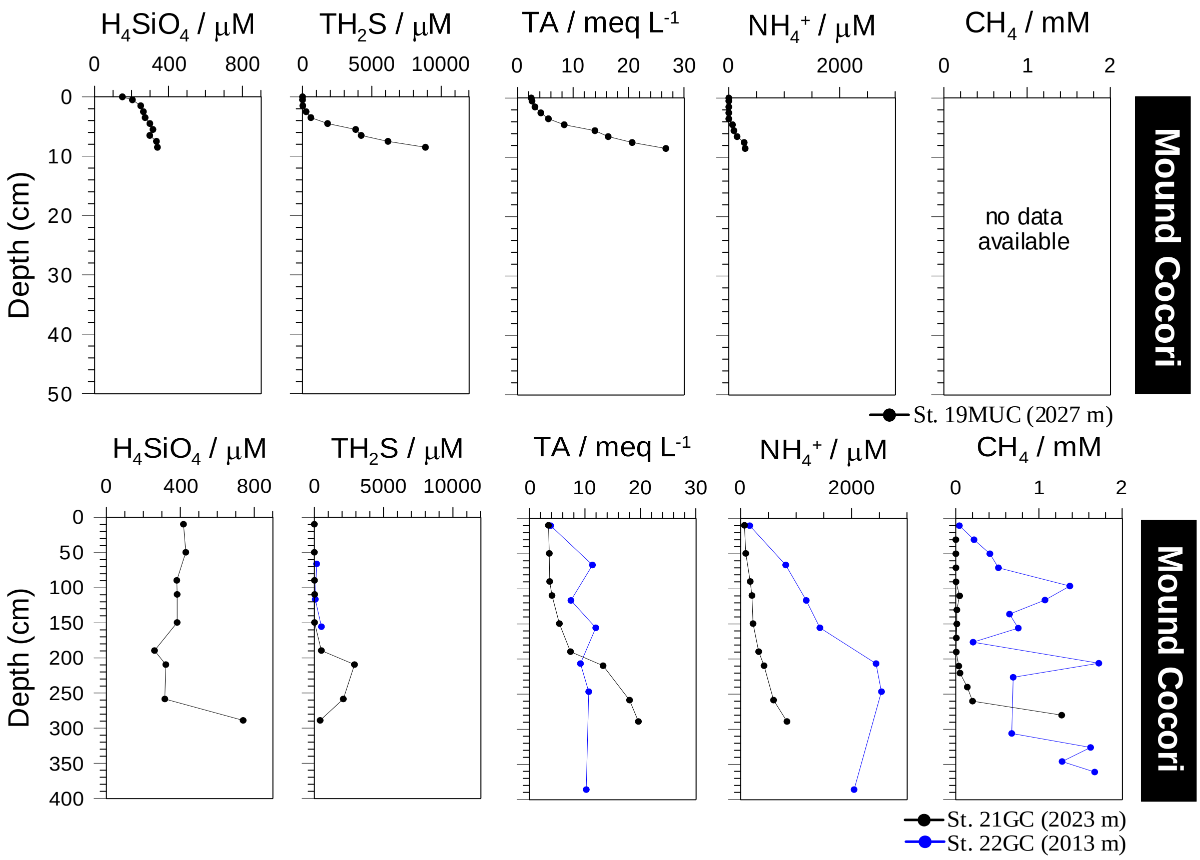


**Figure 5-35:** Porewater profiles from Mound Cocori sampled using the MUC (top) and GC (bottom).

### 5.5.2.2 Mound 11/12

Mounds 11 and 12 on the continental slope off southern Costa Rica at a water depth of ca. 1000 m are small, smooth and closely adjoined structures with only a slight elevation from the surrounding sea floor. In terms of fluid venting, they are known to be among the most active locations in the working area. The geochemistry of the surface sediments at Mound 11 and 12 sampled with the MUC show highly variable trends in the solutes due to the heterogeneity in fluid advection and sediment by bacterial mats (Figure 5-36). The deeper sediments at Mound 11 sampled with the gravity core (38GC and 50GC) show elevated concentrations of methane, sulfide, alkalinity and ammonium compared to the reference sites (51GC and 54GC; (Figure 5-36). The peaks in sulfide and alkalinity between 100 and 25 cm is similarly positioned, but with lower concentrations, as those reported previously at these sites (RV Meteor Cruise Reports M54/2 and M54/3A+B).

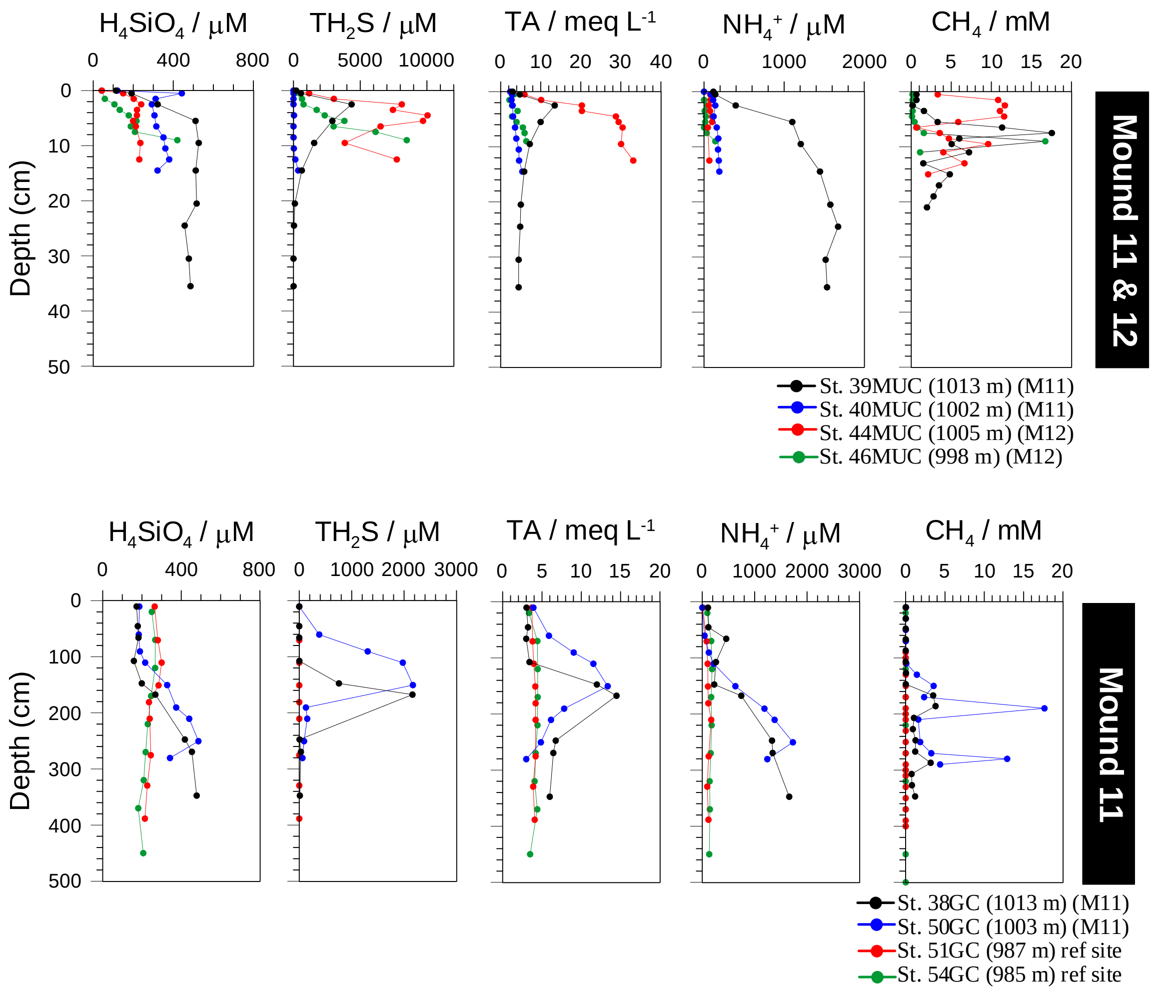


**Figure 5-36:** Porewater profiles from Mound 11/12 sampled using the MUC (top) and GC (bottom).

Analysis of the seawater ions should help elucidate whether fluid advection from below and/or intense sediment irrigation from above are important factors controlling the distribution of the porewater species. The high concentrations of ammonium compared to the reference sites are of particular interest since they allude to much higher rates of organic matter mineralization, much of which is probably ultimately derived from chemosynthetic community thriving at the sediment surface. This would suggest that the mounds have been active for at least as long as the time scale of organic matter burial over ca. 400 cm, which is of the order of $10^3$ years. A compact layer of gas hydrates was recovered at the bottom of core 50GC, and is thought to be issued from the same vein that was sampled during a previous expedition onboard the R/V-Meteor (Schmidt et al., 2005), consistent with the hypothesis that $CH_4$-rich fluid venting is both intense and stable at Mound 11. In this core, the concentration peaks > ca. 5mM are caused by the sampling of dissociated/dissociating gas hydrates.

### 5.5.2.3 Quepos Slide

The sediments at Quepos Slide (Figure 5-37) were sampled using a gravity core (32GC) and 3 TV-MUC deployments (26MUC, 29MUC, 31MUC). The multi-corer data show a high degree of consistency with a rapid increase in silicate, ammonium, sulfide and alkalinity with depth. All MUC sites were covered with a conspicuous layer of white bacterial mats which were presumably sulfide oxidizing bacteria (e.g. *Beggiatoa*, *Thiothrix*) thriving on sulfide produced by AOM in the upper 20 cm of sediment.

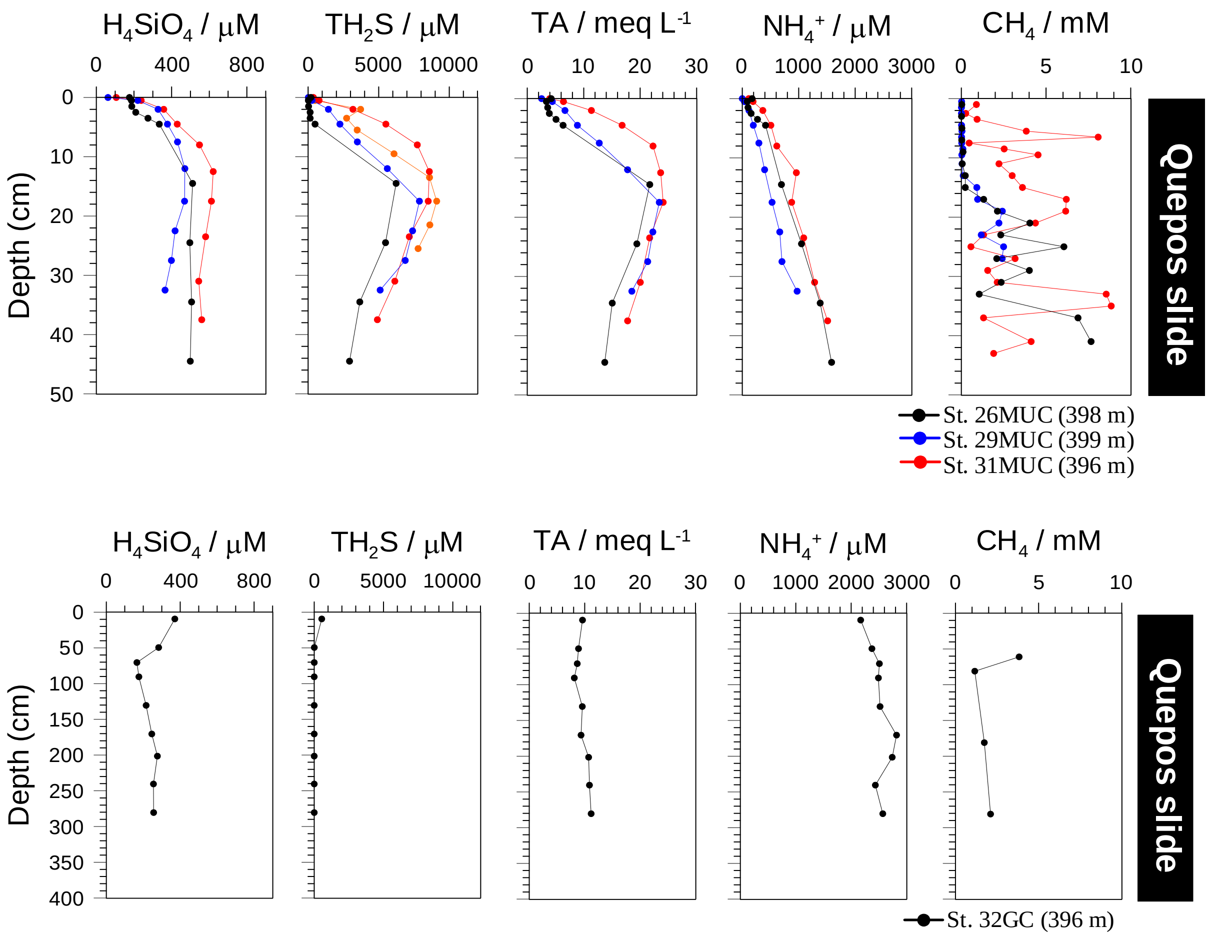


**Figure 5-37:** Porewater profiles from the Quepos Slide sampled using the MUC (top) and GC (bottom).

The sediments at station 26MUC show a well-defined zone of methane consumption where methane concentrations are depleted by 10 cm depth and sulfide and alkalinity show maximum values. The tendency toward lower sulfide and alkalinity concentrations below 15 cm may be caused by the upward advection of fluids from below which are relatively depleted in sulfide and enriched in Ca as observed in previous surveys in the subduction zone (RV Meteor Cruise

Reports M54/2 and M54/3A+B). By contrast, site 32GC shows little evidence of an extensive diagenetic overprint although the concentrations of silicate, ammonium, sulfide and alkalinity at the top of 32GC and bottom of the MUC station are of similar magnitude. It is thus possible that the surface sediments at 32GC were lost by the impact of the gravity core as it penetrated into the sea floor.

#### 5.5.2.4 BGR-Slide

The BGR Slide is a small slide structure located northeast of Jaco Scarp (Figs. 5-24 and 5-31). The porewater was analyzed in 2 gravity cores of ca. 250 cm (16GC) and ca. 750 cm (23GC) in length. The long core is significantly more enriched in silicate, alkalinity and ammonium than the short core. The alkalinity and ammonium trends indicate continual mineralization of organic matter with depth in the sediment. The disappearance of methane by 350 cm at 23GC indicates a deep zone of AOM coupled to sulfate reduction. Sulfate concentrations, to be measured at IFM-GEOMAR, will confirm the depth of this transitional layer.

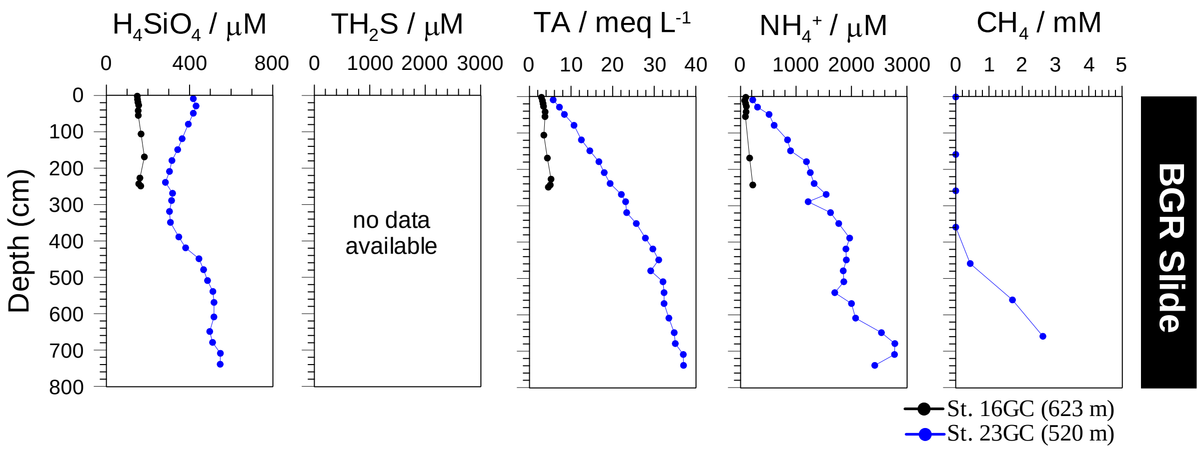


**Figure 5-38:** Porewater profiles from the BGR Slide sampled using the GC.

### 5.6. Geomicrobiology

*(Stefan Krause, Philipp Steeb)*

Aim of this study was to understand the connection between fluid/methane discharge, biological processes, and geochemical reactions along the central 49merican subduction zone. Microbial anaerobic oxidation of methane (AOM) with simultaneous sulfate reduction leads to precipitation of authigenic carbonates and the accumulation of hydrogen sulfide in the sediment. Chemoautotrophic communities (free-living sulfur bacteria or symbiont clams and tubeworms) utilize sulfide to gain energy for primary production

#### 5.6.1 Methodology

During the cruise microbial samples were taken at 8 locations along the subduction zone off Costa Rica (Table 5-3).

Sampling was carried out with a TV-MUC and a gravity corer. Sediment cores taken from the multicorer for biogeochemical analyses were used for (1) sediment solid phase sampling, (2) porewater squeezing, (3) microbial turnover rate measurements, (4) flow through experiments, and (4) sampling of active sediments. For sediment solid phase sampling, the first ten centimeters of the sediment core was sliced into 1-cm intervals. Below ten centimeters, the core was sliced in 2-cm intervals. Each depth section was also sub-sampled for methane and biomarker and RNA/DNA analysis. The porewater core was sliced into 9 intervals. Details on porewater recovery can be found in the porewater geochemistry section. Microbial turnover rates of methane and sulfate were measured in three parallel sub-cores (i.d. 26 mm), respectively, by radiotracer techniques. Fifteen µl of $^{14}$C-methane tracer (activity 2 kBq) and 6µl of the $^{35}$S-sulfate tracer (activity 200 kBq) were injected into the sediment, respectively, in 1-cm intervals. After an incubation time of 24 hours the reactions were stopped by slicing the cores into 1-cm intervals and transferring the sediment into 2.5% (w/w) sodium hydroxide and 20% (w/w) zinc acetate, respectively (Gravity cores were sampled by the same scheme, which was applied to multicorer samples (except for the sampling of the flow-through-core). After slicing of the segments sampling was carried out close to the porewater sampling locations. For sampling glas tubes were pushed into the sediment. After plugging the tubes the samples were processed as previously decribed. From both **types of corers carbonate samples were** taken for further analysis in the home laboratory. Samples were wrapped in aluminum foil and stored frozen. Table 5-4). One sub-core (i.d. 60 mm) was taken from a multicorer core for sediment flow-through experiments in the home laboratory. The core liner was specifically designed to be installed into a flow-through system enabling biogeochemical studies under controlled fluid flow parameters. Active sediments for in-vitro studies were taken from one to two multicorer cores per station. Cores were sliced into the depth sections 0-5, 5-10, and 10-15 cm. Sediments were transferred into glass bottles, topped with anoxic bottom water and sealed with a rubber stopper.

**Table 5-3: Microbiological sampling stations**

| Station | Place | Date | Time UTC | Lat. N | Long E | Depth (m) | Cores sampled | Samples |
|---|---|---|---|---|---|---|---|---|
| So206-10-Muc | Jaco Scarp, Top | 06.06.10 | 02:38 | 9°10.43' | 84°47.74' | 736 | 1 | L |
| So206-12-Muc | Pockmark | 06.06.10 | 14:05 | 8°59.566' | 84°43.6729' | 1923 | 4 | L, S, R, F |
| So206-21-GC | Mound Cocori | 07.06.10 | 19:51 | 9°00.217' | 84°45.8281' | 2025 | 1 | L, S, R |
| So206-29-Muc | Quepos Slide | 08.06.10 | 19:43 | 8°51.2940' | 84°12.6040' | 402 | 4 | L, S, R, F |
| S0206-31-Muc | Quepos Slide | 08.06.10 | 22:07 | 8°51.12' | 84°13.06' | 399 | 6 | L, S, R, F |
| So206-39-Muc | Mound 11 | 09.06.10 | 20:34 | 8°55.3660' | 84°18.2270' | 1005 | 3 | S, R, F |
| So206-40-Muc | Mound 11 | 09.06.10 | 23:23 | 8°55.3520' | 84°18.2260' | 1005 | 1 | L |
| So206-44-Muc | Mound 12 | 11.06.10 | 15:40 | 8°55.7260' | 84°18.8240' | 1007 | 3 | L, S, R, F |
| So206-46-Muc | Mound 12 | 11.06.10 | 20:42 | 8°55.7420' | 84°18.8350' | 1009 | 2 | S, R |
| S0206-50-GC | Mound11 | 14.06.10 | 03:15 | 8°55.3460' | 84°18.2410' | 1003 | 1 | S, R |
| So206-51-GC | Reverenz | 14.06.10 | 04:59 | 8°56.41' | 84°19.00' | 987 | 1 | S, R |

Microbiological sampling stations: L=Live sediment, S= Sediment solid phase sampling, R= Turnover rates, F= Sediment Flow-through system

Gravity cores were sampled by the same scheme, which was applied to multicorer samples (except for the sampling of the flow-through-core). After slicing of the segments sampling was carried out close to the porewater sampling locations. For sampling glas tubes were pushed into the sediment. After plugging the tubes the samples were processed as previously decribed. From both types of corers carbonate samples were taken for further analysis in the home laboratory. Samples were wrapped in aluminum foil and stored frozen.

**Table 5-4:** Subsamples taken from the sediment solid phase and microbial turnover rate cores.

| Parameter | Chemicals | Sample Volume (ml) | Storage |
|---|---|---|---|
| | | *Sediment solid phase* | |
| Methane | 5 ml 2.5% NaOH | 2 ml sediment | room temperature |
| FISH | 1.5 ml 4% formaline | 0.5 ml sediment | stored in PBS/Ethanol at –20°C after washing two times in 1x PBS |
| RNA/DNA | - | ca. 3 ml | -80ºC |
| CNS, BioMarkers | - | ca. 30 ml | -20ºC |
| | | *Microbial turnover rate measurements* | |
| AOM | 20 ml 2.5% NaOH | ca. 5 ml sediment | room temperature |
| Sulfate Reduction | 20 ml 20% ZnAc | ca. 5 ml sediment | room temperature |

### 5.6.2 Results

#### 5.6.2.1 Jaco Scarp and Pockmark area

The seafloor at the top of Jaco Scarp was sandy with no visible signs of bacterial mats, tubeworms or shells. The area was sampled with one TV-MUC (10-MUC). The retrieved cores had a total length of 10 cm. The upper part of the sediment had a grey-brown colour and some carbonate rocks were present. Below 4 cm the colour changed to dark green-grey also including more carbonate material.

The sediments at the location Pockmark were sampled with two TV-MUC (7-MUC, 12-MUC; Figure 5-39). Features at the seafloor included colonies of tubeworms, fields of dead shells, and carbonate rocks. No indications for bacterial mats were observed at the locations of sampling. The cores were approximately 18 cm long. The first 3-4 cm were light grey-brown, followed by dark grey-green sediment indicating the production of sulphide. Carbonate material was present.

Mound Cocori was sampled with one gravity corer (21-GC, Figure 5-40), which had a length of approximately 300 cm. The first 30 cm of the core was disturbed and consisted of dark, soft mud, followed by light grey sediment including carbonate material. In the deeper sections the sediment was compressed. For detailed information on the core description see section 5.4.2.

**Figure 5-39:** Core from Station SO206-12 (MUC).

**Figure 5-40:** Opened gravity core from station SO206-21 (GC). Top left: 0-100 cm, Top right: 100-200 cm, Bottom left: 200-300 cm.

### 5.6.2.2 Mound 11/12

Mound 11 was sampled with 2 TV-MUCs and a GC (39-MUC –Figure 5-41 -, 40-MUC, and 50-GC). Grey-white bacterial mats were frequently present on the sandy sediment. Fields of carbonate blocks were also visible.

The obtained cores varied in length between 27-36 cm. The first centimetre contained black and watery bacterial mat followed by 5 cm of very soft, black sediment indicating sulphide production. Subsequently, the sediment changed to a light grey-green. The cores had a very strong sulphide smell. Methane gas bubbles of varying size were present, especially in the upper and middle part.

**Figure 5-41:** Core from station SO206-39 (MUC).

Two TV-MUC were also deployed at Mound 12 (44-MUC, 46-MUC; Figure 5-42). The sediment appeared to be soft with larger quantities of dead mussels and shell fragments at the surface. Grey-white bacterial mats were present. At the location of 46-MUC fields of large carbonate blocks with living brown mussels attached were observed.

The cores from Mound 12 had a length of 18-20 cm. A grey-white bacterial mat was present on top of the sediment, followed by 3-4 cm of black, soft sediment. Below the sediment changed to a green-grey color and showed numerous gas bubbles. Carbonate material was present at the lower part of the core.

**Figure 5-42:** Cores from stations 44-MUC (left) and 46-MUC (right).

### 5.6.2.3 Quepos Slide

Two TV-MUC (29-MUC, 31-MUC; Figure 5-43) were deployed at in area of Quepos slide. The seafloor was characterized by soft sediment with white and yellow bacterial mats. Red crustaceans were abundant on the sediment and on mats. The sediment cores sampled at station 29-MUC had a total length from 23-32 cm. The top layer of the cores consisted of white bacterial mats followed by 2-3 cm of dark, soft sediment. The sediment then changed to dark grey becoming gradually lighter towards the bottom of the cores. Gas bubbles were observed in the middle part of the cores.

The cores obtained at 31-MUC varied in length between 44-50 cm. White bacterial mats were present at the surface. The following sediment was black and very soft for the first 2 cm, subsequently changing colour to green-grey.

**Figure 5-43:** Cores of stations SO206-29 (MUC) (left) and SO206-31(MUC) (right).

## 5.7 Microbiology of Foraminifera

*(Nicolaas Glock)*

It appears that the pore density in tests of *B. spissa* is sensitive to ambient oxygen- or more propable nitrate-concentrations (GLOCK et al., in press). Furthermore it has been suggested that pores facilitate or promote the uptake of oxygen and to the release of metabolic $CO_2$ (HOTTINGER and DREHER, 1974; LEUTENEGGER and HANSEN, 1979). Some benthic low-oxygen tolerant species showed that their mitochondria, cell organelles involved in respiration, were more abundant near the pores than in other species from well oxygenated waters. This observation may infer an evolutionary linkage between pores and mitochondria (LEUTENEGGER and HANSEN, 1979). Recent studies of *Bolivina pacifica* showed again a clustering of mitochondria at the inner pore face while outer part of the pore void was inhabited by a rod-shaped microbial ectobiont of unknown identity and physiology (BERNHARD et al., in press). Some species of benthic foraminifera from oxygen-poor habitats have recently been shown to respire nitrate via denitrification (RISGAARD-PETERSEN et al., 2006). Intracellular nitrate-stores are used for denitrification as augmented energy sources in times when oxygen is not or poorly available for respiration. The activity of denitrification in benthic foraminifera has not been traced to a specific cell organelle yet (HØGSLUND 2008). Because of the correlation of PD and bottom water nitrogen concentrations (GLOCK et al., in press) the pores may be related to nitrate-uptake. When mitochondria are clustered behind the pore plugs, what indeed has been observed from a *Bolivina* at low-oxygen conditions, the mitochondria might be involved in the mechanism of foraminiferal denitrification, too. Since mitochondria have been documented to serve in nitrate respiration of the primitive eukaryote *Loxodes* (FINLAY, 1983) this assumption is not devious. Furthermore, *Loxodes* switches from oxygen to nitrate-respiration when the number of mitochondria is significantly enhanced. The recent observation of microbial ectobionts of unknown identity and physiology inhabiting the pore void of *B. pacifica* (BERNHARD, GOLDSTEIN and BOWSER, in press) gives a reason to speculate if such ectobionts exist in the pore void of *B. spissa* as well and are indeed denitrifiers. Ultrastructural analyses should prove if indeed in *B. spissa* mitochondria are clustered at the inner pore-room as well and if they get more frequently in oxygen or nitrate depleted habitats. Also it will be investigated if there are ectosymbionts present in the pores of *B. spissa*. These studies could prove if the pores in tests of *B. spissa* are indeed related to the intracellular nitrate or oxygen uptake.

### 5.7.1 Sampling methodology

Two different types of samples were taken from multicorer tubes of several. Within a couple of minutes after the multicorer came on deck, the tubes were brought to a laboratory with a constant room temperature of 4°C. Supernatant water of the core was carefully removed. Then the cores were gently pushed out of the multicorer tube. At five stations (SO206-10, 28, 29, 40, 43; see Figure 5-29) one to two cores were cut into 10 mm thick slices and the untreated samples were transferred to Whirl-Pack™ plastic bags and stored at a temperature of 4°C for morphological studies (i.e. pore-density analysis) of benthic foraminifera. At six stations (SO206-10, 28, 29, 40, 43, 44; see Figure 5-29) samples were taken for cell fixation experiments. Just before the cores were coming on deck a fresh solution of 5% Glutaraldehyde and 0.1 M cacodylate buffer were mixed out of 1 part 25% Glutaraldehyde, 2.5 parts 0.2 M cacodylate buffer, pH 7.2, and 1.5 parts of distilled water. In less the one hour after the cores came on deck they were cut into 10 mm thick slices and 15-16 ml of sediment were transferred into 50 ml centrifuge tubules. These tubules were filled up with the fixative and mixed sufficiently without rigorous shaking and stored at 4° C.

### 5.7.2 Results

Five of the cores were sampled for nitrate analysis of the bottom water and porewater of the first few centimetres. The methodology of sampling and analysis is described in sections 5.5.1.1 and 5.5.1.2. The results are shown in Figure 5-44.

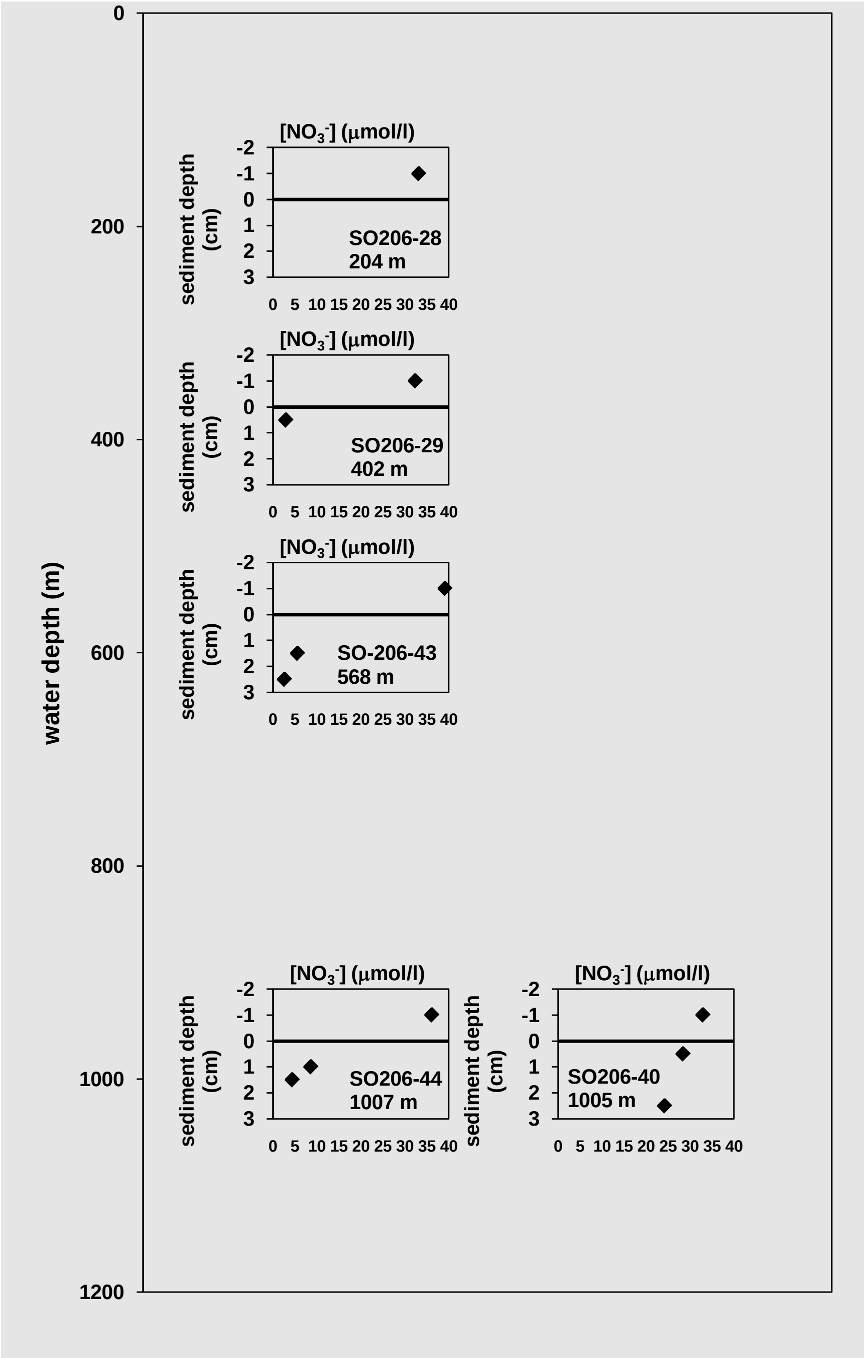


**Figure 5-44:** Concentrations of dissolved nitrate ($NO_3^-$) from the different water depths sampled using the MUC. To facilitate comparison between sites, the analytes are plotted on the same concentration and depth scales.

## Station List SO 206

| SO 206 | | | | | | | | | | | | | | | |
|---|---|---|---|---|---|---|---|---|---|---|---|---|---|---|---|
| | | | Time (UTC) | | | | | Begin / on seafloor | | End / off seafloor | | | | | |
| | | | | | | | | Positon Ship | | | | | | | |
| **Date UTC** | **St. No. SO 206** | **Instrument** | **Begin** | **Start Sci. Program** | **End Sci. Program** | **End** | **Duration hh:mm** | **Latitude N°** | **Longitude W°** | **Latitude N°** | **Longitude W°** | **Water-depth [m]** | **Comment** | **Recovery** | **Area** |
| 02/06/2010 | SO206-01 | CTD | 00:18 | 00:24 | 03:43 | 04:33 | 04:15 | 8°58.91` | 84°53.79` | 8°59.04` | 84°53.84` | 2939 | Releasertest | | Jaco Scarp |
| 02/06/2010 | SO206-02-101 | OBS | 05:58 | | | | | 9°9.417` | 84°48.537` | | | 791 | OBS ausgesetzt | | Jaco Scarp |
| 02/06/2010 | SO206-02-102 | OBS | 06:32 | | | | | 9°8.797` | 84°50.542` | | | 944 | OBS ausgesetzt | | Jaco Scarp |
| 02/06/2010 | SO206-02-103 | OBS | 06:54 | | | | | 9°8.106` | 84°49.213` | | | 922 | OBS ausgesetzt | | Jaco Scarp |
| 02/06/2010 | SO206-02-104 | OBS | 07:18 | | | | | 9°7.417` | 84°47.867` | | | 886 | OBS ausgesetzt | | Jaco Scarp |
| 02/06/2010 | SO206-02-105 | OBS | 07:40 | | | | | 9°07.427` | 84°49.550` | | | 1327 | OBS ausgesetzt | | Jaco Scarp |
| 02/06/2010 | SO206-02-106 | OBS | 07:56 | | | 08:00 | 02:02 | 9°06.805` | 84°49.878` | 9°06.81` | 84°49.88` | 1691 | OBS ausgesetzt | | Jaco Scarp |
| 02/06/2010 | SO206-03 | 2-D MCS | 09:04 | 09:34 | | | 33:42 | 9°03.49` | 84°38.78` | 9°16.06` | 84°45.13` | | | | Jaco Scarp |
| 03/06/2010 | SO206-03 | | | | 18:39 | 18:46 | | | | | | | | | |
| 03/06/2010 | SO206-04 | Posidonia | 19:38 | 19:40 | 00:03 | 00:24 | 04:52 | 9°09.00` | 84°48.75` | 9°9.27` | 84°48.47` | 831 | | | Jaco Scarp |
| 04/06/2010 | SO206-05 | GC | 01:32 | 01:35 | 03:09 | 03:28 | 01:56 | *8° 59,583'* | *84° 43,688'* | 8° 59,57' | 84° 43,71' | 1910 | Gas Hydrates | carbonate nodules | Pockmark |
| 04/06/2010 | SO206-06 | GC | 03:29 | 03:32 | 04:55 | 04:56 | 01:27 | *8° 59,533'* | *84° 43,70'* | 8° 59,53' | 84° 43,71' | 1922 | | 100 cm | Pockmark |
| 04/06/2010 | SO206-07 | TV-MUC | 05:08 | 05:55 | 08:49 | 08:49 | 03:41 | *8° 59,574'* | *84° 43,664'* | 8° 59,57' | 84° 43,67' | 1933 | | | Pockmark |
| 04/06/2010 | SO206-08 | 2-D MCS | 09:05 | 09:44 | | | | 8°59.29` | 84°42.02` | | | | Profilstart | | Jaco Scarp |
| 05/06/2010 | SO206-08 | 2-D MCS | | | 09:53 | 09:55 | 24:50 | | | 9° 1,40' | 84° 42,71' | | Profilende | | Jaco Scarp |
| 05/06/2010 | SO206-09-106 | OBS | 10:52 | 10:56 | 11:27 | | | 9°06.705` | 84°49.799` | | | 1623 | OBS eingeholt | | Jaco Scarp |
| 05/06/2010 | SO206-09-105 | OBS | | 11:44 | 12:02 | | | 9°07,328` | 84°49,487` | | | 1345 | OBS eingeholt | | Jaco Scarp |
| 05/06/2010 | SO206-09-104 | OBS | | 12:23 | 12:39 | | | 9°07,297` | 84°49,785` | | | 886 | OBS eingeholt | | Jaco Scarp |
| 05/06/2010 | SO206-09-103 | OBS | | 13:42 | 13:59 | | | 9°08,106` | 84°49.213` | | | 922 | OBS eingeholt | | Jaco Scarp |

| | | | | | | | | | | | | | | | |
|---|---|---|---|---|---|---|---|---|---|---|---|---|---|---|---|
| 05/06/2010 | SO206-09-102 | OBS | | 13:04 | 13:23 | | | 9°08,566` | 84°50,467` | | | 944 | OBS eingeholt | | Jaco Scarp |
| 05/06/2010 | SO206-09-101 | OBS | | 14:20 | 14:37 | 14:48 | 03:56 | 9°09,261` | 84°48,485` | | | 791 | OBS eingeholt | | Jaco Scarp |
| Port call, Caldera | | | | | | | | | | | | | | | |
| 06/06/2010 | SO206-10 | TV-MUC | 01:38 | 01:42 | 02:38 | 02:39 | 01:01 | 9°10,43' | 84° 47,74' | 9° 10,43' | 84° 47,74' | 736 | | 15 cm | Top-Jaco-Scarp |
| 06/06/2010 | SO206-11 | MB/PS | 03:20 | 03:20 | 09:39 | 09:39 | 06:19 | 9° 9,26' | 84° 50,06' | 9° 7,13' | 84° 37,02' | | | | Jaco Scarp |
| 06/06/2010 | SO206-12 | TV-MUC | 10:50 | 10:59 | 14:05 | 14:09 | 03:19 | 8° 9,566' | 84°3,6729' | 8° 59,54' | 84° 43,70' | 1923 | | until 20 cm | Pockmark |
| 06.06.2010 | SO206-13 | GC | 15:00 | 15:02 | 16:36 | 16:37 | 01:37 | *8° 59,57'* | *84° 43,71'* | *8° 59,58'* | *84° 43,71'* | 1905 | no posidionia | 319 cm | Pockmark |
| 06/06/2010 | SO206-14 | GC | 16:48 | 16:52 | 18:20 | 18:26 | 01:38 | 8° 59,58' | 84° 43,72' | 8° 59,57' | 84° 43,72' | 1896 | no posidionia | 230 cm | Pockmark |
| 06/06/2010 | SO206-15 | GC | 19:46 | 20:34 | 21:11 | 21:19 | 01:33 | 9° 10,69' | 84° 39,72' | 9° 10,69' | 84° 39,72' | 766 | no posidonia | 498 cm | BGR-Slide |
| 06/06/2010 | SO206-16 | GC | 21:33 | 21:37 | 22:08 | 22:23 | 00:50 | 9° 11,54' | 84° 39,72' | 9° 11,54' | 84° 39,71' | 619 | | 262 cm | BGR-Slide |
| 06/06/2010 | SO206-17 | GC | 22:36 | 22:41 | 23:09 | 23:14 | 00:38 | 9° 11,93' | 84° 39,40' | | | 525 | overpenetrated? | 519 cm | BGR-Slide |
| 06/06/2010 | SO206-18 | GC | 23:40 | 23:53 | 00:25 | 00:27 | 00:47 | 9° 11,65' | 84° 37,08' | | | 673 | maybe overpenetrated | 500 cm | BGR-Slide |
| 07/06/2010 | SO206-19 | TV-MUC | 03:45 | 03:49 | 14:24 | 14:28 | 10:43 | 9° 00,18' | 84° 45,86' | | | 2025 | TV-MUC survey | until 20 cm | Mound Cocori |
| 07/06/2010 | SO206-20 | TV-MUC | 14:34 | 14:53 | 17:33 | 17:35 | 03:01 | 9° 00,15' | 84° 45,89' | 9° 00,16' | 84° 45,89' | 2017 | | ? | Mound Cocori |
| 07/06/2010 | SO206-21 | GC | 17:36 | 18:16 | 19:51 | 19:53 | 02:15 | *9° 0,217'* | *84° 5,8281'* | 9° 00,20' | 84° 45,90' | 2025 | | 300 cm | Mound Cocori |
| 07/06/2010 | SO206-22 | GC | 20:05 | 20:15 | 21:45 | 21:47 | 01:42 | *9° 00,21'* | *84° 45,797'* | 9° 00,14' | 84° 45,85' | 2036 | | 386 cm | Mound Cocori |
| 07/06/2010 | SO206-23 | GC | 23:52 | 00:00 | 00:32 | 00:35 | 00:43 | 9° 11,95' | 84° 39,42' | | | 520 | | 759 cm | BGR-Slide |
| 08/06/2010 | SO206-24 | GC | 01:03 | 01:11 | 01:51 | 01:54 | 00:51 | 9° 11,64' | 84° 37,05' | | | 672 | | 450 cm | BGR-Slide |
| 08/06/2010 | SO206-25 | MB/PS | 02:25 | 02:25 | 11:24 | 11:24 | 08:59 | 9° 12,73' | 84° 37,87' | 9° 9,68' | 84° 36,03' | | | | BGR-Slide |
| 08/06/2010 | SO206-26 | TV-MUC | 14:06 | 14:38 | 15:34 | 15:36 | 01:30 | *8°51,1470'* | *84°13,0608'* | 8° 51,14' | 84° 13,06' | 402 | bacterial mats | full | Quepos Slide |
| 08/06/2010 | SO206-27 | TV-MUC | 16:12 | 16:17 | 17:13 | 17:17 | 01:05 | *8° 51,1550'* | *84°13,0461'* | 8° 51,13' | 84° 13,06' | 397 | bacterial mats | full | Quepos Slide |
| 08/06/2010 | SO206-28 | TV-MUC | 17:42 | 17:50 | 18:16 | 18:21 | 00:39 | 8° 51,28' | 84°12,60' | 8° 51,28' | 84° 12,59' | 204 | | | Top Quepos Slide |
| 08/06/2010 | SO206-29 | TV-MUC | 18:34 | 18:43 | 19:43 | 19:45 | 01:11 | *8° 51,053'* | *84°13,0662'* | 8° 51,12' | 84° 13,06' | 402 | | 40-45 cm | Quepos Slide |

| SO 206 | | | | | | | | | | | | | | | |
|---|---|---|---|---|---|---|---|---|---|---|---|---|---|---|---|
| | | | Time (UTC) | | | | | Begin / on seafloor | | End / off seafloor | | | | | |
| | | | | | | | | Positon Ship | | | | | | | |
| Date UTC | St. No. SO 206 | Instrument | Begin | Start Sci. Program | End Sci. Program | End | Duration hh:mm | Latitude N° | Longitude W° | Latitude N° | Longitude W° | Water-depth [m] | Commentx | Recovery | Area |
| 08/06/2010 | SO206-30 | TV-MUC | 20:38 | 20:43 | 21:20 | 21:23 | 00:43 | *8° 51,1560'* | *84°13,0780'* | 8° 51,13' | 84° 13,08' | 401 | nicht ausgeloest | | Quepos Slide |
| 08/06/2010 | SO206-31 | TV-MUC | 21:25 | 21:28 | 22:07 | 22:10 | 00:45 | *8° 51,1360'* | *84°13,0571'* | 8° 51,12' | 84° 13,06' | 399 | white and yellow bacterial mats | 48-60 cm | Quepos Slide |
| 08/06/2010 | SO206-32 | GC | 22:45 | 22:58 | 23:36 | 23:48 | 01:03 | 8° 51,13' | 84°13,06' | | | 400 | | 281 cm | Quepos Slide |
| 09/06/2010 | SO206-33-P301 | OBS | 02:36 | 02:47 | | | | 9° 9,51' | 84°39,70' | | | 965 | OBS ausgesetzt | | BGR-Slide |
| 09/06/2010 | SO206-33-P302 | OBS | | 03:00 | | | | 9° 10,40' | 84°39,70' | | | 810 | OBS ausgesetzt | | BGR-Slide |
| 09/06/2010 | SO206-33-P303 | OBS | | 03:14 | | | | 9° 11,20' | 84° 40,52' | | | 611 | OBS ausgesetzt | | BGR-Slide |
| 09/06/2010 | SO206-33-P304 | OBS | | 03:32 | | | | 9° 11,19' | 84°39,70' | | | 665 | OBS ausgesetzt | | BGR-Slide |
| 09/06/2010 | SO206-33-P305 | OBS | | 03:46 | | | | 9° 11,21' | 84°38,89' | | | 736 | OBS ausgesetzt | | BGR-Slide |
| 09/06/2010 | SO206-33-P306 | OBS | | 04:00 | | 04:01 | 01:25 | 9° 11,95' | 84°39,69' | | | 524 | OBS ausgesetzt | | BGR-Slide |
| 09/06/2010 | SO206-34 | OBS-Seismik | 04:34 | 04:45 | 09:08 | 09:08 | 04:34 | 9° 15,29' | 84° 39,58' | 9° 13,60' | 84° 39,70' | | | | BGR-Slide |
| 09/06/2010 | SO206-35 | OBS-Seismik | 09:08 | 09:55 | 12:18 | 12:22 | 03:14 | 9° 13,60' | 84°39,70' | 9° 11,16' | 84° 37,58' | | | | BGR-Slide |
| 09/06/2010 | SO206-36 | GC | 14:42 | 14:50 | 15:47 | 15:52 | 01:10 | 8° 55,34' | 84°18,21' | 8° 55,34' | 84° 18,22' | 1012 | core catcher did not work, core flushed out | no recovery | Mound 11 |
| 09/06/2010 | SO206-37 | GC | 15:53 | 16:09 | 17:06 | 17:07 | 01:14 | *8°55,3620'* | *84°18,2170'* | *8°55,3650'* | *84°18,2190'* | 1007 | 1007 | | Mound 11 |
| 09/06/2010 | SO206-38 | GC | 17:08 | 17:25 | 18:24 | 18:27 | 01:19 | *8°55,3580'* | *84°18,2240'* | *8°55,3570'* | *84°18,2260'* | 1016 | 1016 | | Mound 11 |

| | | | | | | | | | | | | | | | |
|---|---|---|---|---|---|---|---|---|---|---|---|---|---|---|---|
| 09/06/2010 | SO206-39 | TV-MUC | 18:28 | 19:08 | 20:34 | 20:35 | 02:07 | *8°55,3620'* | *84°18,2290'* | *8°55,3660'* | *84°18,2270'* | 1005 | white bacterial mats | 38 cm | Mound 11 |
| 09/06/2010 | SO206-40 | TV-MUC | 20:38 | 20:57 | 23:23 | 23:25 | 02:47 | *8°55,3520'* | *84°18,2260'* | *8°55,3520'* | *84°18,2260'* | 1005 | in small grey mats, no posidonia | 17 cm | Mound 11 |
| 10/06/2010 | SO206-41 | OBS-Seismik | 01:59 | 02:04 | 06:43 | 06:47 | 04:48 | 9° 12,69' | 84°41,40' | 9° 12,71' | 84°40,56' | | | | BGR-Slide |
| Port call, Caldera | | | | | | | | | | | | | | | Caldera |
| 11/06/2010 | SO206-42-306 | OBS | 04:48 | 04:52 | 05:06 | | | 9° 12,01' | 84°39,88' | | | 523 | OBS eingeholt | | BGR-Slide |
| 11/06/2010 | SO206-42-305 | OBS | | 05:23 | 05:56 | | | 9° 11,27' | 84°39,14' | | | | OBS eingeholt | | BGR-Slide |
| 11/06/2010 | SO206-42-304 | OBS | | 06:19 | 06:40 | | | 9° 11,29' | 84°39,99' | | | | OBS eingeholt | | BGR-Slide |
| 11/06/2010 | SO206-42-303 | OBS | | 07:08 | 07:19 | | | 9° 11,28' | 84°40,75' | | | | OBS eingeholt | | BGR-Slide |
| 11/06/2010 | SO206-42-302 | OBS | | 07:21 | 07:43 | | | 9° 10,97' | 84°40,47' | | | | OBS eingeholt | | BGR-Slide |
| 11/06/2010 | SO206-42-301 | OBS | | 07:45 | 08:01 | 08:07 | 03:13 | 9° 9,90' | 84°39,85' | | | | OBS eingeholt | | BGR-Slide |
| 11/06/2010 | SO206-43 | MUC | 10:58 | 11:04 | 11:43 | 11:52 | 00:54 | 8° 52,27' | 84°14,10' | | | 568 | | 20 cm | Region Mounds 11-12 / Quepos Slide |
| 11/06/2010 | SO206-44 | TV-MUC | 12:39 | 12:44 | 15:40 | 15:43 | 03:04 | *8°55,7290'* | *84°18,8280'* | *8°55,7260'* | *84°18,8240'* | 1007 | Lotschacht nicht ausgefahren | 14 cm | Mound 12 |
| 11/06/2010 | SO206-45 | TV-MUC | 15:44 | 16:11 | 17:52 | 17:54 | 02:10 | *8°55,7470'* | *84°18,8210'* | *8° 55,7500'* | *84°18,8200'* | 1002 | small, grey bacterial mats | no recovery | Mound 12 |
| 11/06/2010 | SO206-46 | TV-MUC | 19:00 | 19:08 | 20:42 | 20:43 | 01:43 | *8°55,7460'* | *84°18,8310'* | *8° 55,7420'* | *84°18,8350'* | 1009 | Bacterial mat | 12 cm | Mound 12 |
| 11/06/2010 | SO206-47 | OBS/OBH | 21:03 | 21:07 | | 21:08 | 00:05 | 8° 55,63' | 84°18,40' | | | 1021 | OBS ausgesetzt | | Mound 12 |
| 11/06/2010 | SO206-48 | 3D-MCS | 21:48 | 22:29 | | | | 8° 59,60' | 84°21,83' | | | | Profilstart | | Mounds 11&12 |
| 14/06/2010 | SO206-48 | 3D-MCS | | | 00:30 | 00:35 | 50:47 | | | 8° 53,90' | 84°17,83' | | Profilende | | Mounds 11&12 |
| 14/06/2010 | SO206-49 | OBS/OBH | 01:05 | 01:06 | 01:26 | 01:27 | 00:22 | 8° 55,79' | 84°18,49' | | | 1003 | OBS eingeholt | | Mound 12 |

| SO 206 | | | | | | | | | | | | | | | | |
|---|---|---|---|---|---|---|---|---|---|---|---|---|---|---|---|---|
| | | | Time (UTC) | | | | | Begin / on seafloor | | End / off seafloor | | | | | | |
| | | | | | | | | Positon Ship | | | | | | | | |
| **Date UTC** | **St. No. SO 206** | **Instrument** | **Begin** | **Start Sci. Program** | **End Sci. Program** | **End** | **Duration hh:mm** | **Latitude N°** | **Longitude W°** | **Latitude N°** | **Longitude W°** | **Water-depth [m]** | **Commentx** | **Recovery** | **Area** |
| 14/06/2010 | SO206-50 | GC | 01:50 | 02:06 | 03:15 | 03:19 | 01:29 | *8°55,3470'* | *84°18,2410'* | *8°55,3460'* | *84°18,2410'* | 1003 | massive gas hydrates, at least 25 cm, OFOP time incorrect | 300 cm | Mound 11 |
| 14/06/2010 | SO206-51 | GC | 03:54 | 04:07 | 04:59 | 05:00 | 01:06 | 8° 56,41' | 84°19,00' | 8° 56,41' | 84°19,00' | 987 | | 395 cm | Reference Location (Mound 11/12) |
| 14/06/2010 | SO206-52 | MB/PS | 06:28 | 06:28 | 11:12 | 11:12 | 04:44 | 9° 7,68' | 84°20,81' | 9° 9,41' | 84°18,72' | | | | Shelf break |
| 14/06/2010 | SO206-53 | 3D-MCS | 12:06 | 12:30 | | | | 9° 0,64' | 84°22,54' | | | | Profilstart | | Mound 11&12 |
| 16/06/2010 | SO206-53 | 3D-MCS | | | 15:31 | 15:36 | 51:30 | | | 9° 4,37' | 84°39,68' | | Profilende | | Mound 11&12 |
| 16/06/2010 | SO206-54 | GC | 16:24 | 16:33 | 17:24 | 17:26 | | 8° 56,39' | 84°19,02' | 8° 56,39' | 84°19,02' | | | 500 cm | Reference Location (Mound 11/12) |
| 16/06/2010 | SO206-55 | 2D-MCS | 20:00 | 21:04 | | | | 9° 2,33' | 84°39,81' | | | | Profilstart | | BGR-Slide |
| 17/06/2010 | SO206-55 | 2D-MCS | | | 12:28 | 12:30 | 16:30 | | | 9° 9,87' | 84°48,82' | | Profilende | | BGR-Slide |
| 18/06/2010 | SO206-56 | MB/PS | 14:43 | 15:40 | 01:35 | 02:13 | 10:52 | 9° 16,55' | 84°27,96' | 9° 9,00' | 84°10,66' | | massive gas hydrates at last 25 cm, OFOP time incorrect | | Shelf break |

**Acknowledgments**

We thank Captain Oliver Meyer and the entire crew of RV SONNE for their excellent support during the cruise. We are grateful to Ulrike Lomnitz and Christine Utecht for editorial support in preparation of this report. Cruise SO 206 was funded by the "Deutsche Forschungsgemeinschaft" (DFG) through the "SO 206 – Costa Rica Mounds" grant.

**Data and sample storage and availability**

The raw data acquired during cruise SO 206 were archived allowing for an immediate exchange of the data within the project group. Subsequent results may be added in the same context avoiding redundant metadata input. CTD data of the cruise are already uploaded to the server at IFM-GEOMAR (https://portal.ifm-geomar.de). DSHIP data of this cruise are available at the BSH (http://dship.bsh.de).

The metadata is already publicly accessible immediately. The associated scientific data will be made public after a limited time period. Published data and data out of moratorium will be submitted to World Data Centers (WDC) such as PANGAEA. The IFM-GEOMAR/University Kiel data management team will take care of the data transfers to long-term archives in order to ensure the data availability worldwide and for the far future.

**References**

Bernhard, J., Bowser and Goldstein, S., 2010. An ectobiont-bearing foraminiferan, Bolivina pacifica, that inhabits microxic porewaters: Cell-biological and paleoceanographic insights. Environmental Microbiology, 12, 2107-2119.

Elvert, M., Boetius, A., Knittel, K., and Jørgensen, B. B., 2003. Characterization of specific membrane fatty acids as chemotaxonomic markers for sulphate reducing bacteria involved in anaerobic oxidation of methane. Geomicrobiology Journal 20, 403-419.

Finlay, B. J., Span. A. S. W.. and Harman. J. M. P., 1983. Nitrate respiration in primitive eukaryotes. Nature, 303, 333-335.

Glock, N., Eisenhauer, A., Milker, Y., Liebetrau, V., Schönfeld, J., Mallon, J., Sommer, S., Hensen, C. Environmental influences on the pore-density in tests of Bolivina Spissa. Journal of Foraminiferal Research, in press.

Grasshoff, K., Ehrhardt, M., and Kremling, K., 1999. Methods of Seawater Analysis. Wiley-VCH, Weinheim, 600pp.

Hensen, C., Wallmann, K., Schmidt, M., Ranero, C. R., and Suess, E., 2004. Fluid expulsion related to mud extrusion off Costa Rica continental margin - a window to the subducting slab. Geology 32, 201-204.

Høgslund, S., Revsbech, N. P., Cedhagen, T., Nielsen, L. P. and Gallardo, V. A., 2008. Denitrification, nitrate turn over, and aerobic respiration by benthic foraminiferans in the oxygen minimum zone off Chile. J. Exp. Mar. Biol. Ecol., 359, 85–91.

Ivanenkov, V.N., Lyakhin, Y.I., 1978. Determination of total alkalinity in seawater. In: Bordovsky, O.K., Ivanenkov, V.N. (Eds.). Methods of Hydrochemical Investigations in the Ocean. Nauka Publ. House, 110–114, in Russian.

Kahn, L. M., Silver, E. A., Orange, D. L., Kochevar, R., and McAdoo, B., 1996. Surficial evidence of fluid expulsion from the Costa Rica accretionary prism. Geophys. Res. Lett. 23, 887-890.

Leutenegger, S. and Hansen, H. J., 1979. Ultrastructural and radiotracer studies of pore function in foraminifera. Marine Biology, 54, 11-16.

Mau, S., 2004. Methane output from cold seep structures along the Central American continental margin. Dissertation, Christian-Albrechts-Universität, Kiel, 132pp.

McAullife, C. 1971. GC determination of solutes by multiple phase equilibration. Chemical Technology, 1, 46–51.

Ranero, C. R., Grevemeyer, I., Sahling, H., Barckhausen, U., Hensen, C., Wallmann, K., Weinrebe, W., Vannucchi, P., von Huene, R., and McIntosh, K., 2008. Hydrogeological system of erosional convergent margins and its influence on tectonics and interplate seismogenesis. Geochem. Geophys. Geosyst 9.

Ranero, C. R. and Von Huene, R., 2000. Subduction erosion along the Middle America convergent margin. Nature 404, 748-752.

Risgaard–Petersen, N., Langezaal, A.M., Ingvardsen, S., Schmid, M.C., Jetten, M.S., Op den Camp, H.J.M., Derksen, J.W.M., Pina–Ochoa, E., Eriksson, S.P., Nielsen, L.P., Revsbech, N.P., Cedhagen, T. and van der Zwaan, G.J., 2006. Evidence for complete denitrification in a benthic foraminifer. Nature, 443, 93–96-

Sahling, H., Masson, D. G., Ranero, C. R., Hühnerbach, V., Weinrebe, W., Klaucke, I., Bürk, D., Brückmann, W., and Suess, E., 2008. Fluid seepage at the continental margin offshore Costa Rica and southern Nicaragua. Geochem. Geophys. Geosyst 9.

Schmidt, M., Hensen, C., Mörz, T., Müller, C., Grevemeyer, I., Wallmann, K., Mau, S., and Kaul, N., 2005. Methane hydrate accumulation in "Mound 11" mud volcano, Costa Rica forearc. Mar. Geol. 216, 83-100.

Von Huene, R., Ranero, C. R., and Watts, P., 2004. Tsunamigenic slope failure along the Middle America Trench in two tectonic settings. Mar. Geol. 203, 303-317.

# Appendix A: Core descriptions and core photos

Documentation of gravity cores

## Legend for stratigraphic columns

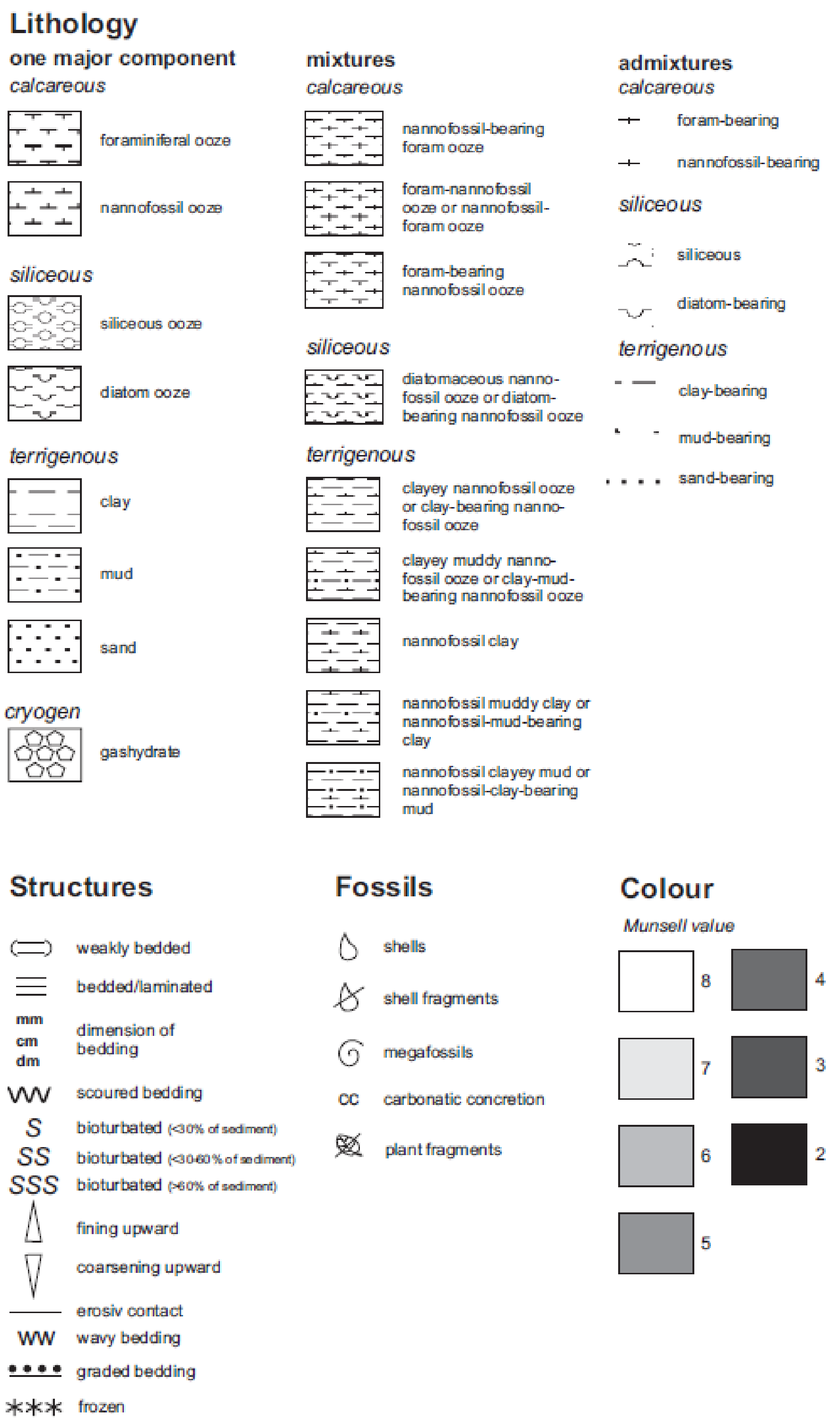

**SO206-06 GC** Date: 4.6.2010 Pos: 8° 59,53‘ N, 84° 43,70‘ W
Water Depth:1922 m Core Length: 100 cm

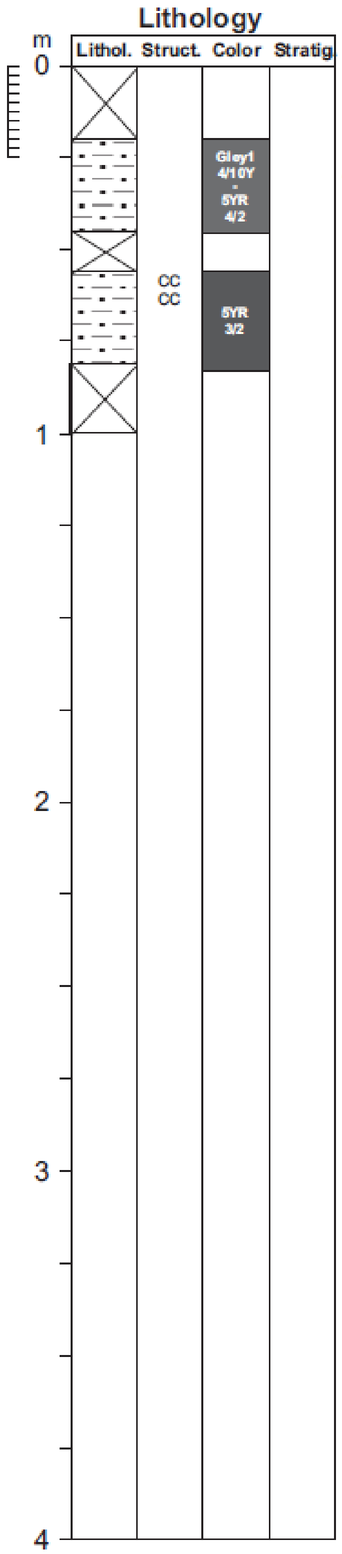


dark greenish grey

19-41 and 62-100 cm: mud (clayey silt), homogenous, shell framents, forams, distinct smell of $H_2S$; lower part in segment with dark olive grey color.
62-71 cm: concretions of authigenic carbonate (greenish grey nodules, angular, sub-angular or rounded, porous surface, up to 7 cm in diameter)

olive grey

NOTE: Due to difficulties in core splitting the archive half is fragmentary while the working recovered the full meter.

Appendix 1: Core discription and photograph – SO206-06 GC

**SO206-13 GC**

Date: 6.6.2010 Pos: 8° 59,58‘ N, 84° 43,72‘ W
Water Depth:1905 m Core Length: 319 cm

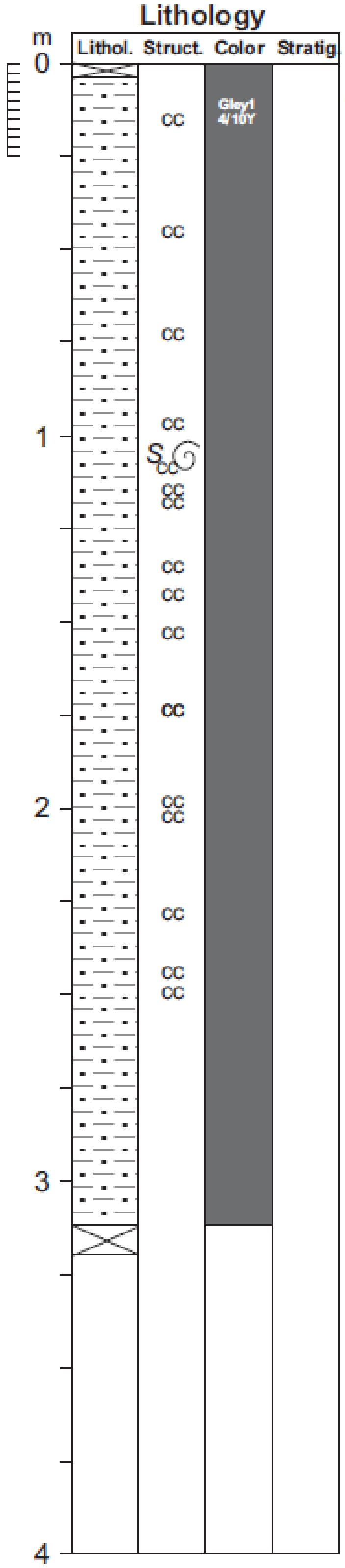


dark greenish grey

0-319 cm: mud (clayey silt), homogenous, some degree of carbonate cementation in pore space affecting the consistence of the mud; forams, carbonaceous shell fragments.

rounded to sub-angular authigenic carbonate nodules at:
10-15 cm, 40-48 cm, 69-74 cm, 89-99 cm, 102-104 cm, 110-119 cm, 134-135 cm, 141-146 cm, 152-159 cm, 173-174 cm, 195-207 cm, 227-230 cm, 237-241 cm, 245-251 cm

106-111 cm: burrows of tubeworms (including tub fragments)

NOTE: top sediment surface was tilted (working half: full recovery of upper 19 cm)


**Appendix 2: Core discription and photograph – SO206-13 GC**

**SO206-16 GC** Date: 6.6.2010 Pos: 9° 11,54‘ N, 84° 39,72‘ W
Water Depth: 623 m Core Length: 262 cm

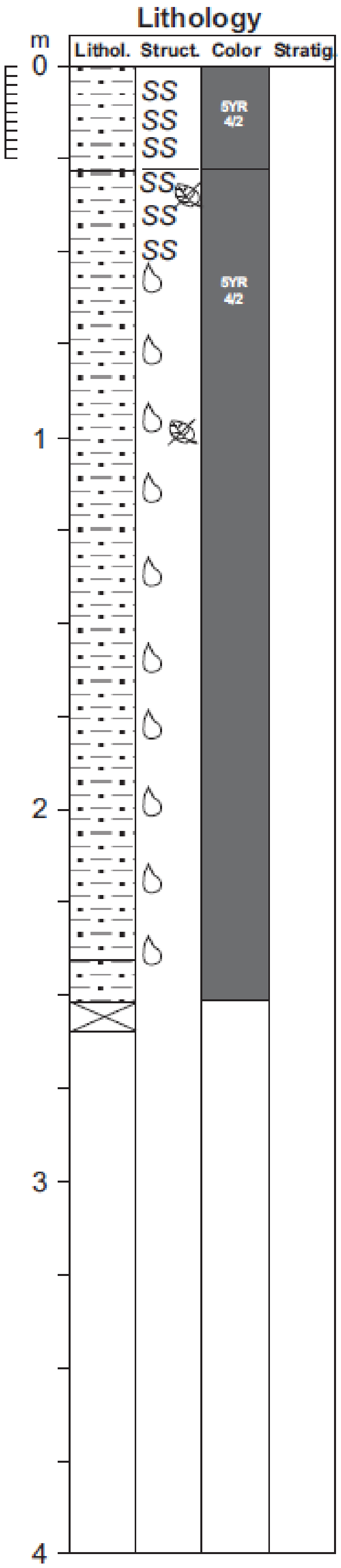


olive grey — 0-30 cm: mud (clayey silt), high water content, homogenous, shell framents, forams, bioturbation into underlaying unit with clear (erosive) boundary at 30 cm bsf. to:

olive grey — 30-252 cm: mud (clayey silt), consolidated (indicating hiatus at boundary), homogenous, forams, carbonate shells and shell fragments, makroskopic bioturbation with burrows (originating from overlaying unit) down to 55 cm bsf, filled with soft mud from top unit.
Larger organic material (probably wood/plant pieces) at:
34-35 cm, 99-100 cm,

Apparent boundary at 240 cm bsf. is a core splitting artefact.

NOTE: lowermost 10 cm (252-262 cm) in core catcher.


**Appendix 3: Core discription and photograph – SO206-16 GC**

| **SO206-21 GC** | Date: 7.6.2010 Pos: 9° 0,21' N, 84° 45,83' W<br>Water Depth: 2025 m Core Length: 300 cm |
|---|---|

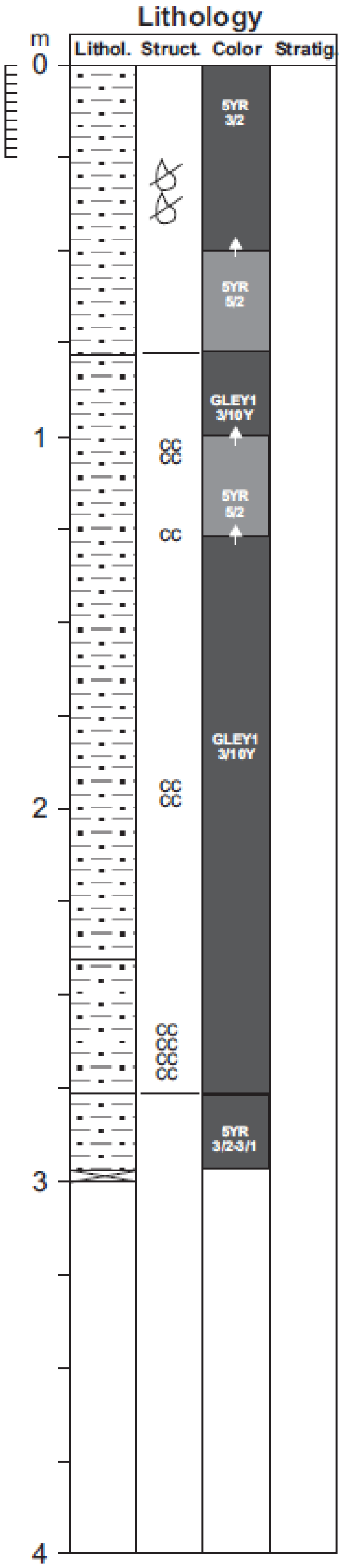


dark olive grey — 0-73/76 cm: mud (silty clay), high water content (sludge), homogenous, large shell frament (clamys, probably in situ before coring) at 25-40 cm bsf., transition to lighter colors around 50 cm bsf.

olive grey

at 73/76 cm: sharp tilted (erosive) boundary to:

dark greenish grey — 73/76-277/280 cm: mud (clayey silt), consolidated (indicating hiatus at boundary),homogenous (apparently, no makroskopic bioturbation visible), intensive smell of $H_2S$.

Intervals with diffuse boundaries, brighter color and higher rate of authigenic carbonate cementation at:
100-130 cm, 191-198 cm, 257-277/280 cm.

dark olive grey

dark greenish grey

sharp irregular contact to:

dark olive grey (almost black) — 277/280-294 cm: mud (silty clay), less consolidated (softer than above), homogenous (apparently, no makroskopic bioturbation visible).
[! possible coring artefact !]


**Appendix 4: Core discription and photograph – SO206-21 GC**

**SO206-23** Date: 8.6.2010 Pos: 9° 11,95' N, 84° 39,42' W
Water Depth: 7,59 m Core Length: 520 cm

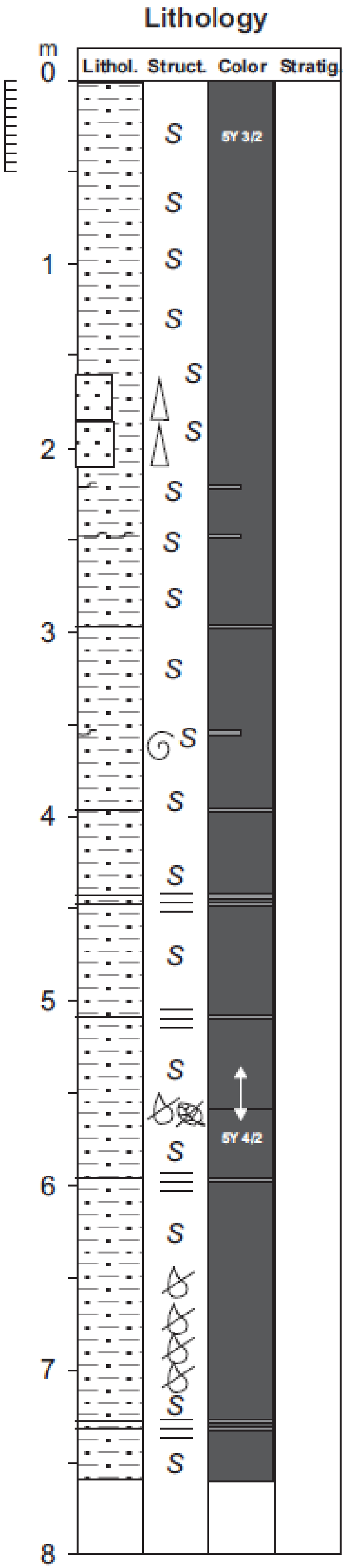


olive grey — mud (clayey silt), bioturbated, abundant forams, small shells, shell fragments, gastropods, homogenous appaerance, upper 2 cm with water content (slurry) with „normal" gradient in compaction downcore.

139-141 cm: interval with higher abundancy of forams

170-184 cm: interval with pathes of sand (reworked turbidite), coarse sand to fine gravel (forams, bioclasts, opaque lithic grains: basaltic/andesitic volcanics)

188-194 cm: reworked sandy turbidite (mainly foram and bioclasts, opaque lithic grains probably basaltic/andesitic volcanics),

222-223 cm: interval with brownish grey mudclasts (tephra, bioturbated)

240-248 cm: interval with bluish grey (Gley2 5/10B) mudclasts (tephra, reworked by bioturbation)

293-294 cm: slightly brighter (greenish grey) tephra layer, diffuse boundaries, slightly bioturbated

356-358 cm: slightly brighter (greenish grey) tephra clast, from bioturbation

396-397 cm: slightly brighter (greenish grey) tephra layer, diffuse boundaries, slightly bioturbated

443-445 cm: bluish grey (Gley2 5/10B) tephra layer, clear boundaries,
448-449 cm: bluish grey (Gley2 5/10B) tephra layer, clear boundaries,

508-509 cm: bluish grey (Gley2 5/10B) tephra layer, clear boundaries.

560-561 cm: layer of larger bioclasts (mainly bivalves)
565-567 cm: layer bivalve and organic plant material (probably wood fragment)

olive grey — 596-598,5 cm: bluish grey (Gley2 5/10B) tephra layer, clear boundaries.

654-656 cm: larger bioclasts

729-730 cm: bluish grey (Gley2 4/10B) tephra layer, clear boundaries, slightly bioturbated.
737-738 cm: bluish grey (Gley2 3/10B) tephra layer, clear boundaries. slightly bioturbated


**Appendix 5: Core discription and photograph – SO206-23 GC**

**SO206-32 GC** Date: 8.6.2010 Pos: 8° 51,13‘ N, 84° 13,06‘ W
Water Depth: 400 m Core Length: 281 cm

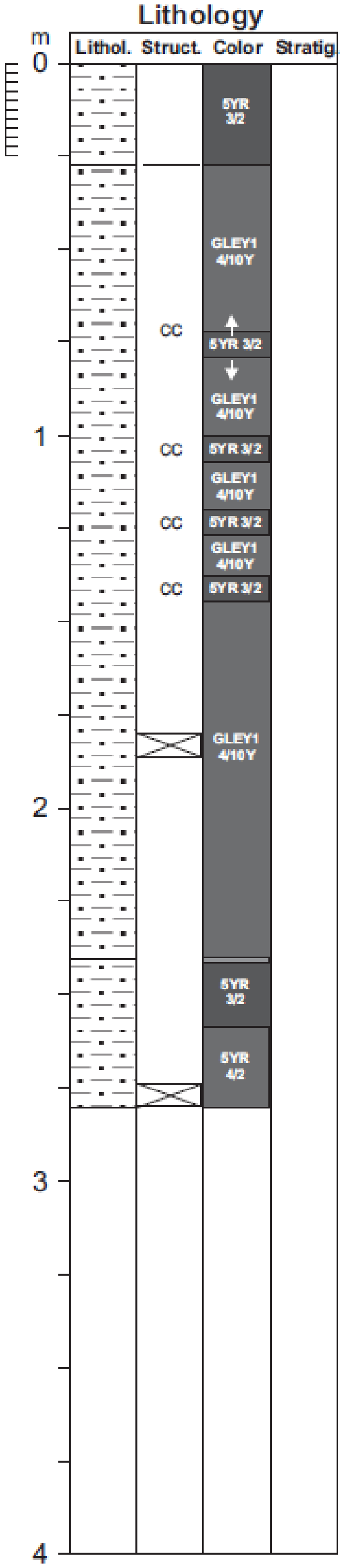


dark olive grey — 0-22/27 cm: mud (clayey silt), high water content (sludge), homogenous, foram-bearing, at 9 cm: sharp tilted erosive boundary to:

dark greenish grey — 22/27-230 cm: mud (clayey silt), consolidated (indicating hiatus at boundary), foram-bearing, few scattered carbonate shell fragments. homogenous (apparently, no makroskopic bioturbation visible), darker band (tilted) at 97-99 cm.

dark olive grey — Intervals with diffuse boundaries, darker color and higher rate of authigenic carbonate cementation (and absence / reduced content of forams) at: 70-81 cm, 99-108 cm, 122-129 cm, 138-144 cm.

dark greenish grey

dark olive grey

dark greenish grey

dark olive grey

dark greenish grey

dark olive grey

dark greenish grey

sharp inclinated contact to:

dark olive grey — 239-242 cm: mud (clayey silt), consolidated, homogenous (apparently, no makroskopic bioturbation visible), diffuse color change at 255 cm.

dark olive grey

NOTE: The lower section (181-281 cm) was squeezed for Helium-Analysis. The Section ends are therefore inundated!


O206-32 GC
181 → 281 cm
SO206-32 GC
81 → 181 cm
SO206-32 GC
0 → 81 cm

**SO206-38 GC** Date: 9.6.2010 Pos: 8° 55,33‘ N, 84° 18,22‘ W
Water Depth: 1016 m Core Length: 357 cm

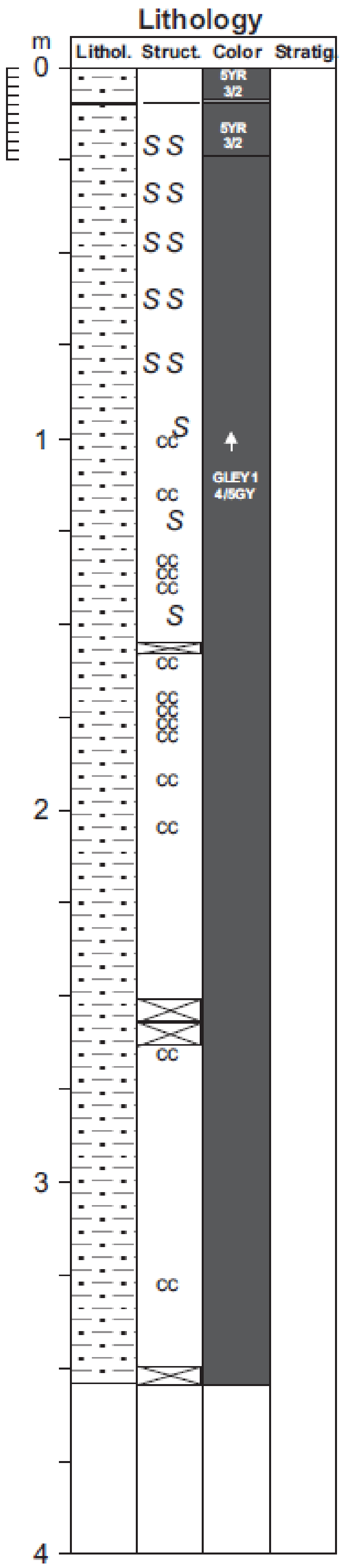


dark olive grey 0-9 cm: mud (clayey silt), high water content (sludge), homogenous, foram-bearing, at 9 cm: sharp boundary (erosive) to:

dark olive grey 9-249 cm: mud (clayey silt), consolidated (indicating hiatus at boundary), foram-bearing, few scattered carbonate shell fragments.
Bioturbation: filled burrows: 1-1,5 cm Ø, individual burrows originate from the boundary at 9 cm (being filled with sludge) and reach up to 80 cm bsf.
Below 120: bioturbation less clearly visible.

80-120cm: smooth color transition from dark olive grey to dark greenish grey

dark greenish grey

81-249cm: scattered small (and individual larger) authigenic carbonate concretions, some black nodules (1-2 mm Ø, probably FeS)

Larger authigenic carbonate nodules (1-7 cm Ø) at:
100 cm, 115 cm, 132-139 cm, 161-163 cm, 169-184 cm, 189 cm, 207 cm, 266 cm, 327 cm.

NOTE: The lower two sections (157-257 cm, 257-357 cm) were squeezed for Helium-Analysis. The Section ends are therefore inundated!


**Appendix 7: Core discription and photograph – SO206-38 GC**

**SO206-50 GC** Date: 14.6.2010 Pos: 8° 55,33‘ N, 84° 18,23‘ W
Water Depth: 1028 m Core Length: 300 cm

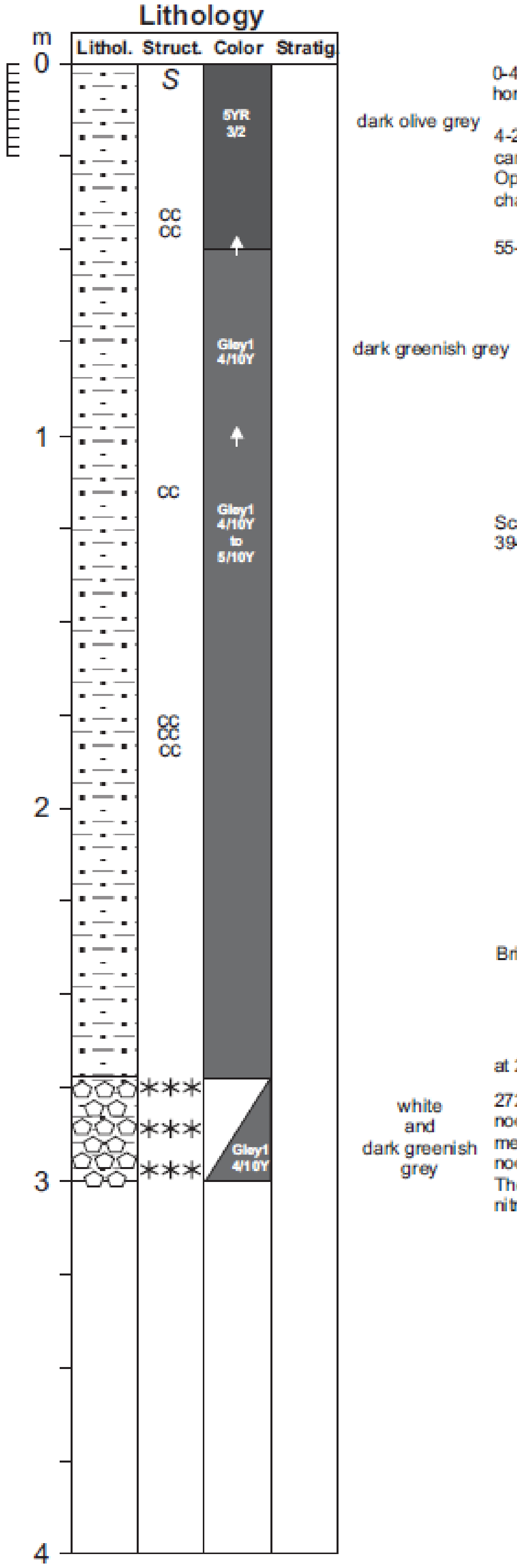


0-4 cm: mud (clayey silt), high water content (sludge), homogenous, foram-bearing, carbonate shell fragments with boundary to:

4-272 cm: mud (clayey silt), consolidated,foram-bearing, few scattered carbonate shell fragments.
Open holes with 0,5-1 cm Ø, at 61-62 and 85-86 cm bsf., interpretation: fluid channels or unfilled burrows.

55-55 cm: smooth color transition from-dark olive grey to dark greenish grey

Scattered small (and individual larger) authigenic carbonate concretions at: 39-47 cm, 114-116 cm, 176-181 cm,

Brighter interval of authigenic carbonates cementation at 237-245 cm.

at 272 cm: sharp contact to:

272-300 cm: gashydrate (fast desintegrating), conglomerate of originally single nodular hydrate aggregates, contains small amount of burnable gas (probably methane). Nodules of the conglomerate up to 3 cm Ø. Space between the nodules filled with relict sediment (mud as above). Hydrate to sediment: 9:1. The compact body was sampled and stored at -20°C (due to lacking liquid nitrogene aboard) to preserve at least the cryogene structure.


SO206-50 GC
200 → 300 cm
SO206-50 GC
100 → 200 cm
O206-50 GC
0 → 100 cm

Appendix 8: Core discription and photograph – SO206-50 GC

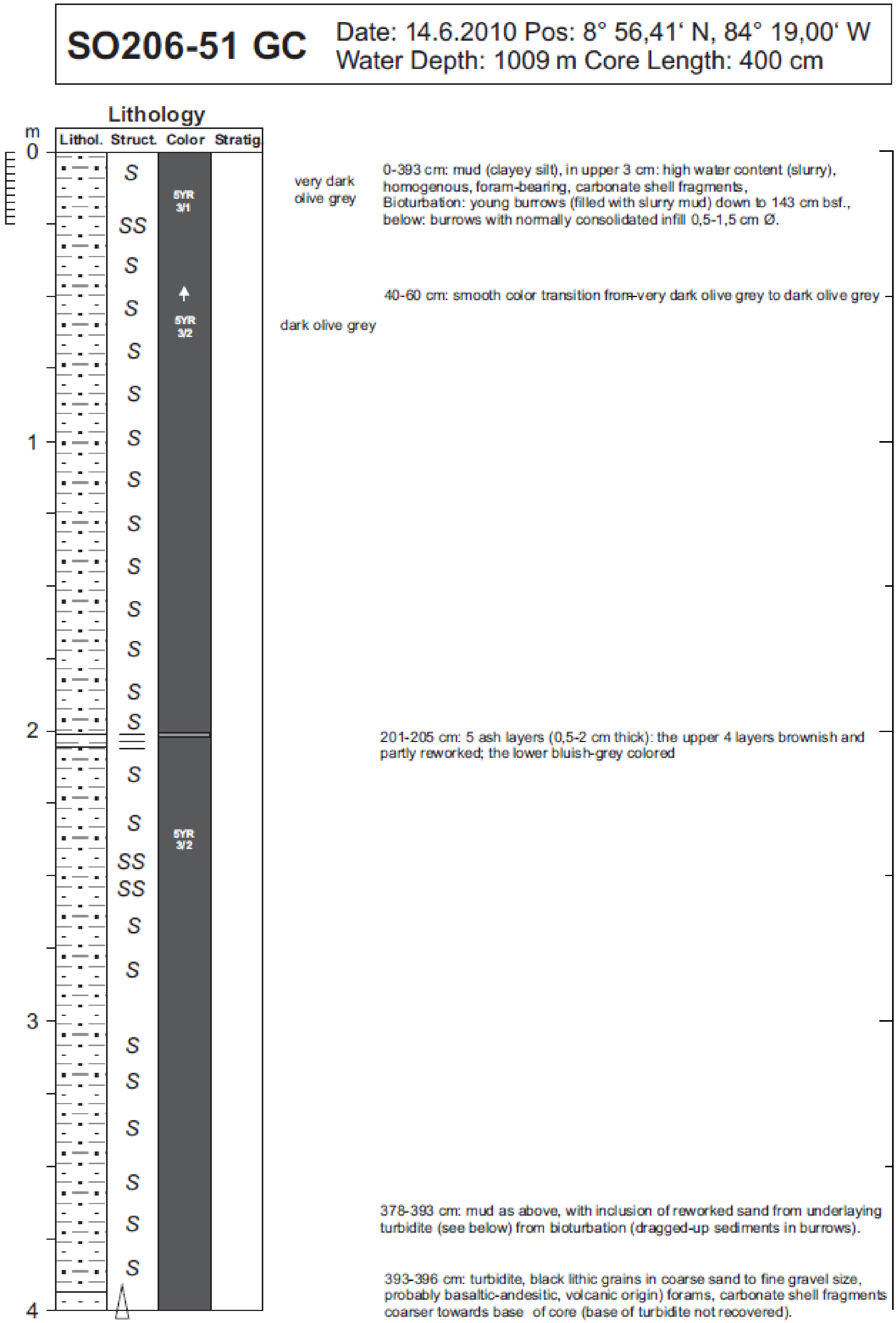


**Appendix 9: Core discription and photograph – SO206-51 GC**

**SO206-54**

Date: 16.06.2010 Pos: 8° 56,39‘ N, 84° 19,02‘ W
Water Depth: 988 m Core Length: 500 cm

## Lithology

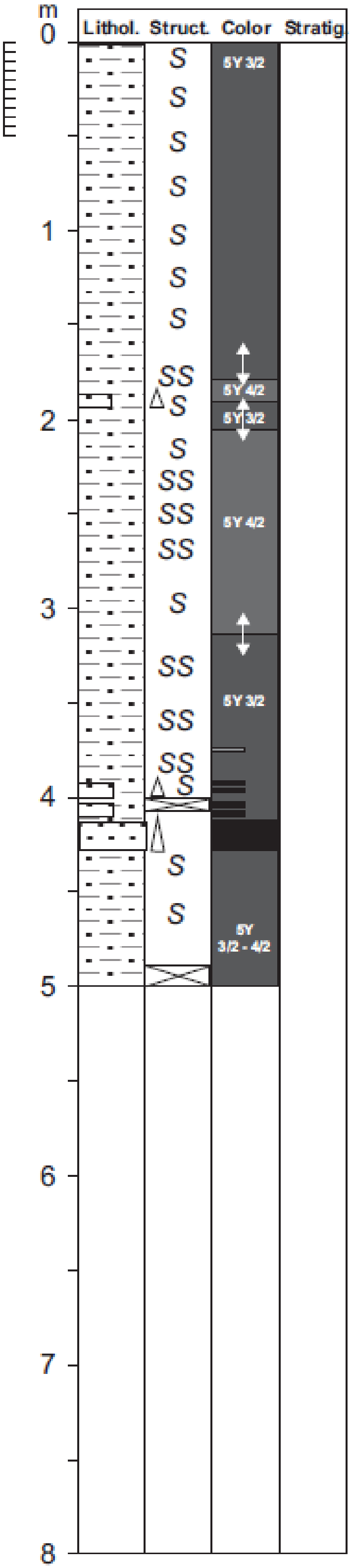


dark olive grey 0-500 cm: mud (clayey silt), forams, shells and shell fragments, homogen, upper 15 cm with high water content (slurry), bioturbated: burrows filled with slurry mud down to 63 cm.

75-77 cm: darker mud clast (reworked tephra ?)
87-96 cm: darker mud clast (reworked tephra ?)

160-200 cm: curved structure (large burrow?)

185-191 cm: sand layer fragments: reworked turbidite(s) (components: opaque lithic grains, forams, shell fragments, quartz grains)

olive grey

dark olive grey

olive grey

dark olive grey

368-369 cm: lense of brighter clay (reworked tephra ?)

379-400 cm: reworked upper turbidite (components see below)

400-427 cm: turbidite (coarse to medium sand; components: opaque lithic grains probably basaltic and/or andesitic, forams, shell fragments, quartz grains and feldspar), upper part: silty and reworked by bioturbation.
[NOTE: Apparent load cast structures are an artefact from squeezing section 400-500 cm: mud underlying the turbidite was squeezed towards thesampling holes!]

427-477 cm: sand-filled burrows (originating in the turbidite)

NOTE: core „shot through“ - uppermost app. 20 cm not recored!

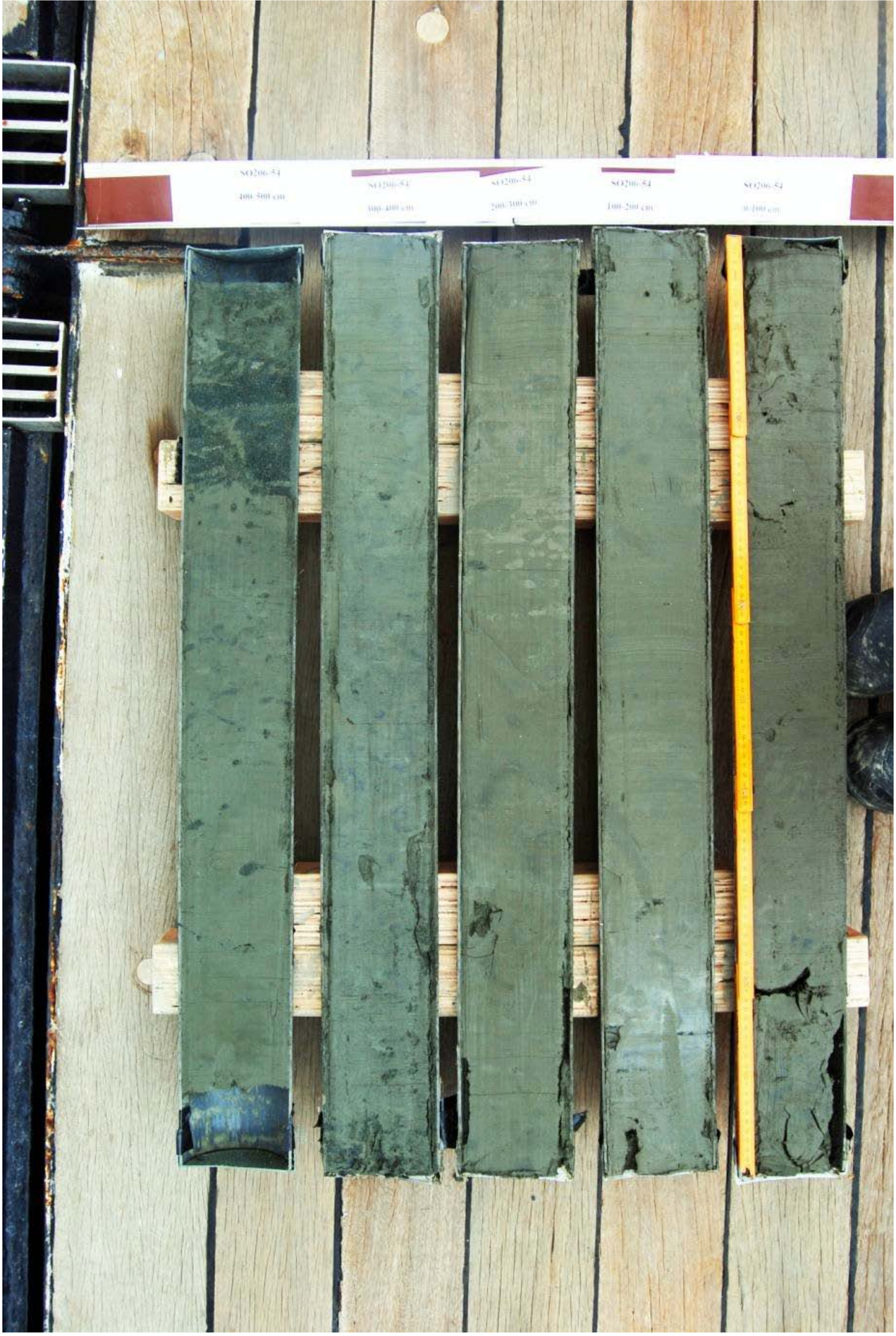


**Appendix 10: Core discription and photograph – SO206-54 GC**

IFM-GEOMAR
Leibniz-Institut für Meereswissenschaften
an der Universität Kiel

# IFM-GEOMAR Reports

| No. | Title |
|---|---|
| 1 | RV Sonne Fahrtbericht / Cruise Report SO 176 & 179 MERAMEX I & II (Merapi Amphibious Experiment) 18.05.-01.06.04 & 16.09.-07.10.04. Ed. by Heidrun Kopp & Ernst R. Flueh, 2004, 206 pp.<br>In English |
| 2 | RV Sonne Fahrtbericht / Cruise Report SO 181 TIPTEQ (from The Incoming Plate to mega Thrust EarthQuakes) 06.12.2004.-26.02.2005. Ed. by Ernst R. Flueh & Ingo Grevemeyer, 2005, 533 pp.<br>In English |
| 3 | RV Poseidon Fahrtbericht / Cruise Report POS 316 Carbonate Mounds and Aphotic Corals in the NE-Atlantic 03.08.–17.08.2004. Ed. by Olaf Pfannkuche & Christine Utecht, 2005, 64 pp.<br>In English |
| 4 | RV Sonne Fahrtbericht / Cruise Report SO 177 - (Sino-German Cooperative Project, South China Sea: Distribution, Formation and Effect of Methane & Gas Hydrate on the Environment) 02.06.-20.07.2004. Ed. by Erwin Suess, Yongyang Huang, Nengyou Wu, Xiqiu Han & Xin Su, 2005, 154 pp.<br>In English and Chinese |
| 5 | RV Sonne Fahrtbericht / Cruise Report SO 186 – GITEWS (German Indonesian Tsunami Early Warning System 28.10.-13.1.2005 & 15.11.-28.11.2005 & 07.01.-20.01.2006. Ed. by Ernst R. Flueh, Tilo Schoene & Wilhelm Weinrebe, 2006, 169 pp.<br>In English |
| 6 | RV Sonne Fahrtbericht / Cruise Report SO 186 -3 – SeaCause II, 26.02.-16.03.2006. Ed. by Heidrun Kopp & Ernst R. Flueh, 2006, 174 pp.<br>In English |
| 7 | RV Meteor, Fahrtbericht / Cruise Report M67/1 CHILE-MARGIN-SURVEY 20.02.-13.03.2006. Ed. by Wilhelm Weinrebe und Silke Schenk, 2006, 112 pp.<br>In English |
| 8 | RV Sonne Fahrtbericht / Cruise Report SO 190 - SINDBAD (Seismic and Geoacoustic Investigations Along The Sunda-Banda Arc Transition) 10.11.2006 - 24.12.2006. Ed. by Heidrun Kopp & Ernst R. Flueh, 2006, 193 pp.<br>In English |
| 9 | RV Sonne Fahrtbericht / Cruise Report SO 191 - New Vents "Puaretanga Hou" 11.01. - 23.03.2007. Ed. by Jörg Bialas, Jens Greinert, Peter Linke, Olaf Pfannkuche, 2007, 190 pp.<br>In English |
| 10 | FS ALKOR Fahrtbericht / Cruise Report AL 275 - Geobiological investigations and sampling of aphotic coral reef ecosystems in the NE-Skagerrak, 24.03. - 30.03.2006, Eds.: Andres Rüggeberg & Armin Form, 39 pp. In English |

IFM-GEOMAR
Leibniz-Institut für Meereswissenschaften
an der Universität Kiel

| No. | Title |
|---|---|
| 11 | FS Sonne / Fahrtbericht / Cruise Report SO 192-1: MANGO: Marine Geoscientific Investigations on the Input and Output of the Kermadec Subduction Zone, 24.03. - 22.04.2007, Ernst Flüh & Heidrun Kopp, 127 pp.<br>In English |
| 12 | FS Maria S. Merian / Fahrtbericht / Cruise Report MSM 04-2: Seismic Wide-Angle Profiles, Fort-de-France – Fort-de-France, 03.01. - 19.01.2007, Ed.: Ernst Flüh, 45 pp.<br>In English |
| 13 | FS Sonne / Fahrtbericht / Cruise Report SO 193: MANIHIKI Temporal, Spatial, and Tectonic Evolution of Oceanic Plateaus, Suva/Fiji – Apia/Samoa 19.05. - 30.06.2007, Eds.: Reinhard Werner and Folkmar Hauff, 201 pp.<br>In English |
| 14 | FS Sonne / Fahrtbericht / Cruise Report SO195: TOTAL TOnga Thrust earthquake Asperity at Louisville Ridge, Suva/Fiji – Suva/Fiji 07.01. - 16.02.2008, Eds.: Ingo Grevemeyer & Ernst R. Flüh, 106 pp.<br>In English |
| 15 | RV Poseidon Fahrtbericht / Cruise Report P362-2: West Nile Delta Mud Volcanoes**,** Piräus – Heraklion 09.02. - 25.02.2008, Ed.: Thomas Feseker, 63 pp.<br>In English |
| 16 | RV Poseidon Fahrtbericht / Cruise Report P347: Mauritanian Upwelling and Mixing Process Study (MUMP), Las-Palmas - Las Palmas, 18.01. - 05.02.2007, Ed.: Marcus Dengler et al., 34 pp.<br>In English |
| 17 | FS Maria S. Merian Fahrtbericht / Cruise Report MSM 04-1: Meridional Overturning Variability Experiment (MOVE 2006), Fort de France – Fort de France, 02.12. – 21.12.2006, Ed.: Thomas J. Müller, 41 pp.<br>In English |
| 18 | FS Poseidon Fahrtbericht /Cruise Report P348: SOPRAN: Mauritanian Upwelling Study 2007**,** Las Palmas - Las Palmas**,** 08.02. - 26.02.2007, Ed.: Hermann W. Bange, 42 pp.<br>In English |
| 19 | R/V L'ATALANTE Fahrtbericht / Cruise Report IFM-GEOMAR-4: Circulation and Oxygen Distribution in the Tropical Atlantic, Mindelo/Cape Verde - Mindelo/Cape Verde, 23.02. - 15. 03.2008, Ed.: Peter Brandt, 65 pp.<br>In English |
| 20 | RRS JAMES COOK Fahrtbericht / Cruise Report JC23-A & B: CHILE-MARGIN-SURVEY, OFEG Barter Cruise with SFB 574, 03.03.-25.03. 2008 Valparaiso – Valparaiso, 26.03.-18.04.2008 Valparaiso - Valparaiso, Eds.: Ernst Flüh & Jörg Bialas, 242 pp.<br>In English |
| 21 | FS Poseidon Fahrtbericht / Cruise Report P340 – TYMAS "Tyrrhenische Massivsulfide"**,** Messina – Messina**,** 06.07.-17.07.2006, Eds.: Sven Petersen and Thomas Monecke, 77 pp.<br>In English |

| No. | Title |
|---|---|
| 22 | RV Atalante Fahrtbericht / Cruise Report HYDROMAR V (replacement of cruise MSM06/2), Toulon, France - Recife, Brazil, 04.12.2007 - 02.01.2008, Ed.: Sven Petersen, 103 pp. In English |
| 23 | RV Atalante Fahrtbericht / Cruise Report MARSUED IV (replacement of MSM06/3), Recife, Brazil - Dakar, Senegal, 07.01. - 31.01.2008, Ed.: Colin Devey, 126 pp. In English |
| 24 | RV Poseidon Fahrtbericht / Cruise Report P376 ABYSS Test, Las Palmas - Las Palmas, 10.11. - 03.12.2008, Eds.: Colin Devey and Sven Petersen, 36 pp, In English |
| 25 | RV SONNE Fahrtbericht / Cruise Report SO 199 CHRISP Christmas Island Seamount Province and the Investigator Ridge: Age and Causes of Intraplate Volcanism and Geodynamic Evolution of the south-eastern Indian Ocean, Merak/Indonesia – Singapore, 02.08.2008 - 22.09.2008, Eds.: Reinhard Werner, Folkmar Hauff and Kaj Hoernle, 210 pp. In English |
| 26 | RV POSEIDON Fahrtbericht / Cruise Report P350: Internal wave and mixing processes studied by contemporaneous hydrographic, current, and seismic measurements, Funchal – Lissabon, 26.04.-10.05.2007 Ed.: Gerd Krahmann, 32 pp. In English |
| 27 | RV PELAGIA Fahrtbericht / Cruise Report Cruise 64PE298: West Nile Delta Project Cruise - WND-3, Heraklion - Port Said, 07.11.-25.11.2008, Eds.: Jörg Bialas & Warner Brueckmann, 64 pp. In English |
| 28 | FS POSEIDON Fahrtbericht / Cruise Report P379/1: Vulkanismus im Karibik-Kanaren-Korridor (ViKKi), Las Palmas – Mindelo, 25.01.-12.02.2009, Ed.: Svend Duggen, 74 pp. In English |
| 29 | FS POSEIDON Fahrtbericht / Cruise Report P379/2: Mid-Atlantic-Researcher Ridge Volcanism (MARRVi), Mindelo- Fort-de-France, 15.02.-08.03.2009, Ed.: Svend Duggen, 80 pp. In English |
| 30 | FS METEOR Fahrtbericht / Cruise Report M73/2: Shallow drilling of hydrothermal sites in the Tyrrhenian Sea (PALINDRILL), Genoa – Heraklion, 14.08.2007 – 30.08.2007, Eds.: Sven Petersen & Thomas Monecke, 235 pp. In English |
| 31 | FS POSEIDON Fahrtbericht / Cruise Report P388: West Nile Delta Project - WND-4, Valetta – Valetta, 13.07. - 04.08.2009, Eds.: Jörg Bialas & Warner Brückmann, 65 pp. In English |
| 32 | FS SONNE Fahrtbericht / Cruise Report SO201-1b: KALMAR (Kurile-Kamchatka and ALeutian MARginal Sea-Island Arc Systems): Geodynamic and Climate Interaction in Space and Time, Yokohama, Japan - Tomakomai, Japan, 10.06. - 06.07.2009, Eds.: Reinhard Werner & Folkmar Hauff, 105 pp. In English |
| 33 | FS SONNE Fahrtbericht / Cruise Report SO203: WOODLARK Magma genesis, tectonics and hydrothermalism in the Woodlark Basin, Townsville, Australia - Auckland, New Zealand 27.10. - 06.12.2009, Ed.: Colin Devey, 177 pp. In English |

| **No.** | **Title** |
|---|---|
| 34 | FS MARIA S. MERIAN Fahrtbericht / Cruise Report MSM 03-2: HYDROMAR IV: The 3rd dimension of the Logatchev hydrothermal field, Fort-de-France - Fort-de-France, 08.11. - 30.11.2006, Ed.: Sven Petersen, 98 pp. In English |
| 35 | FS SONNE Fahrtbericht / Cruise Report SO201-2 **KALMAR: K**urile-Kamchatka and **AL**eutian **MAR**ginal Sea-Island Arc Systems: Geodynamic and Climate Interaction in Space and Time Busan/Korea – Tomakomai/Japan, 30.08. - 08.10.2009, Eds.: Wolf-Christian Dullo, Boris Baranov, and Christel van den Bogaard, 233 pp. In English |
| 36 | RV CELTIC EXPLORER Fahrtbericht / Cruise Report CE0913: Fluid and gas seepage in the North Sea, Bremerhaven – Bremerhaven 26.07. - 14.08.2009, Eds.: Peter Linke, Mark Schmidt, CE0913 cruise participants, 90 pp. In English |
| 37 | FS SONNE Fahrtbericht / Cruise Report: TransBrom SONNE, Tomakomai, Japan - Townsville, Australia, 09.10. - 24.10.2009, Eds.: Birgit Quack & Kirstin Krüger, 84 pp. In English |
| 38 | FS POSEIDON Fahrtbericht / Cruise Report POS403, Ponta Delgada (Azores) - Ponta Delgada (Azores), 14.08. - 30.08.2010, Eds.: Torsten Kanzow, Andreas Thurnherr, Klas Lackschewitz, Marcel Rothenbeck, Uwe Koy, Christopher Zappa, Jan Sticklus, Nico Augustin, 66 pp. In English |
| 39 | FS SONNE Fahrtbericht/Cruise Report SO208 Leg 1 & 2 Propagation of Galápagos Plume Material in the Equatorial East Pacific (PLUMEFLUX), Caldera/Costa Rica – Guayaquil/Ecuador 15.07. - 29.08.2010, Eds.: Reinhard Werner, Folkmar Hauff and Kaj Hoernle, 230 pp, In English |
| 40 | Expedition Report "Glider fleet", Mindelo (São Vincente), Republic of Cape Verde, 05. – 19.03.2010, Ed.: Torsten Kanzow, 26 pp, In English |
| 41 | FS SONNE Fahrtbericht / Cruise Report SO206, Caldera, Costa Rica – Caldera, Costa Rica, 30.05. – 19.06.2010, Ed.: Christian Hensen, 95 pp, In English |

IFM-GEOMAR

Leibniz-Institut für Meereswissenschaften
an der Universität Kiel

Das Leibniz-Institut für Meereswissenschaften ist ein Institut der Wissenschaftsgemeinschaft Gottfried Wilhelm Leibniz (WGL)

The Leibniz-Institute of Marine Sciences is a member of the Leibniz Association (Wissenschaftsgemeinschaft Gottfried Wilhelm Leibniz).

**Leibniz-Institut für Meereswissenschaften / Leibniz-Institute of Marine Sciences**
IFM-GEOMAR
Dienstgebäude Westufer / West Shore Building
Düsternbrooker Weg 20
D-24105 Kiel
Germany

**Leibniz-Institut für Meereswissenschaften / Leibniz-Institute of Marine Sciences**
IFM-GEOMAR
Dienstgebäude Ostufer / East Shore Building
Wischhofstr. 1-3
D-24148 Kiel
Germany

Tel.: ++49 431 600-0
Fax: ++49 431 600-2805
www.ifm-geomar.de